DROPLET-BASED MICROEXTRACTION OF DNA ENABLED BY ELECTROWETTING-ON-DIELECTRIC DIGITAL MICROFLUIDICS

by

SHUBHODEEP PAUL

Presented to the Faculty of the Graduate School of

The University of Texas at Arlington in Partial Fulfillment

of the Requirements

for the Degree of

DOCTOR OF PHILOSOPHY

THE UNIVERSITY OF TEXAS AT ARLINGTON

December 2019

To my parents and my wife

for their endless love & support

Acknowledgments

First and foremost, I would like to thank and convey my deepest gratitude to my Ph.D. supervisor Dr. Hyejin Moon. Over the years in her lab, she has provided the ideal environment to think freely and grow as an independent researcher. I thank her for investing her time and efforts to teach me to – ask the right questions, design meaningful experiments, analyze data, and communicate results in the most effective way. The training under her supervision has proven indispensable towards the completion of this dissertation.

I was fortunate to have very helpful supervising committee members: Dr. Rhonda Prisby, Dr. Ashfaq Adnan, Dr. Debabrata Saha, Dr. Junha Jeon, and Dr. Wen Shen. I want to thank them for their time and for providing valuable criticism.

My sincerest appreciation goes to all my colleagues in the IMNfL lab. I thank all of them for the ideas that we have shared and the fun time that we had in the lab. Special thanks to Matin for his help on numerous occasions in my research. I also want to take this opportunity to thank the UTA MAE department for the generous funding, which was essential to support my education.

In conclusion, I would like to thank my family and friends. My wife Debapriya for the endless love, support, and for enduring the last five years of grad school. I have been lucky enough to share my passion for scientific research with Debapriya, and she continues to be my most significant inspiration everyday.

Abstract

DROPLET-BASED MICROEXTRACTION OF DNA ENABLED BY ELECTROWETTING-ON-DIELECTRIC DIGITAL MICROFLUIDICS

Shubhodeep Paul

The University of Texas at Arlington, 2019

Supervising Professor: Hyejin Moon

In recent years there have been significant advances in micro/nanotechnologies employing miniaturized platforms to achieve efficient sample pre-processing, separation, and quantification processes. The idea of bringing several lab-scale protocols on to a single chip, i.e., a lab-on-a-chip (LOC) device along with automation, is a reality now. Miniaturization of biochemical operations usually handled in a laboratory has numerous advantages, such as cost effectiveness, multiplexing, assay speed, and sensitivity. Microfluidic technologies used in LOC devices can manipulate tiny volumes of samples and reagents to perform on-chip protocols with minimal human intervention. Electrowetting-on-dielectric (EWOD)-based digital microfluidics (DMF) is one of the LOC platforms that show the potential to achieve rapid processing through its capabilities, such as multiplexed operation, simple instrumentation, flexible device geometry, and easy coupling with other technologies. There has been much effort in integrating protocols of DNA analysis workflow into EWOD microfluidics recently. However, much of the sample preparation (mainly DNA extraction) is still done hands-on using standard lab protocols. In this work, an EWOD microfluidic

platform has been designed to demonstrate and integrate the microscale drop-to-drop (DTD) DNA extraction via the liquid-liquid extraction (LLE) method.

The first study is focused on the demonstration of LLE protocol in a DTD format on EWOD DMF devices. The study done was to show the separation of color dye analytes in a binary solution mixture using an EWOD platform. Absorbance-based concentration measurement was miniaturized and integrated with the platform to evaluate the performance of the on-chip LLE protocol. The study showed the capability of EWOD-based LLE to separate molecules in a sample.

The second and the third studies are focused on extending the capability of EWOD DTD LLE for the separation of DNA molecules from other impurities in the sample. Plasmid DNA was used as the model DNA, and bovine serum albumin (BSA) protein molecules were used as impurities to show the capability of EWOD LLE to isolate the DNA molecules selectively. Different liquid-liquid systems were studied for the on-chip DNA extraction other than the traditional phenol extraction method. The second study is focused on the LLE of DNA using ionic liquid (IL) as an extractant. Hydrophobic IL, which forms a two-phase system with the aqueous sample, is an excellent solvent for DNA isolation. The capability of EWOD devices to isolate DNA molecules using aqueous/IL (Aq./IL) is highlighted in the second study. The third study is focused on the integration of aqueous two-phase systems (ATPS) for DNA extraction on the EWOD device. EWOD has already shown the capability to handle ATPSs, and this last study was done to demonstrate the integration of a aqueous two-phase extraction (ATPE) process for isolating DNA molecules on EWOD devices for the first time. It was observed that by changing the liquid-liquid systems, there were significant changes in the final extraction yield from the on-chip LLE process.

This research validates the initial steps for the creation of an efficient on-chip system for DNA based sample preparation, recognized by the miniaturization of DNA LLE and novel DTD

extraction techniques. This DNA sample preparation can eventually be integrated with post-extraction based manipulations of DNA utilized by genomic analysis modules.

Table of Contents

List of Illustrations

Chapter 1

Introduction

Nucleic acids, which are regarded as the central database of the cells, have an implication on the biochemical processes of every organism [1]. It controls cell growth and replication [1]. DNA analysis is routinely done in many fields such as DNA as biomarkers for disease diagnosis [2]; therapeutics [3]; anthropology [4]; genetics [5] and pharmaceuticals [6]. Sample preparation in these analyses can be labor-intensive using several different instruments and kits to extract DNA from the sample. A high-quality DNA is required as the analysis is affected by the purity of the DNA [7-9]. Impurities such as proteins, small organic molecules, and phospholipids often cause a challenge in downstream assays as interfering agents [10 - 12]. The following detection and analysis steps in the workflow can also be very time-consuming. With the advancements in the technology of miniaturization, devices are developed that can integrate some or all the DNA analysis steps into a single chip for specific applications. These devices dramatically reduce reagent consumption, analysis time, and eliminate the use of expensive, bulky laboratory instruments. They are often referred to as lab-on-a-chip (LOC) devices.

LOC devices can integrate multiple laboratory functions on a single integrated circuit (commonly called a “chip”) [13]. These chips can automate complicated biochemical protocol steps ranging from sample preparation to detection on micro to pico-scale levels [13]. These devices combine microfluidics, electronics, optical, and biosensing procedures to achieve the biochemical protocols on a platform sized typically between few square millimeters to few

centimeters. Thus, LOC devices can provide a compact, disposable, automated closed system for DNA analysis that could be used in clinical and forensic laboratories for faster analysis [13].

The concept of a LOC device for DNA analysis is shown in Fig. 1.1. Different steps of the workflow, including DNA extraction, assay, and detection, can be integrated into a single chip. In the example shown in Figure 1.1, a LOC device is developed for the extraction of nucleic acid in this work [14]. The extraction is followed by performing polymerase chain reaction (PCR) assay for the amplification of specific genes and finally detect single nucleotide polymorphism (SNP) by looking at the SNP markers in the genome [14].

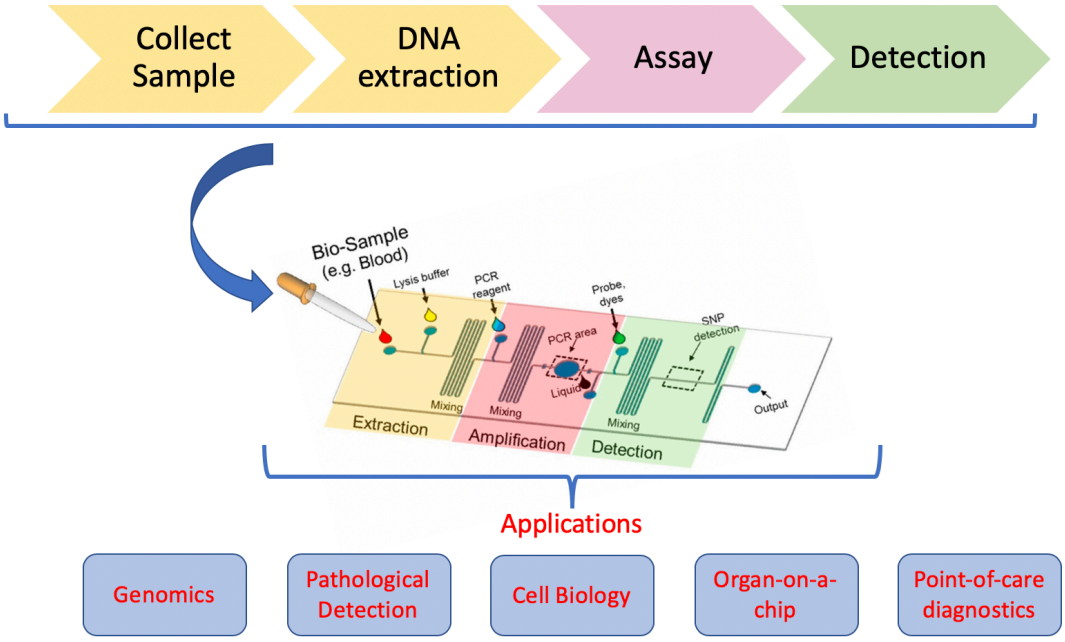

Figure 1.1: Concept of a lab-on-a-chip device for DNA analysis and its applications.

LOC devices make use of microfluidics either in the forms of continuous microfluidics [14] or droplet microfluidics [15, 16]. The example in Figure 1.1 uses continuous microfluidics, which is the most common format of microfluidics and is based on enclosed microchannels in planar platforms.

A distinct type of droplet microfluidics system known as digital microfluidic (DMF), which works on the principle of electrowetting on dielectric (EWOD), is also an excellent candidate for LOC devices for nucleic acid analysis [17,18]. DMF microfluidic devices can handle and move microdroplets in a discrete format with the application of electric signals (detailed working of EWOD devices is provided in chapter 3). The capability of the EWOD DMF device to operate individual droplets makes it a very suitable platform for running multiple nucleic acid assays with varying conditions on the same chip to achieve high-throughput gene screening [19, 20]. Many downstream protocols (assay and detection) for DNA analysis workflow have already been developed on EWOD devices [21-24]. For all these devices, the DNA extraction steps are still done off-chip using standard lab-scale protocols. Some efforts have been made to integrate DNA extraction on EWOD devices, but they rely on using solid particles (magnetic beads) for the isolation, making it an elaborate multistep process [25, 26]. The other conventional and more straightforward method for DNA isolation, known as the liquid-liquid extraction (LLE), has not been studied on EWOD devices. The real advantage of EWOD devices for DNA analysis will be leveraged with the inclusion of a simpler DNA extraction protocol, such as LLE, along with the downstream protocol modules.

1.1 Dissertation Overview

The objective of this dissertation is to improve the state-of-the-art in DNA analysis workflow, with a particular focus on developing sample preparation, integrating LLE protocol, and bead free DNA extraction on EWOD microfluidics. The methods of LLE of DNA on EWOD is explored in this research. It is potentially cost-efficient, easy to integrate with further assay steps, and highly likely for possible automation.

The first part of the work focuses on building an EWOD device, which can perform a traditional LLE process in a drop-to-drop format using color-based dyes. The integration of the LLE process on EWOD was ascertained by studying the extraction of the color dye molecules. The second and the third part of the dissertation extends this capability of EWOD-based LLE for the isolation of DNA molecules from its impurities. The LLE process adopted in the study for DNA extraction uses different liquid-liquid systems other than the traditional phenol extraction method.

Chapter 2 describes the most common methods used in current DNA extraction protocols. This chapter further introduces DNA extraction in microfluidics-based platforms. It gives an overview of approaches adopted in microfluidics devices and the development over the years.

Chapter 3 introduces EWOD DMF devices highlighting the fundamentals of the theory of microdroplet motion on a solid substrate under the application of electric potential. The working of the platform and device fabrication steps are explained in detail.

Chapter 4 is about the proof of concept study for liquid-phase extraction (LLE) on EWOD devices. It covers the study of selective extraction of dye molecules from a binary mixture sample with the LLE process on the EWOD device. The steps of the LLE process were studied for better performance of the device and to develop the LLE protocol for the following DNA extraction study. The on-chip real-time concentration monitoring system was developed to measure the yield of extraction from the process. A comparison between the results obtained from the designed microfluidic device and the standard lab-scale LLE protocol was made in this chapter.

Chapter 5 introduces ionic liquid (IL) as an extractant for DNA extraction, and the LLE of DNA is developed on the EWOD chip. The optimized conditions and steps for LLE obtained from chapter 4 were utilized. Control samples of pure plasmid DNA (pDNA) was used to show the working of the extraction process on EWOD. The chapter further reports the selective extraction of pDNA from a sample mixture of pDNA and protein. The partition of pDNA molecules was quantified by analyzing the residual pDNA left in the sample.

In Chapter 6, an introduction to the aqueous two-phase system (ATPS) is provided. This chapter demonstrates the technique of DNA extraction by ATPS on EWOD devices. Two ATPSs were studied, and a comparison of performance for DNA extraction was made between the two systems. The increase in the yield by changing the liquid-liquid system and the ease of doing so on EWOD devices is highlighted here.

Chapter 2

Introduction to DNA Extraction

As discussed in the previous chapter, the first step in DNA analysis workflow involves isolating or extracting DNA from cells. A high-quality DNA is required since the downstream analysis is affected by the purity of the DNA [1]. Impurities such as proteins, small organic molecules, and phospholipids can often be a hindrance in the downstream applications. A review of the standard methods of DNA extraction followed by the adaptation of these methods in microfluidic devices is provided in this chapter.

2.1 Standard DNA extraction methods

DNA extraction and purification methods fall under two main categories – i) solid-phase extraction (SPE) and ii) liquid phase extraction (LPE). A detailed description of the two types is as follows:

2.1.1 Solid-phase extraction

SPE methods work on the principle of DNA molecules selectively binding to a solid surface [27]. A silica surface is typically used for SPE. The steps involved are lysis of cells, adsorption of DNA, washing, and elution of DNA. Silica surfaces used for DNA extraction are in the form of silica filters or columns packed with silica particles. They come under the category of silica filtration. Magnetic beads coated with silica or charged ligands are also widely used for DNA extraction [28]. Hence, the two most common DNA extraction technologies under SPE are silica filtration and magnetic beads-based extraction, the steps of which are described below.

(1) Silica filtration

The first step in this procedure is cell lysis using alkaline conditions. The cell lysate is then loaded into a silica packed column or a silica filter. The presence of chaotropic salts in the system makes the DNA bind to the silica surface owing to electrostatic shielding between them [29]. Unlike DNA, the other components of the cells fail to attach to the silica beads. The next step is to wash away the contaminants to leave the DNA as the sole components bound to the silica surface. A low salt-based elution buffer is then used to detach the DNA from silica [29]. Centrifugation is required for all the steps of DNA binding, washing, and elution to force the liquid through the silica column or filter.

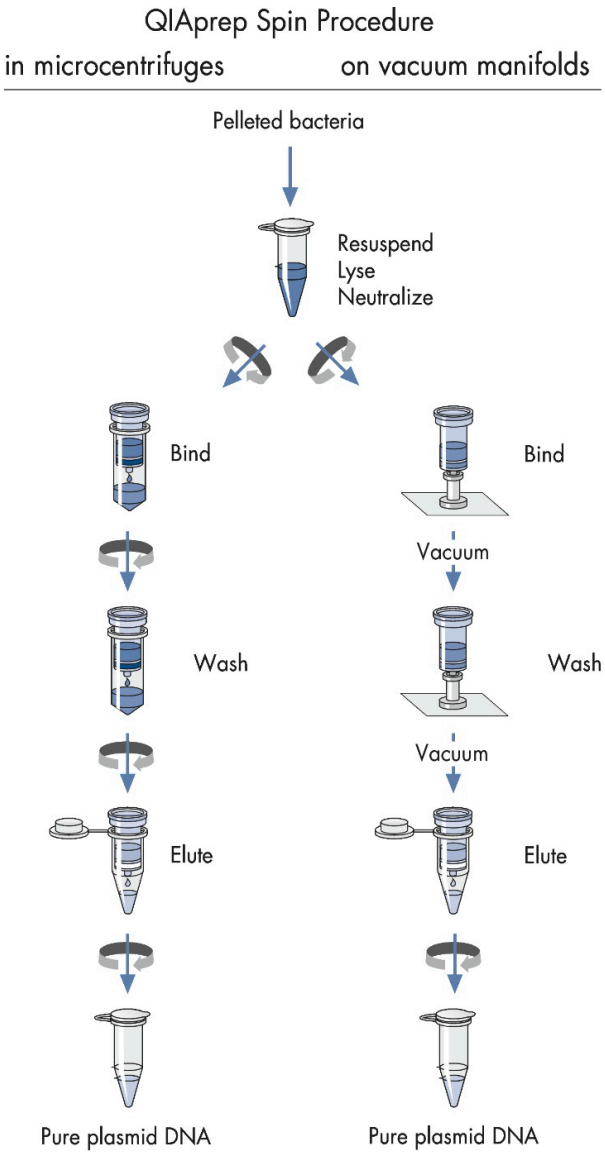

Figure 2.1: Silica filtration protocol steps with Qiagen QIAprep kit [30].

This procedure of DNA extraction has been implemented in several commercially-available protocols, including Qiagen QIAamp®, Clontech NucleoSpin™, Mo Bio Laboratories Ultraclean™ BloodSpin™, Promega Wizard™, Akonni TruTip®, and Sigma Aldrich GenElute™. These kits primarily used silica in the form of microporous filters in order to separate

the DNA. Figure 2.1 shows the detailed steps of silica filtration using Qiagen QIAprep kit® [30]. One of the protocols in Figure 2.1 requires centrifugation steps at specific steps to flush liquid through the filter, whereas the other protocol makes use of a vacuum manifold to do the same task [30].

(2) Magnetic bead-based extraction

The magnetic beads, as opposed to silica filtration, consists of several layers, namely, a super magnetic core, a protective coating, and a surface layer at the top to functionalize DNA [29]. The DNA binding to the top layer of the magnetic bead can then be eluted and resuspended in the pure form [29].

The process starts with lysing the cells to release the genetic material into the solution, as well as denaturing the nucleases that could degrade the DNA. The magnetic beads are then added to the lysate and mixed. The DNA molecules selectively bind to the magnetic beads. The beads are aggregated at one corner of the tube when it is placed in an external magnetic separation rack. The supernatant is then discarded. The beads are resuspended and thoroughly mixed with a washing buffer to remove impurities from the beads. After another round of aggregation of the beads with the magnetic separation rack, the wash buffer is removed. Finally, the purified DNA is eluted from the beads by resuspending the beads in the elution buffer. The beads are then again aggregated, and the isolated DNA in the elution buffer is removed and stored for analysis. The steps of DNA extraction using magnetic beads is illustrated in Figure 2.2.

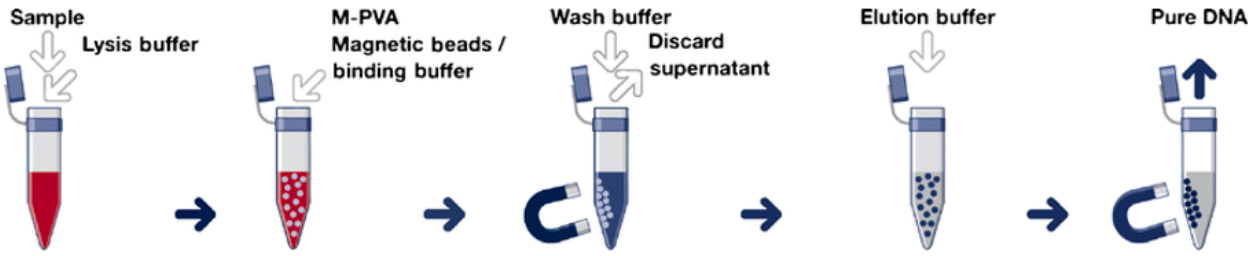

Figure 2.2: Schematic illustration of nucleic acids isolation using magnetic beads [31].

Magnetic bead-based DNA extraction is different from silica filtration in a way that the repeated centrifugation in the silica filtration protocol is replaced by the magnetic bead aggregation utilizing the magnetic separation rack. This process has been well adopted in many automated platforms and is capable of handling a large sample volume by scaling up in a 96 well plate [32]. However, the initial investment purchasing the automated platforms and their subsequent maintenance costs are imperative.

2.1.2 Liquid-phase extraction

The isolation of DNA using the LPE methods performs all steps of extraction, purification, and isolation of DNA in the liquid phase itself. Centrifugation serves as an integral component in the protocol. The conventional DNA extraction methods using liquid phase are cesium hloride gradient centrifugation, phenol-chloroform, salting-out, alkaline, and chelex. Among these methods, the phenol-chloroform method is described below, which is most relevant to this work.

Phenol-chloroform extraction:

This method makes use of phenol, an organic liquid, in combination with the aqueous or sample phase [33]. The phenol/chloroform method has been shown to be able to purify DNA mixtures by extracting the RNA, lipid, and proteins from the sample phase [34]. This separation technique is based on the affinity of the molecules for their preferred liquid phase. The steps of this process include digestion of cells, mixing the phases where impurities like proteins and lipid molecules separate into the phenol or organic phase, leaving the DNA behind in the aqueous phase. Precipitation can later be used to separate the DNA from the purified aqueous phase.

The LPE process starts with cell lysis, which can be achieved using a chemical, thermal, or mechanical rupture of the cells. The protocol is usually carried out in 1.5 ml tubes, and volumes in the range of 100 μl to 500 μl are used for easy manipulation of the sample with micropipettes. The sample (aqueous) and the extractant (phenol) phases are mixed in the tube and vortexed vigorously with the use of a benchtop vortex for proper mixing of the phases. During the mixing process, the components of the cell separate in the two-phase system based on their affinity and the interaction energies. The DNA molecules stay back in the aqueous phase, whereas the other (impurities) molecules separate into the organic phase. The separation occurs at the interface of the two liquids, and hence increasing the interfacial area is an important parameter to have a high yield of extraction. After the mixing step, the tube is centrifuged so that the phases separate due to their density difference. The aqueous phase due to its lower density compared to the organic phase remains at the top, and the organic phase settles at the bottom. The top aqueous phase with the DNA is now removed very carefully with a micropipette. The entire process can be repeated with a fresh organic phase to get a higher purity of DNA or with a different extractant phase to get rid of some other cellular component. In addition to phenol-based extraction, chloroform is finally

added to the aqueous phase in order to retract any leftover phenol from the final purified sample. The sample now can be directly used for analysis or can be precipitated using an ethanol-based precipitation method to get rid of all the salts in the sample. The ethanol precipitation method involves mixing the sample with ice-cold ethanol centrifuged at a very high speed that precipitates the DNA into a pellet. The supernatant is removed, and the sample is washed with 80% ethanol to get rid of the remaining salts in the sample. The pellet at the end is collected and resuspended into DI water or Tris-EDTA (TE) buffer.

Barring the obvious advantages of obtaining pure DNA, the disadvantages of the phenol-chloroform extraction method are that it is highly labor-intensive, reducing its cost-effectiveness significantly in using inexpensive reagents. Moreover, cautionary steps are required while handling chemicals such as phenol since it is extremely corrosive and requires operation inside a fume hood [35]. Owing to the disadvantages mentioned above, experienced and skilled personnel must be available to run the protocol. There have been recent developments in many other liquid-liquid systems without the use of phenol to perform LLE of DNA. This dissertation addresses the use of other liquid-liquid systems that will be studied on the EWOD platform for effective DNA extraction.

Drawing a comparison between the above two techniques, namely, SPE and LPE, each of them have their respective pros and cons. SPE is advantageous over the latter because it does not deal with organic solvents like phenol and their potential hazards, not to mention the possibility of contaminating the purified DNA by organic solvents so much so that downstream procedures are affected [36]. However, SPE is limited by the surface area available on the silica particles or magnetic meads for DNA extraction to occur efficiently. It is also more likely to get contaminated by other biomolecules like proteins due to non-specific binding to the silica surface. Moreover,

SPE is primarily a batch procedure where solutions are required to be introduced at each step as opposed to LPE. In LPE, a continuous flow suffices its protocol.

Ionic Liquids (ILs), on the other hand, are great substitutes for organic solvents in LPE systems [37, 38]. Aqueous two-phase systems (ATPS) are also another arena for exploration into phenol-free LPE systems [39]. Our EWOD DMF platform studies the above two LPE system in details.

2.2 Microfluidic DNA extraction

Microfluidics has a significant advantage of miniaturizing, automating the complicated steps of DNA extraction and minimizing human-related errors [40]. The Development of the unit process of DNA extraction will enable integration with other downstream assays for LOC devices. Microfluidics aiming to integrate DNA extraction has mainly focused on the miniaturization of SPE methods [41], and few studies on LPE methods (utilizing phenol extraction method) [42]. Primarily two categories of microfluidic devices have been discussed below. They are a) continuous and b) EWOD based microfluidic devices.

2.2.1 Continuous microfluidics-based DNA extraction

The early era in microfluidics research is predominantly marked by continuous microfluidics. It is characterized by a fluid phase that flows continuously through microchannels [43]. For maintaining a constant pressure difference that drives the flow of fluid from one spot to another inside the microchannel, several regulators have been devised. Some of them are micropumps and microvalves [44].

Some early attempts to develop a continuous microfluidics-based unit process for DNA extraction involved mimicking SPE lab bench techniques on chip-scale. These devices suffered from the challenge of handling multiple chemical reagents in multistep assays. Michael et al. [41] showed that when hybrid silica particle/sol-gel packed in a microchannel can extract DNA to purify the human genome DNA (Figure 2.3 a).

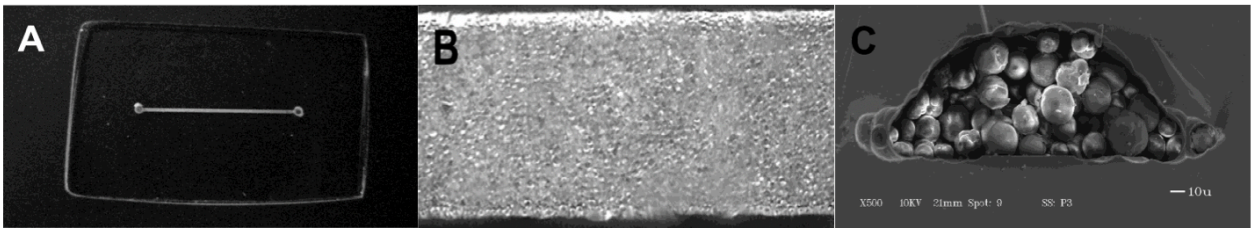

Figure 2.3. Microchip packed with silica particles and immobilized with sol-gel: (A) 1× magnification; (B) 10× magnification; (C) cross section of packed channel at 500× magnification [41].

The flow rate, pH, and DNA loading were optimized to get results comparable with the benchtop microcentrifuge method [41]. The chip requires an off-chip lysis step and loading of sample lysate. Following adsorption, by the particles, it needs a washing and elution steps, and both require separate buffers.

Cady et al. [45], in their work, showed the integration of silica-coated micropillar in a microfluidic device having a serpentine design channel, as shown in Figure 2.4. Samples containing DNA and other impurities, when passed through this channel, DNA molecules would selectively bind to the micropillars. The silica-coated micropillars were microfabricated during the fabrication process using standard techniques [45]. This method has an advantage because it is not

required to fill the channels with silica beads or particles. Like [41], this chip also requires a post-process of washing and elution to retrieve the DNA molecules from the pillars.

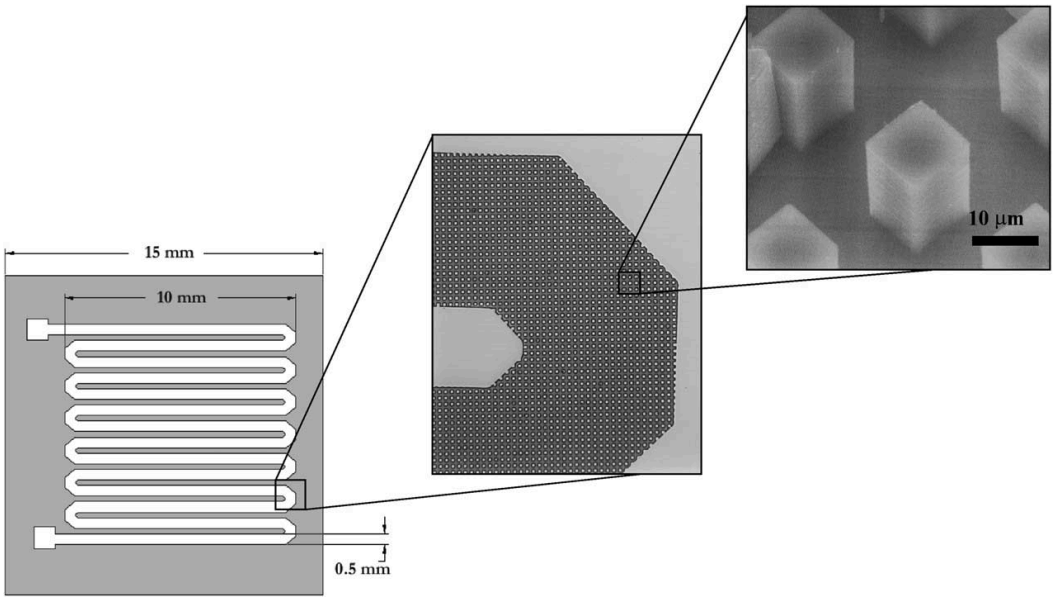

Figure 2.4: Schematic representation of channels containing microfabricated silica pillars. The spacing between pillars and the pillar width was constant at 10 mm, while the depth of the channels and height of the pillars could be adjusted between 20 and 50 mm [45].

Recent efforts have also been made to incorporate the sample preparation step with downstream analysis processes using multiple devices in line, as shown in Figure 2.5 [46]. In this work, the DNA extraction module uses a magnetic bead fluidized bed. The DNA is isolated on the beads using standard SPE techniques. The extracted DNA is transferred to a second emulsifying chip, which can encapsulate the DNA molecules with droplet microfluidics. On-chip droplet digital PCR (ddPCR) is then performed, and the drops are sorted for analysis.

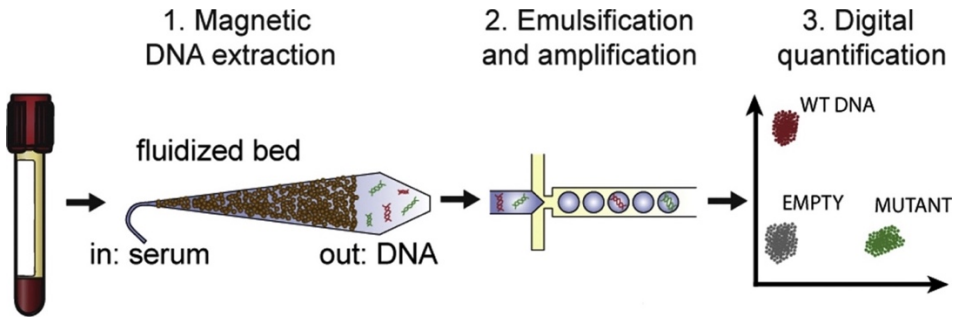

Figure 2.5: Schematic of the integrated procedure for DNA extraction and emulsification for ddPCR analysis [46].

Morales et al. [42] reported the development of a continuous microfluidic device using the phenol extraction method for DNA purification (Figure 2.6). The work explored two different microfluidics flow regimes, namely parallel flow and droplet flow, for better mixing and higher purification yield [42]. BSA protein molecules were successfully extracted to the phenol phase, leaving the sample concentrated with the DNA molecules. However, the improper splitting of the phases at the end in these kinds of microfluidic platforms, the process might lead to the unwanted presence of the organic phase in the downstream sample analysis.

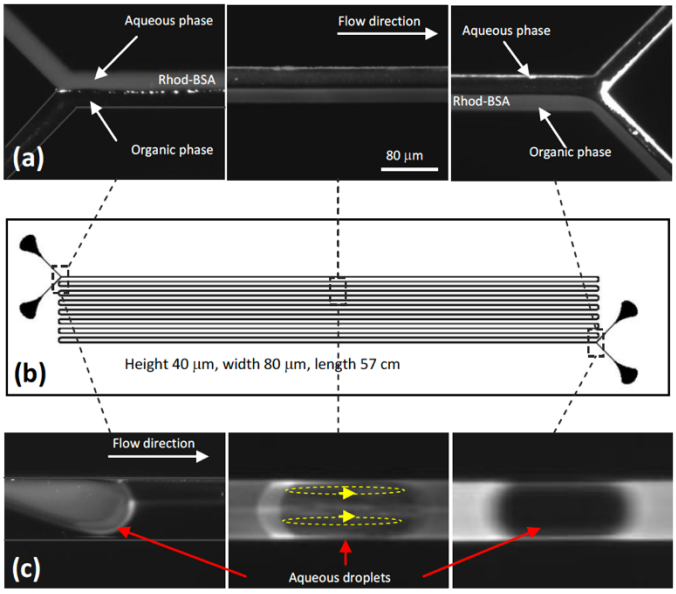

Figure 2.6: BSA extraction using two types of flow - parallel and droplet-based flow in a Serpentine microfluidic device: (a) images of BSA partition into organic phase using parallel flow, (b) the device geometry and dimensions, and (c) images of BSA partition using droplet-based flow [42].

In another microfluidic-based LPE of nucleic acid was reported by Zhang et al. [47], in which a chip with 900 microwell array was used. The volume of the wells corresponded to 125 $nl/well$ where the aqueous sample phase was stored, and the immiscible organic phase was continuously flowing over the microwells. This protocol was adopted to have a significant contact time between the two phases for higher extraction yield. The protein molecules and other impurities were isolated into the organic phase. This work also achieved on-chip PCR of the extracted nucleic acid. Figure 2.7 illustrates the entire process. After the organic phase is introduced in the device, the chip is inverted (Figure 2.7 b). The inverted position facilitates the extraction of the protein molecules. In this illustration, RNA is concentrated in the wells by extracting out the protein and DNA molecules. In the case where DNA needs to be concentrated,

the pH of the solution can be adjusted accordingly so that the protein and RNA molecules extract out to the organic phase. Although it is a confined process in a microfluidic chip, it is still somewhat manual at the steps where the chip is inverted. The device also could only achieve limited mixing of the phases with a small interfacial area between the phases.

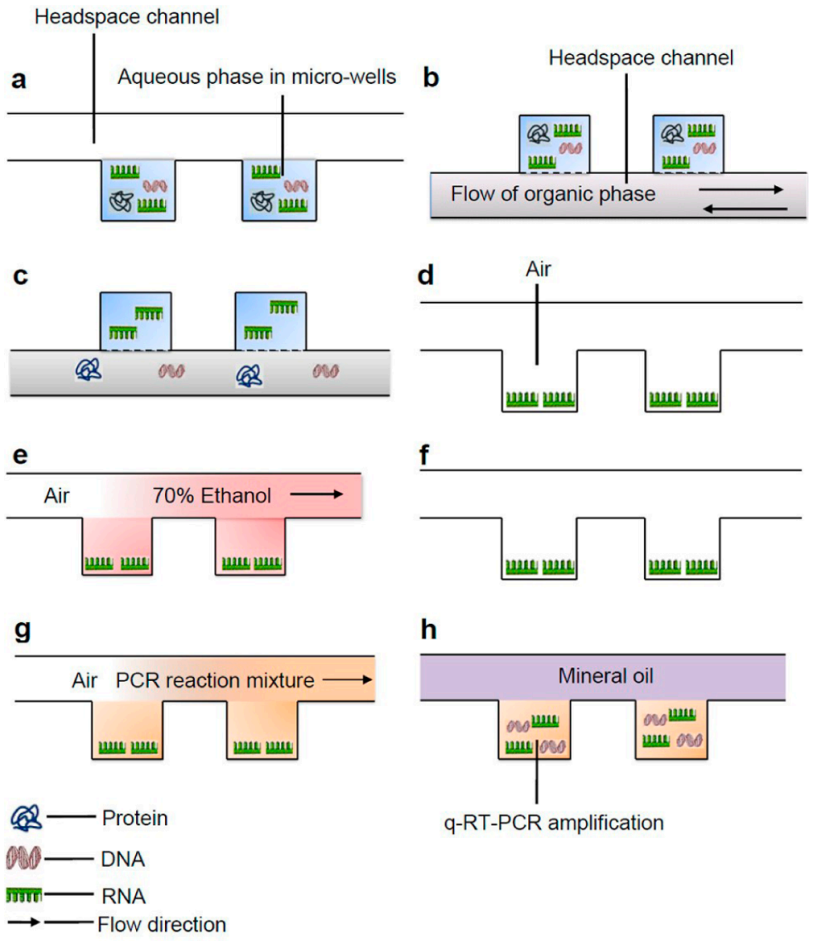

Figure 2.7: (a) Aqueous phase containing DNA, RNA, and protein mixture loaded into the microwells, (b) Organic phase introduced into the channel with continuously made to flow. The chip was inverted for nucleic acid purification in this step, (c) Protein and DNA were transferred from the aqueous phase into the organic phase, while RNA remained in the aqueous phase, (d) Organic phase was taken out from the channel and the fluid was evaporated while purified RNA remained in the microwell (e, f). The remaining organic phase was washed, and vacuum evaporated with 70% ethanol. (g) q-RTPCR reaction mixture was loaded into the microwells. (h) Mineral oil introduced and on-chip q-RTPCR was performed [47].

Microfluidics based liquid phase DNA extraction has not been much explored, and all the reported works are done by using microchannel based continuous microfluidics. Most of these devices that implemented liquid-liquid extraction mode suffer from the drawbacks of improper phase splitting at the end and limited extraction time. Besides, integrating any downstream process into one single chip is challenging.

2.2.2 EWOD DMF-based DNA extraction

EWOD involves the generation of discreet microdroplets that are controlled with the application of an external electric field. The microdroplets generated can be moved and interacted with other droplets generated from different reservoirs. This interaction forms the basis of the liquid-based extraction of solutes presented in this work. They can later be split, applying similar electric fields across various electrodes. The principles of EWOD droplet motion have been covered in greater detail in Chapter 3. EWOD has been utilized for various applications like chemical [48, 49] and enzymatic reactions [50], PCR [51], proteomics [52], etc. Since the application of an electric field across various electrodes drives the movement of the droplets generated, the application of pumps and valves along the system is rendered superfluous, which in turn makes the device appropriately miniaturized. Moreover, this elimination of such complicacies in the device makes it less likely for failure and more open to the integration of other electronic parts like heaters, sensors, etc. for assay integration. The following short review is only about the works that reported DNA extraction on EWOD, or protocols developed on EWOD that could be used for DNA extraction.

Kim et al. [26] reported their findings regarding using the EWOD platform for automated sample preparation of next-generation sequencing (NGS). One of the protocols highlighted in this

paper was the integration of the buffer exchange protocol on EWOD. Buffer exchange protocol is an integral step in NGS sample preparation. At the several stages of the process, a buffer exchange step is required. The protocol was integrated and automated on EWOD [26] with the help of magnetic beads. The device was successful in integrating all the steps of buffer exchange, as shown in Figure 2.8. The steps involved binding of DNA molecules to the beads, washing, and elution to the new buffer solution. The steps of buffer exchange demonstrated in this work are similar to the DNA extraction protocol with magnetic beads.

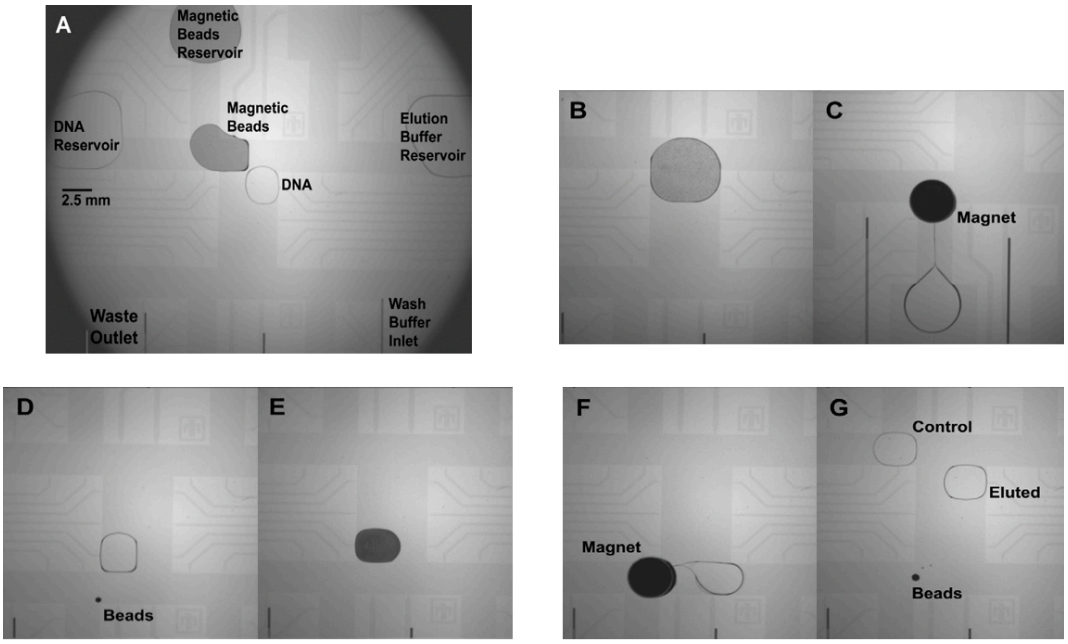

Figure 2.8: Video stills showing the buffer exchange assay performed on EWOD. A) Droplets of DNA and magnetic bead solution are generated from reservoirs. B) merged together and actively mixed. C) Cylindrical magnets placed on the device to hold the DNA-bound beads in place to remove supernatant. D-F) Elution buffer droplet introduced and mixed with the beads to unbind the DNA from the beads, which are then magnetically separated from the eluted sample [26].

Hung et al. [25] demonstrated the DNA extraction from raw blood on EWOD using magnetic beads. All the steps of DNA extraction, starting from the lysis of the sample to the elution of DNA in the final elution buffer were integrated on the platform (Figure 2.9). An external magnet was used in the steps when aggregation of the beads is required for changing buffer. The final elution droplet containing the extracted DNA was retrieved from the device and analyzed off-chip by measuring the fluorescence intensity upon the intercalation of SYBR green dye with the DNA molecules. As shown in Figure 2.9, the protocol involves several mixing steps (as is common with magnetic bead-based DNA extraction), and the success of the process depends mainly on efficient mixing at each step and binding of the DNA molecules with the magnetic beads. The repeatability of the process was not reported, and the yield of extraction achieved from the process on-chip was not clear.

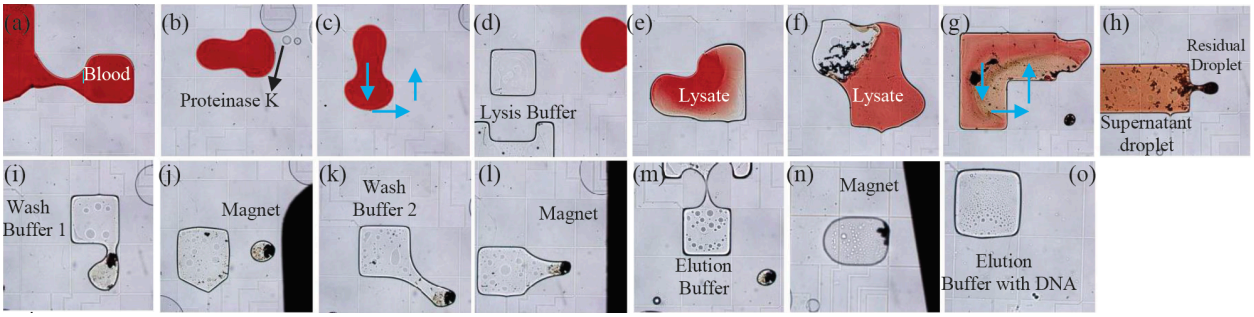

Figure 2.9: Magnetic beads DNA extraction on an EWOD device [25]. (a) A droplet of the whole blood generated. (b)-(c) Proteinase K degrading nucleases added into the blood droplet and mixed. (d)-(e) Lysis Buffer breaking cell membranes then added and mixed. (f)- (g) Binding buffer binding DNA onto the beads added and mixed. (h) Beads were attracted by a magnet. The supernatant droplet was split and expelled. (i)-(l) Washing Buffer1 and Washing Buffer 2 were sequentially added with a residual droplet in order to remove salts and Proteinase K. (m)-(n) Elution Buffer added to rinse the DNA from beads. After rinsing, beads without DNA were taken out from Elution Buffer by magnet (o) DNA obtained from blood [25].

The last work in this review does not involve working with DNA molecules; instead, RNA was extracted, and qPCR was performed on an EWOD device [53]. This work highlights the LOC capability of EWOD platforms for nucleic acid analysis. As shown in Figure 2.10, RNA was extracted from cell samples using a magnetic bead extraction method. The on-chip RNA extraction was followed by preparing the sample (adding qRT mix with the extracted RNA droplet) for qPCR.

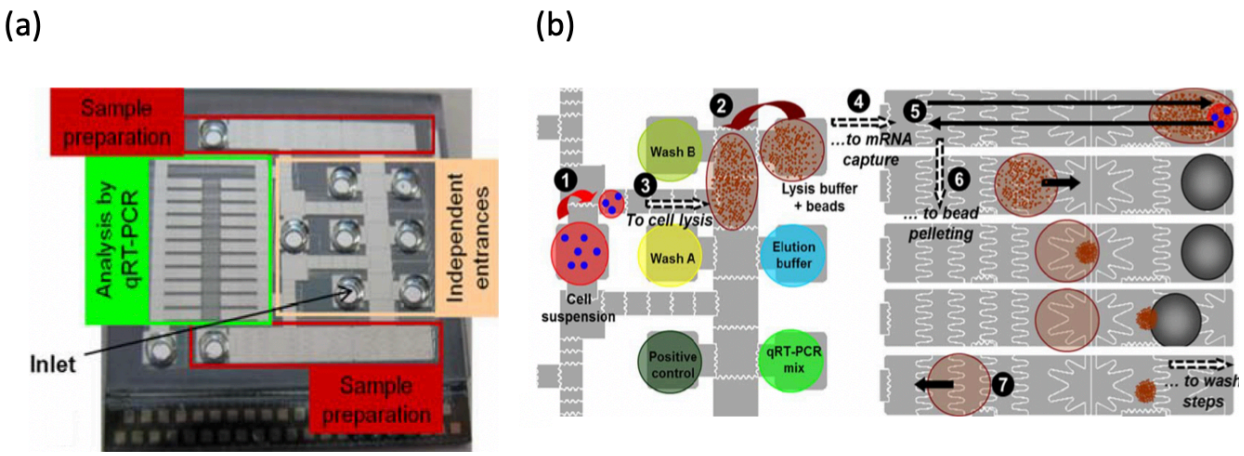

Figure 2.10: a) EWOD based qPCR device for RNA extraction from single cell and perform qPCR, b) the protocol of RNA extraction on EWOD using magnetic bead extraction method [53].

Chapter 3

Electrowetting-on-dielectric (EWOD) digital microfluidic devices

3.1 Introduction

High importance and interest in miniaturized systems have given rise to LOC devices [13]. The main advantages of these systems are portability, flexibility, and capability of automating complex biochemical protocols [54]. In microscale, surface tension forces dominate over gravitational and other body forces [55]. EWOD devices use this principle to actuate droplets. In EWOD devices, nano to pico liter-sized droplets can be manipulated by changing the wetting behavior of conductive liquid droplets placed on a conductive solid surface by applying a voltage on the surface. In order to prevent electrolysis, the solid surface is generally coated with a dielectric layer. The medium surrounding the liquid droplet, can either be air or another immiscible liquid depending upon the requirements of the system [56]. The principle of EWOD relies upon the possibility to change the contact angle of a polar microdroplet resting on a solid conductive surface, which is coated with a dielectric layer, as shown in Figure 3.1. The working principle of EWOD is described in the following section.

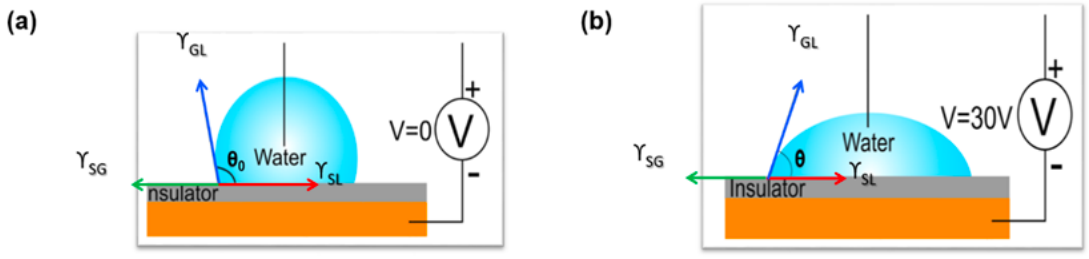

Figure 3.1: Electrowetting-on-dielectric principle. (a) A droplet resting on a solid surface with a contact angle θ_0 *at 0 voltage. (b) Contact angle changes to θ after applying voltage,* V. γ_{SL}, γ_{SG} *and* γ_{GL} *are the interfacial tensions between solid-liquid, solid-gas and gas-liquid respectively [57].*

3.2 Theory of EWOD

When voltage is applied, across the dielectric-liquid interface, charges accumulate, and an electric double layer is formed. Due to these accrued charges, the effective solid-liquid surface tension reduces. The change in the surface tension, in turn, reduces the contact angle to balance the interfacial energies at the three-phase contact line. The process is reversible, i.e., when the voltage is removed, the droplet regains the initial contact angle. In Figure 3.1, θ and θ_0 are the contact angles corresponding to the applied voltage V and 0, respectively. γ represents the three surface tension coefficients between solid-liquid, solid-gas, and gas-liquid.

When an electric potential is applied, the droplet wets or spreads on the surface, as shown in Figure 3.1. The relationship between the applied electrical potential and the resulting surface tension obtained by Lippmann's equation is shown in Equation 1. It describes the relationship between the applied electric potential (V) and the resulting surface tension (γ) The Lippmann's equation is derived through a thermodynamic analysis of the interface.

$$\gamma_{SL} = \gamma_{SL0} - \frac{1}{2} cV^2 \qquad (1)$$

where γ_{SL0} is the solid-liquid surface tension at the potential zero charge and c is the capacitance per unit area.

Young's equation provides a relationship for the contact angle of a liquid droplet on a solid surface, with surface tension, as seen below in Equation 2:

$$\gamma_{SL} = \gamma_{SG} - \gamma_{GL} cos\theta \qquad (2)$$

where θ_0 is the contact angle when the electric field across the interfacial layer is zero, γ_{SL} is the solid-liquid surface tension, γ_{SG} is the solid-gas surface tension, and γ_{GL} is the gas-liquid surface tension.

By combining Equations 1 and 2, the Lippmann-Young equation, as seen in Equation 3 below, has been described to explain the contact angle changes brought about by EWOD.

$$cos\theta = cos\theta_0 + \frac{1}{\gamma_{GL}}\frac{1}{2}cV^2 \qquad (3)$$

3.3 Droplet actuation with EWOD

Using the principle of electrowetting pico-liter to microliter sized droplets can be manipulated and driven on a series of electrodes. The two types of EWOD configurations are as follows:

- Sessile drop configuration
- Sandwiched drop configuration

Figure 3.1 demonstrates the sessile drop configuration of EWOD. In this dissertation, sandwiched drop configuration-based devices were used for all the studies. Figure 3.2 demonstrates how the droplet actuation happens in the sandwiched drop configuration EWOD device (Figure 3.2 shows the side view of the device). The device consists of two parallel plates – top plate and the bottom plate. The bottom plate contains an array of electrodes, with a dielectric layer coated to increase charge accumulation. The top plate consists of a single electrode that can be grounded. The electrodes in the bottom plate have switches that can be turned on or off and

thus controlling the droplet wetting behavior on the surface. Both the plates have a layer of hydrophobic coating at the top, which is in direct contact with the droplet.

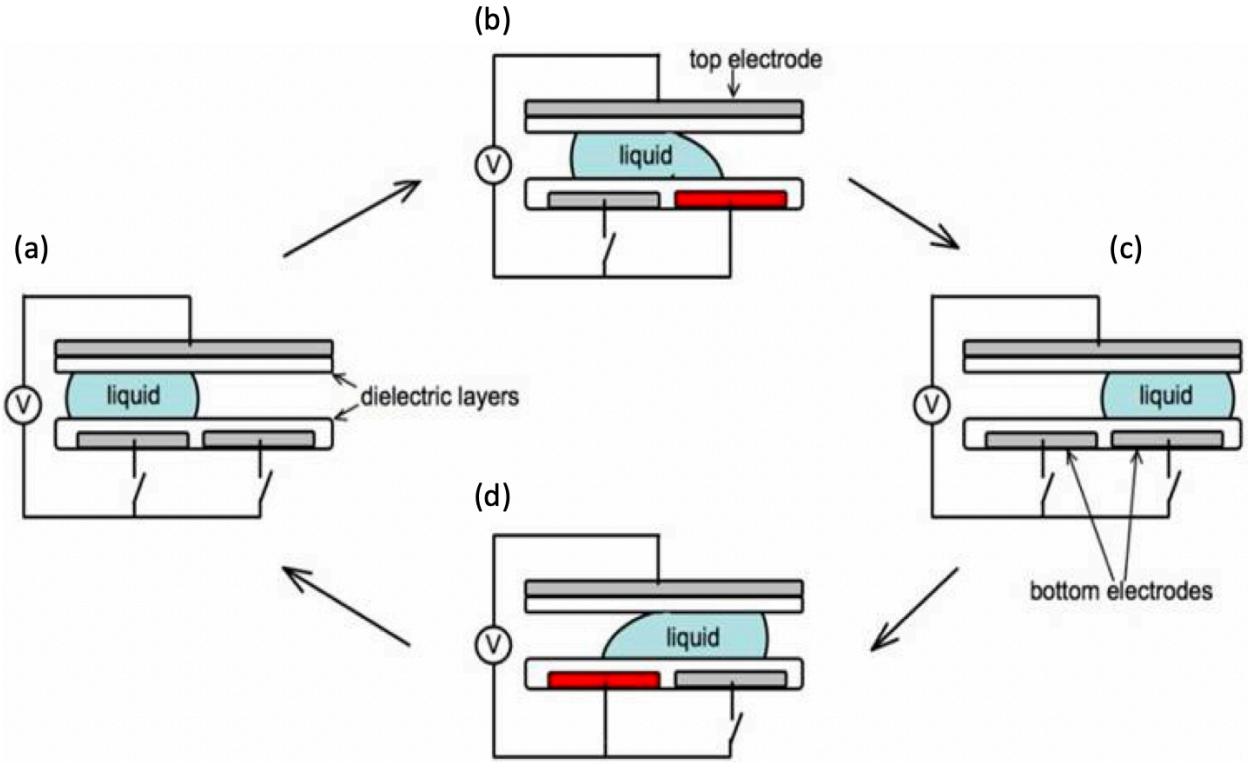

Figure 3.2: Actuation of a droplet at sandwiched drop configuration, using EWOD concept [58].

Initially, the droplet sits on one electrode, which is not activated (off), as shown in Figure 3.2 (a), and at the same time, a part of the droplet is touching the adjacent electrode. By applying a voltage to the next electrode (turning the next electrode on), the droplet can be moved to that electrode. The reason is, the part of the droplet touching the adjacent electrode start wetting the activated electrode surface due to electrowetting phenomena (Figure 3.2 b). The asymmetric curvatures at the two sides of the droplet, creating a pressure gradient inside the droplet. The pressure gradient then drives the droplet toward the activated electrode until the droplet completely

covers that electrode, as shown in Figure 3.2 (c). The droplet can be moved back to its initial location by deactivating the current electrode and turning on the previous electrode (Figure 3.2 d). This operation, when repeated, droplets can be moved around on the device along the desired path by merely changing the device design.

3.4 EWOD device design

For the sandwiched drop configuration type, the device design mainly involved the design of the bottom plate. The arrangement of electrodes should be designed by considering the desired droplet actuation patterns. Software tools, such as LayoutEditor, are used to design the electrode patterns. Unless for complicated devices that need separate elements, such as sensors, typically, the top electrode completely covers the top plate and does not need any designing.

The device design for the bottom plate used in this research, which is to be fabricated on a circular wafer, is shown in Figure 3.3. The bottom plate of EWOD devices generally consists of (i) electrodes, which are separated by a small gap ($\sim$10 μm), (ii) contact pads, which facilitate the electrical connection between electrodes and the voltage supply, and (iii) contact lines that connect electrodes with their corresponding electrode pads. The electrode pads are powered to provide a voltage across each electrode (turn electrode ON). The voltage supply is coming through external switches, each of which corresponds to one electrode on the bottom plate of the device. Signals to the switches, with the information whether the corresponding electrode should be on or off, are sent by the custom-built LabView program as per the user request. How the device is assembled and operated will be presented in section 3.6.

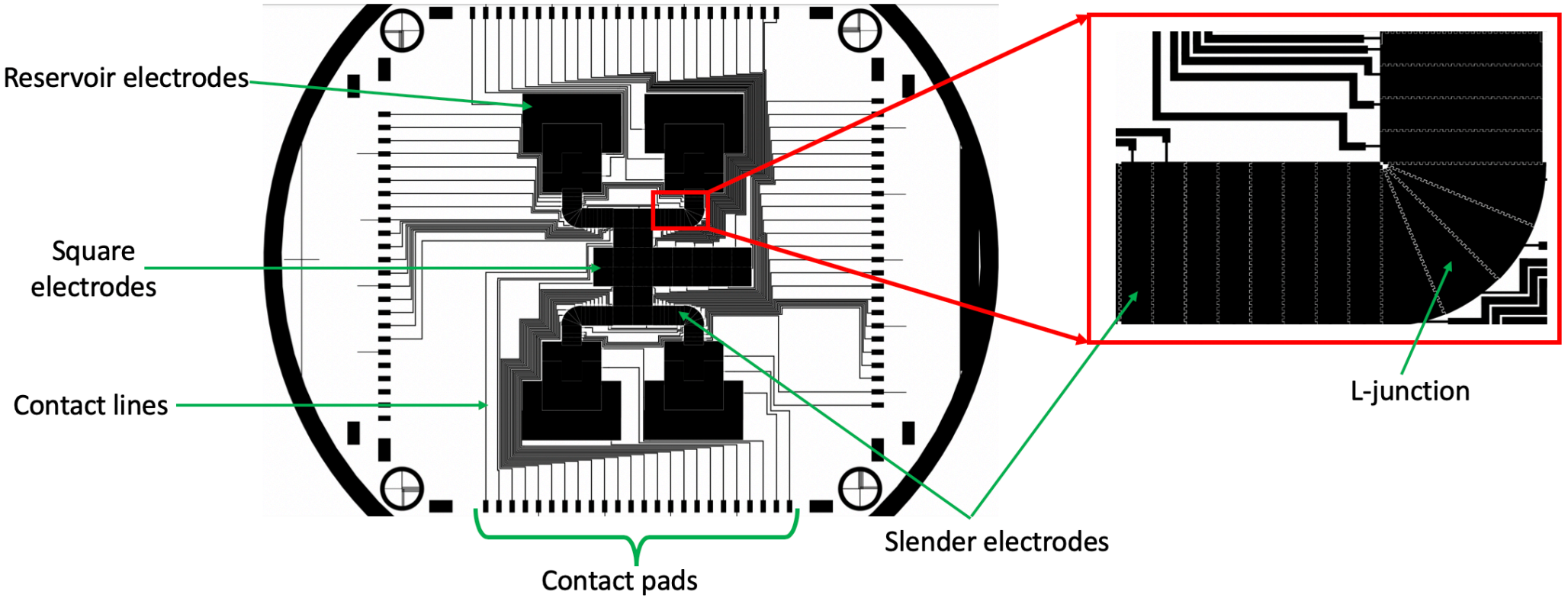
Reservoir electrodes
Square electrodes
Contact lines
Contact pads
Slender electrodes
L-junction

Figure 3.3: Pattern on the mask for the bottom plate.

The mask design, as shown in Figure 3.3, is used in the study to develop the LLE protocol in this work. It has a combination of – i) L-junction reservoirs for equal volume droplet generation, and ii) typical square electrodes for the rest of the LLE protocol (mixing and splitting phases). L-junction reservoirs were first introduced by Nikapitiya et al. [59], and the details of the droplet generation mechanism can be found in [59]. The L shape was created by thin strips of electrodes, which are called slender electrodes. L-junction reservoirs were selected because they are capable of generating an equal volume of droplets continuously and consistently [59]. A more elaborate scheme of droplet generation for the LLE application studied in this work will be explained later in section 4.2.3.

3.5 EWOD device fabrication

The top and bottom plates of our device are fabricated in a cleanroom that allows micro/nanofabrication facilities. Bottom plate fabrication is done using standard photolithography and wet etching processes, as shown in Figure 3.4. An Indium tin oxide (ITO, obtained from Delta technologies Ltd., Stillwater, MN) coated glass substrate, is used as the top and bottom plates.

The process starts with cleaning the wafer thoroughly with non-halogenated hydrocarbons: acetone, methanol, isopropanol, and then rinsing with deionized (DI) water. The wafer is then dehydrated at 150 ^{0}C for 5 minutes. For the bottom chip, at first, a chemical hexamethyldisilazane (HMDS) is coated on the wafer with a spin coater. The following recipe for spin coating is used: spin speed of 500 rpm with a ramping rate of 100 rpm/s for 5 s; ramping with 900 rpm/s to 4000 rpm for 30 s. The thin HMDS layer provides excellent adhesion between the ITO layer and

the photoresist (PR), which will be deposited next. After the coating of the HMDS layer, the wafer is baked at 150 ^{0}C for 3 minutes.

Next, a positive resist PR (Microchem S1813) is spin-coated on the wafer with the following recipe: spin speed of 500 rpm with a ramping rate of 100 rpm/s for 5 s; ramping with 900 rpm/s to 3000 rpm for 30 s. The spin coat results in a uniform 1.2 μm thick PR layer. The glass substrate with the coated PR layer is then baked at 120 ^{0}C for 2 minutes. Next, the mask and the wafer are aligned using a backside aligner (OAI 806MBA). Particular areas of the PR layer are exposed to UV light with a light dose of 140 mJ/cm^2 for 7.5 s, and the rest is protected with the mask. The UV exposure step is followed by baking the wafer at 115 ^{0}C for 1 minute 30 s.

After the UV exposure, the wafer is dipped in a developer solution (Microchem, MF-319) and rinsed with DI water and dehydrated. The PR layer takes up the shape of the mask, with the exposed areas being washed away. The resulted PR pattern is checked under the microscope for accuracy. The wafer is then dipped in a mixture of Hydrochloric (HCL) acid, Nitric (HNO3) acid and DI water (H2O) (wt. %- 20% HCl, 5% HNO3, 75% H2O or vol %- 8:1:15, HCl: HNO3: H2O) for 2.5 minutes at 55 ^{0}C to etch the ITO layer in the areas where the PR does not cover it. At the end of the etching process, the PR is removed by dipping the wafer in a PR stripper solution (PR Remover 1165, Microchem). After removing the PR layer, the wafer is dehydrated at 150 ^{0}C for 5 minutes.

Next to provide an insulation layer, a dielectric material (SU-8-5, Microchem) is spin-coated on the wafer with the following recipe; the spin speed of 500 rpm with a ramping rate of 100 rpm/s for 5 s; spin speed 2000 rpm with a ramping rate of 900 rpm/s for 30 s. The spin coat results in a 5 μm thick uniform dielectric layer. The wafer is next baked to harden the layer at 65 ^{0}C for 1 minute, followed by a second baking step at 95 ^{0}C for 3 minutes. For further

hardening the dielectric layer, it is then exposed to UV light with a light dose of 140 mJ/cm^2 for 9 s. The wafer is then baked at three temperatures: 65 ^{0}C for 1 minute, 95 ^{0}C for 1 minute, and 150 ^{0}C for 5 minutes. A hydrophobic layer is next created by spin coating a 300 nm thick uniform Teflon layer with the following recipe: spin speed of 1000 rpm with a ramping rate of 300 rpm/s for 30 s. For the top chip, an ITO coated wafer is first cleaned thoroughly with non-halogenated hydrocarbons: acetone, methanol, isopropanol, and then rinsed with DI water. It is then dehydrated at 150 ^{0}C for 5 minutes. A 300 nm thick Teflon layer is deposited using the same recipe described before. Figure 3.4 shows the complete process of the bottom plate fabrication (Figure 3.4 a) and assembled bottom and top plates (Figure 3.4 c).

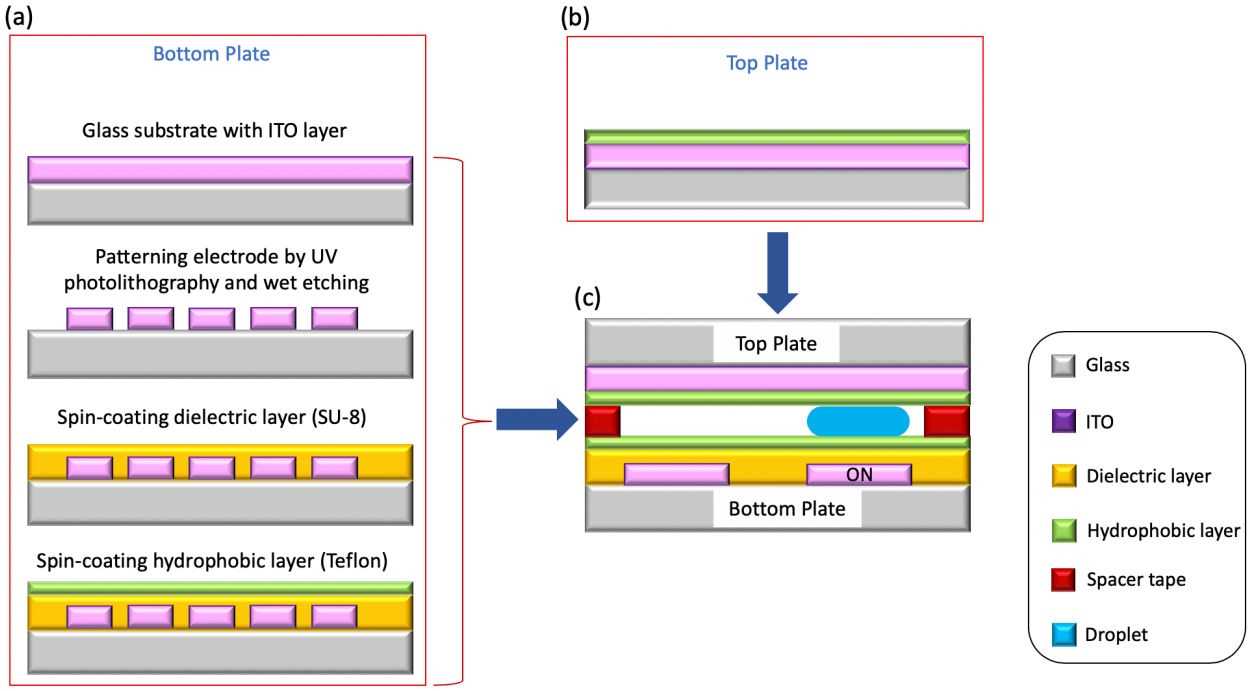

Figure 3.4: a) Process steps for fabricating bottom plate of EWOD device, b) Top plate, c) Side view of the assembled device with the liquid droplet sandwiched between the top and bottom plates.

3.6 Device assembly

The complete device assembly consists of a printed circuit board (PCB), a plexiglas holder, the EWOD bottom and top plates, four z-directional conducting strips, as shown in Figure 3.5. The EWOD bottom plate is attached to the plexiglas holder using tape. Small strips of Kapton tape (DuPont™ Kapton® HN polyimide film) are attached to the bottom chip to create the gap with the top chip. To accommodate the z-directional conducting strips, the plexiglas holder has via holes to hold them and make the connection between the switches on the PCB and the contact pads located on the bottom chip. Before doing the experiments, the reservoir is filled with the desired liquid, and the top plate is placed on the Kapton tape strips, therefore, sandwiching the liquid between the top and bottom plates. Finally, the assembly is connected to the switching circuit via data cables.

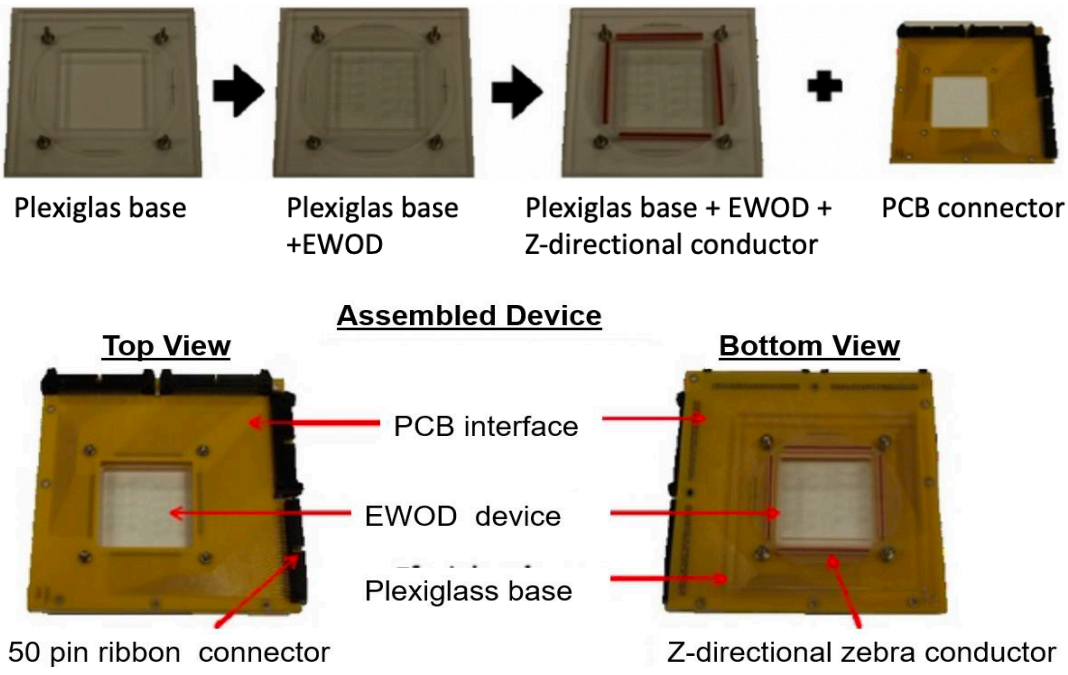

Figure 3.5: Assembly of EWOD device into the holder.

Device Control: Firstly, the assembled device is connected to the switchboard. Through a customized LABVIEW program, instructions for switching the electrodes are sent to the switches. Voltage 5V or 0V is supplied to each switch when the signal for switching on or off is sent from the computer through the Input /Output device and I/O connector accordingly. Electrodes corresponding to a particular switch will be activated or deactivated according to on or off status of switches. A power source and voltage amplifier are used to amplify the supplied potential, as shown in Figure 3.6. A multimeter is used to monitor the applied voltage continuously. The actual experimental setup is shown in Figure 3.7.

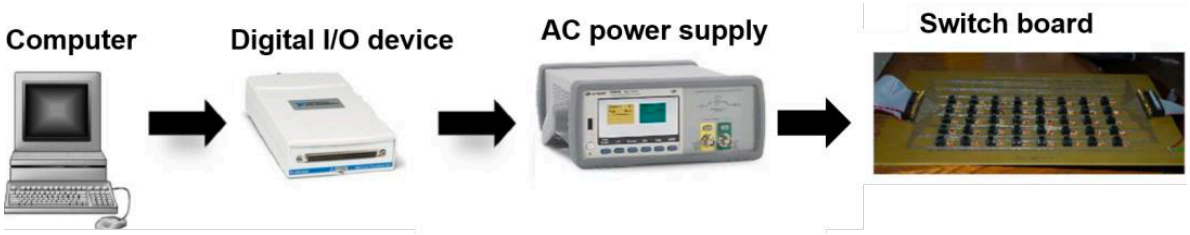

Figure 3.6: Device control flow.

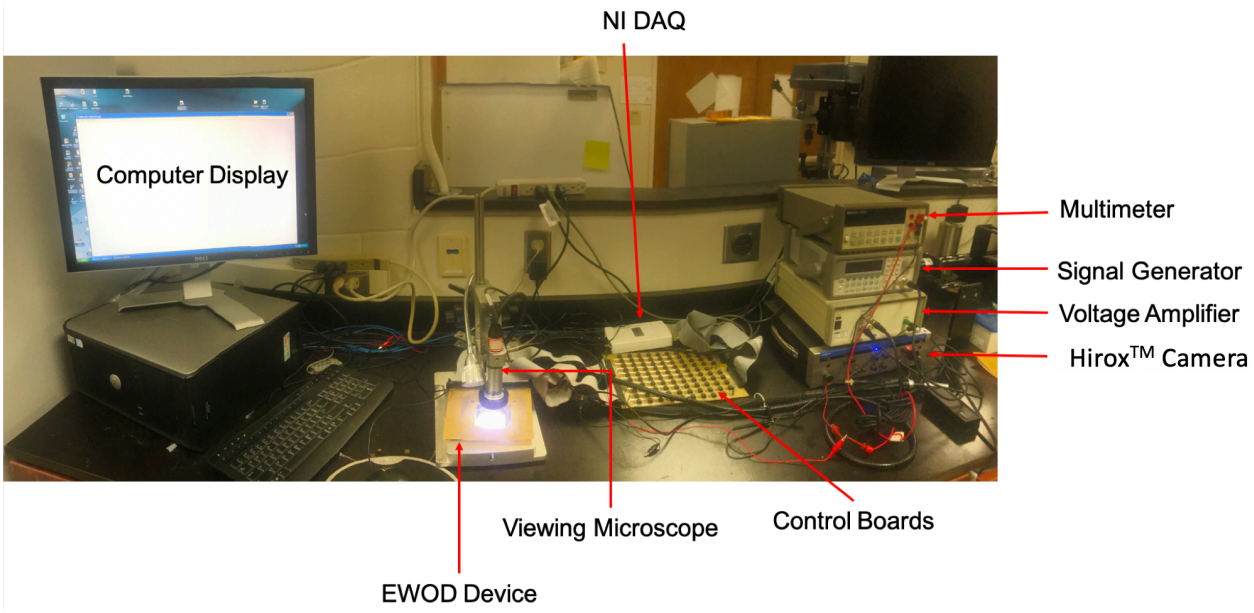

Figure 3.7: Experiment setup.

Chapter 4

Liquid-liquid Microextraction enabled by EWOD Digital Microfluidics to separate binary solution mixture

This chapter demonstrates the first drop-to-drop (DTD) extraction of an analyte from a sample of binary solution mixture using the principle of LLE enabled by EWOD DMF chips. A very well-known process of sample extraction and purification, LLE is based on the relative solubility of the compounds in the two-phase system formed by two immiscible liquids. In this study, the EWOD DMF platform was used to generate two immiscible liquid droplets, one of which is the ionic liquid (IL), and the other is an aqueous binary sample solution phase. The droplets were moved along electrodes, merged to form a two-phase system, mixed thoroughly to facilitate the extraction of the target analyte into the IL phase and finally were split after successful extraction. This process of LLE on EWOD resulted in the separation of each compound in the binary solution and finally concentrated on each liquid droplet phase. The effect of different mixing schemes of the two liquid phases on the extraction yield was studied. A spectrophotometry system was miniaturized and integrated into the platform for real-time concentration measurement. Finally, multistage liquid-liquid extraction (MLLE) was studied to obtain a higher recovery of target analytes from the process. After two cycles of serial LLE, molecules of green organic dye were successfully removed from the binary solution droplet and left the droplet concentrated with yellow dye molecules. This chapter reports the foundation of the device and the LLE process integration towards our goal of DNA extraction from a sample, which will be demonstrated in the subsequent chapters.

4.1 Introduction

Chemical and biochemical analysis play vital roles in drug discovery, medical diagnoses, and food and drug regulation [60-62]. These analysis procedures involve several processing steps, ranging from simple to laboriously complicated steps. Before the chemical analysis, it requires various sample-pretreatment steps, including purification [60]. Purification is essential in any chemical analysis for the pre-concentration of the target molecules and removal of the unwanted analytes, followed by concentration measurement. The sample purity is a significant player in determining the accuracy of the downstream analysis results. Thus, it becomes essential at the start of any chemical analysis to have a clean sample.

LLE, also called solvent extraction, is one of the most common extractions and purification techniques [63]. It is a passive extraction process in which the transfer of components takes place from one liquid phase into another due to their unbalanced chemical potentials [64]. In LLE based extraction, the solutes exchange across the interface formed by the two liquid phases, until the system reaches an equilibrium state. This method can be used to selectively extract the compound of interest from a mixture of various components. Hence, it is considered as a fundamental sample pre-processing technique in chemical and bioanalytical fields. The success of the LLE method depends on the difference in solubility of the compound to be extracted between the two solvents. A higher separation yield can be achieved by having an MLLE process.

As discussed so far, the LLE process is very efficient in separating target molecules. However, traditional LLE is time-consuming, labor-intensive, and requires large quantities of samples. With the advent of microfluidics, LOC devices are gaining more popularity. Miniaturization and integration of these sample purification techniques provide an excellent opportunity for the advancement of the next generation LOC devices [65]. Moreover, the

simplicity of the LLE process makes it a perfect candidate for miniaturization into these platforms. Early liquid-liquid microextraction (LLME) has been reported, which involved the use of syringe needles [64]. Although the sample volume was drastically reduced, it was still labor-intensive, and the protocol was difficult to automate. Wijethunga et al. reported the first demonstration of LLE in the EWOD DMF platform, which overcame most of these challenges [66].

EWOD DMF devices enable manipulation of discrete droplets in the micro-scale dimensions on an array of electrodes [67]. Since the EWOD principle can be used effectively to actuate a droplet from one position to another, electrowetting has been used to develop a variety of microfluidic LOC devices [68-73]. EWOD based LOC devices are versatile compared to other traditional devices due to several advantages such as low power consumption, no pumps or mechanically moving parts, independent control of droplets, and flexible and programmable droplet paths.

Wijethunga et al. demonstrated the diffusion of a single type of organic molecule from the aqueous phase to the ionic liquid phase [66] on an EWOD based platform. This chapter reports the development of the EWOD device for selective extraction and separation of a binary mixture solution based on the principle of LLE. The separation is possible because of the significant difference in the partition coefficients of the analytes in the liquid-liquid system. As proof of concept, here we performed two cycles of LLE to demonstrate the capability of EWOD DMF to perform an MLLE process. The successful separation of the compounds in the binary solution was hence achieved. The device was also integrated with an absorbance-based concentration measurement system to quantify the yield from the process on EWOD.

4.2 ***Experimental***

4.2.1 Working fluids

To demonstrate the separation of a binary solution on EWOD DMF by LLE, we selected two organic dyes, acid green 25 ($C_{28}H_{20}N_2Na_2O_8S_2$) and reactive yellow 17 ($C_{20}H_{20}K_2N_4O_{12}S_3$) (provided by Organic Dyestuffs Corporation), as the solutes. The sample phase was prepared by mixing equal amounts of these two dyes. The final concentration of each analyte in the sample mixture formed was 1250 $\mu g/ml$ for all the EWOD LLE experiments.

Water-immiscible IL (1-butyl-3-methylimidazolium hexafluorophosphate (BMIM-PF_6) was used as the other phase, which we call the extractant phase. The IL was purchased from Sigma Aldrich. ILs have been previously reported in several studies as an extractant for different molecules, including DNA [74]. Some of the other properties of IL, such as negligible evaporation, high thermal stabilities, compatible medium for biomolecules, and tunable chemical and physical properties make it a suitable medium for downstream processing of the extracted material [75].

The other properties of BMIM-PF_6 is a viscous, colorless, hydrophobic, and non-water-soluble ionic liquid with a melting point of -8 °C. It is known to be the most widely studied IL along with 1-butyl-3-methylimidazolium tetrafluoroborate. BMIM-PF_6 is also known to decompose very slowly in the presence of water [76]. The chemical structure is shown in Figure 4.1. It consists of BMIM cation and PF_6 anion.

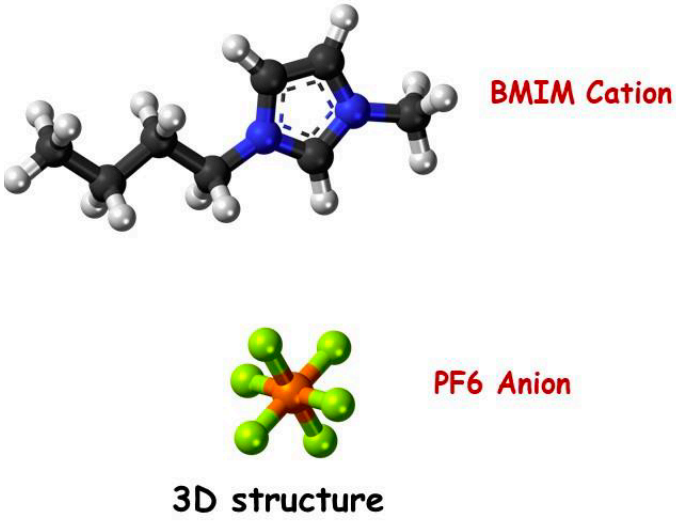

Figure 4.1: Chemical formula of ionic liquid BMIM-PF_6 [76].

4.2.2 Device design, fabrication and operating conditions

As presented in Chapter 3, the same device design and fabrication, as well as experimental setup, were used. A standard parallel plate EWOD DMF device was utilized. Briefly, each device was assembled using an ITO coated glass substrate on top. After dispensing the sample and extractant phase into the reservoirs, the top plate was assembled. A spacer of 100 μm was maintained to separate the top and bottom plates from each other. A 100 to 110V at 1kHz was used to facilitate the droplet movement. A Hirox^{TM} camera was used for visualization and documentation of the procedure.

For the LLE process on an EWOD DMF electrode array, the droplets were generated, mixed, and split during the process. The integrated real-time concentration measurement system consisted of two LED light sources and a photodiode for the measurement of light intensity passing through the sample. The light intensity was converted to voltage measurements, the values of which were used to obtain the sample concentration after the LLE process. The on-chip

concentration method quantified the yield of the LLE process. The detailed description of the steps of on-chip concentration measurement is described in section 4.2.5.

4.2.3 Drop-to-drop LLE process on EWOD

Droplet generation: The sample and the IL phase droplets (extractant) were generated from two different 'L-junction' reservoirs, which can generate equal volumes of droplets fabricated in the LLE device (details provided in section 3.4). Figure 4.2 shows the entire process of droplets generations for the LLE study.

The fluids are initially introduced on the electrode marked as 1, as shown in Figure 4.2 a. In the first step of droplet generation, the entire liquid volume is pulled to fill the L-junction electrodes, as shown in Figure 4.2 b, by turning them on and turning off electrode 1. Next, the electrodes 2, 3, and junction electrodes are turned off, and electrode 1 is switched back on. Consequently, the electrowetting forces create a neck at the L-junction between the activated electrodes, and the liquid instability at the neck finally forms a droplet (Figure 4.2 c). After generation, the droplets were moved to the mixing region where the LLE takes place.

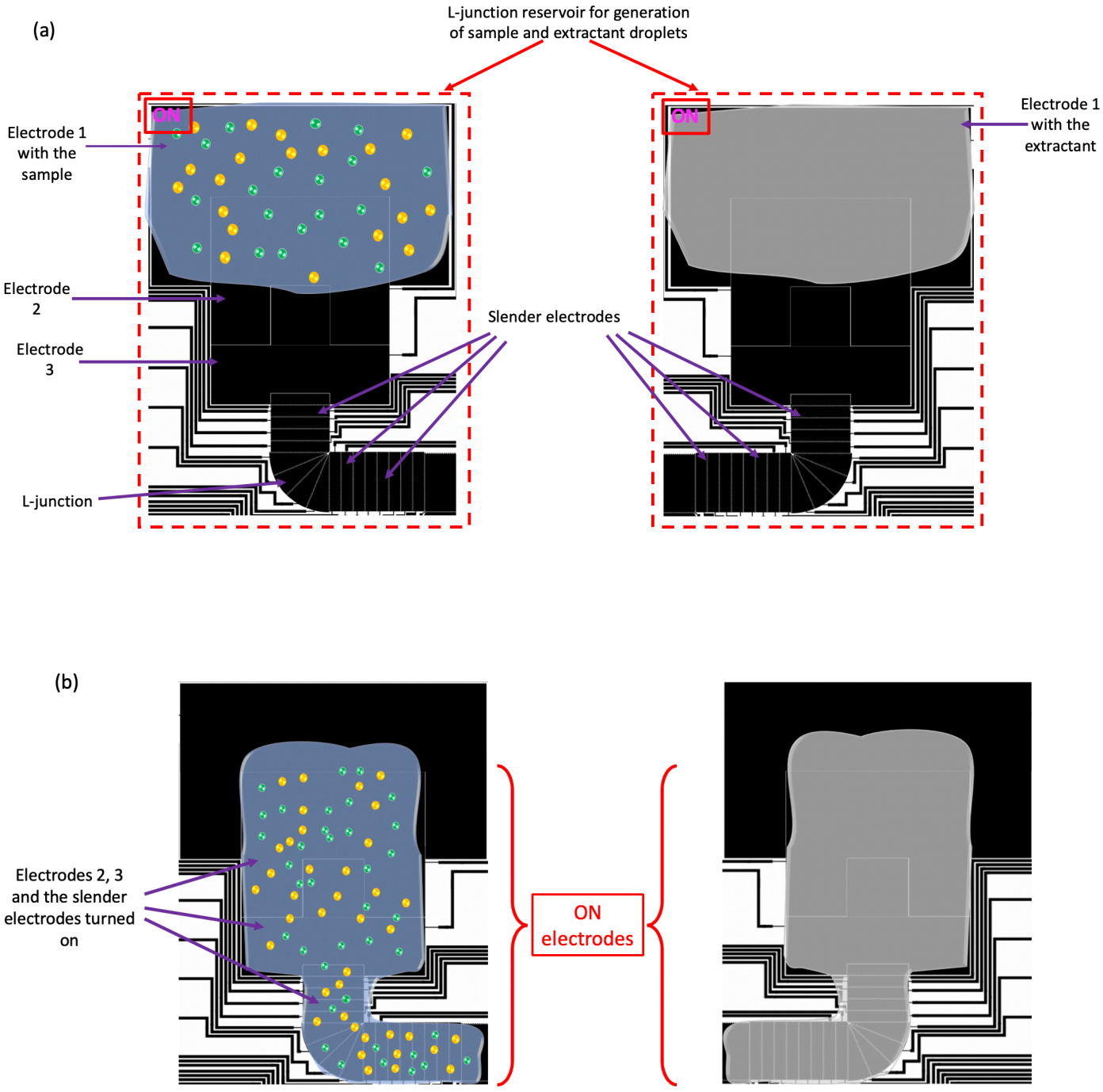
(a)
L-junction reservoir for generation of sample and extractant droplets
ON
ON
Electrode 1 with the sample
Electrode 1 with the extractant
Electrode 2
Electrode 3
Slender electrodes
L-junction
(b)
Electrodes 2, 3 and the slender electrodes turned on
ON electrodes

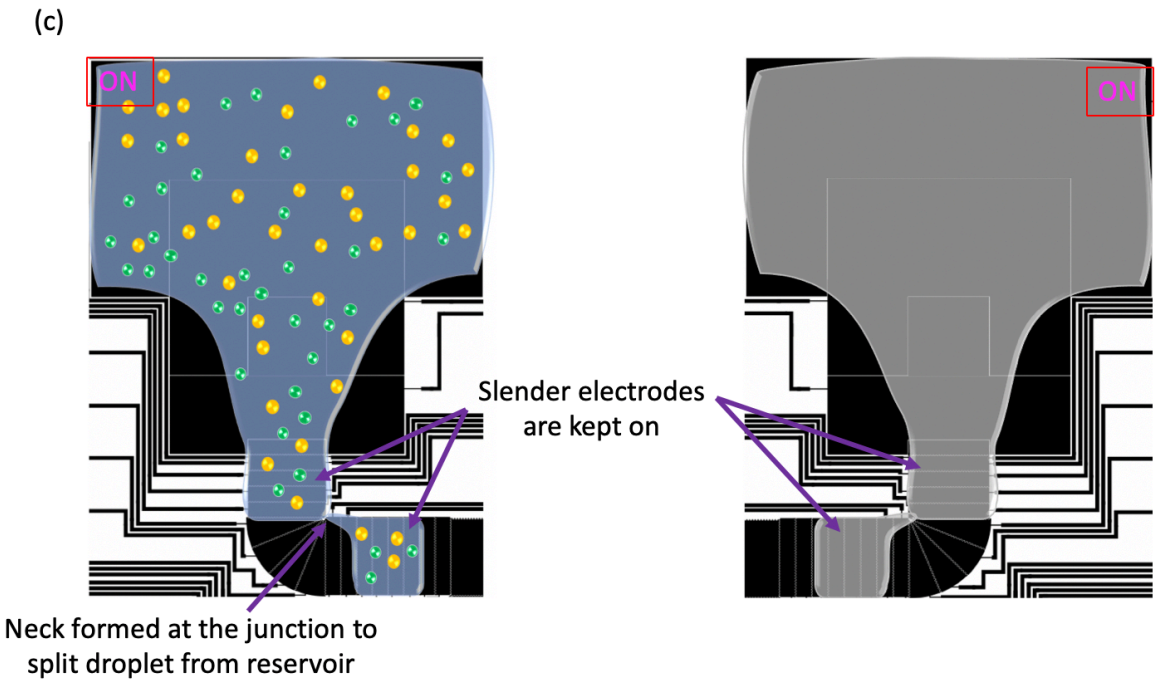

Figure 4.2: Droplet generation scheme from the reservoir: a) The fluids are introduced to the reservoir and electrode 1 turned on; b) The electrodes 2, 3 and the slender electrodes turned on to fill them with the fluid while electrode 1 turned off and c) Electrodes 2 and 3 turned off while turning on electrode 1 which forms a neck at the L-junction and droplet is generated from the reservoir.

Droplets merging, mixing, and splitting: Figure 4.3 illustrates the entire procedure post droplet generation of the LLE process on the EWOD chip. Dispensed droplets are further actuated along the electrode paths simply by activating the consecutive square electrodes one after the other. Merging sample and extractant droplets is done by bringing the two droplets onto to adjacent electrodes (Figure 4.3 a). Then the merged sample and extractant droplets are mixed by systematically activating electrodes (Figure 4.3 b). Separate experiments were conducted to study the effects of different mixing schemes on the LLE yield described in section 4.3.2. Once the extraction is completed, phase splitting was also done by driving the two phases onto two separate

opposite electrodes, as shown in Figure 4.2 c-d. After the splitting of the phases, one cycle of the LLE process is completed.

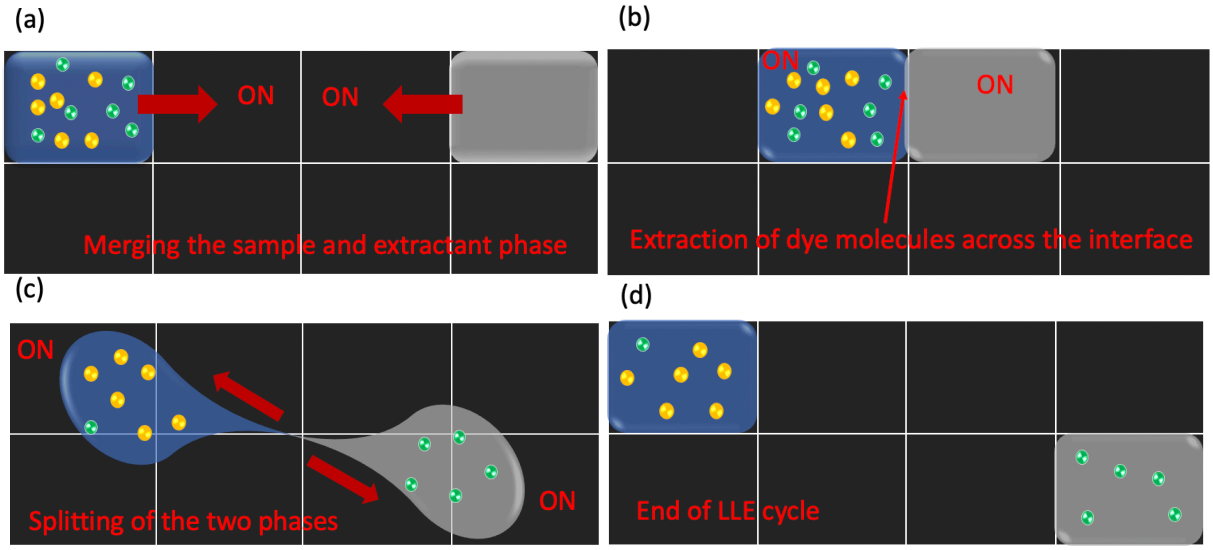

Figure 4.3: Concept of DTD LLE. The arrows show the direction of droplets. (a) driving the sample (blue) droplet containing the solutes (green and yellow dye molecules) and the IL droplet to merge, (b) the merged droplets are mixed with fastening the extraction, solutes diffuse from sample to the extractant, (c) splitting the two phases after the extraction is completed, and (d) sample (without green solute) and extractant (with green solute) after the successful splitting of the phases.

The extraction can be observed in real-time through the digital microscope. Spectrophotometry was integrated into the system to measure real-time concentration change at the end of the LLE process. After obtaining linear calibration curves on-chip for each of the analytes, this method of quantification was adopted. Details of the method are described in section 4.2.5.

4.2.4 Off-chip LLE and dye characterization

Off-chip LLE experiments were conducted in Eppendorf tubes for each of the dyes separately. Their extraction yield for the liquid-liquid system was studied. Separate green and yellow dye samples with a concentration of 1 mg/ml were used. An equal volume of the sample and IL were introduced in the tube and vortexed for a few minutes for proper mixing. At the end of the LLE, phases were split, and samples were transferred to a plate-based spectrophotometer for concentration measurement.

Wavelengths at which absorbance is maximum for each analyte were obtained by sweeping over a range in a plate-based spectrophotometer. The wavelength of maximum absorptivity was found to be 650 nm for green dye and that of 430 nm for the yellow dye. These wavelengths were used for all the on-chip and off-chip absorbance measurements.

4.2.5 On-chip concentration measurement

On-chip concentration measurement was done by the absorbance method to quantify the change in the concentration of individual analytes in the sample. Concentration measurement based on the same principle on EWOD devices was first demonstrated in [77], where the concentration measurement of various samples was studied. The setup for the concentration measurement is illustrated in Figure 4.4. Two LEDs with 650 nm and 430 nm dominant wavelengths were used as the light source. The LEDs were housed in 3D printed boxes with opening smaller than the droplet size so that not much of the light was dispersed in other directions. Photodiode TSL257 was used to measure the voltage, corresponding to the sample concentration of each dye in the sample.

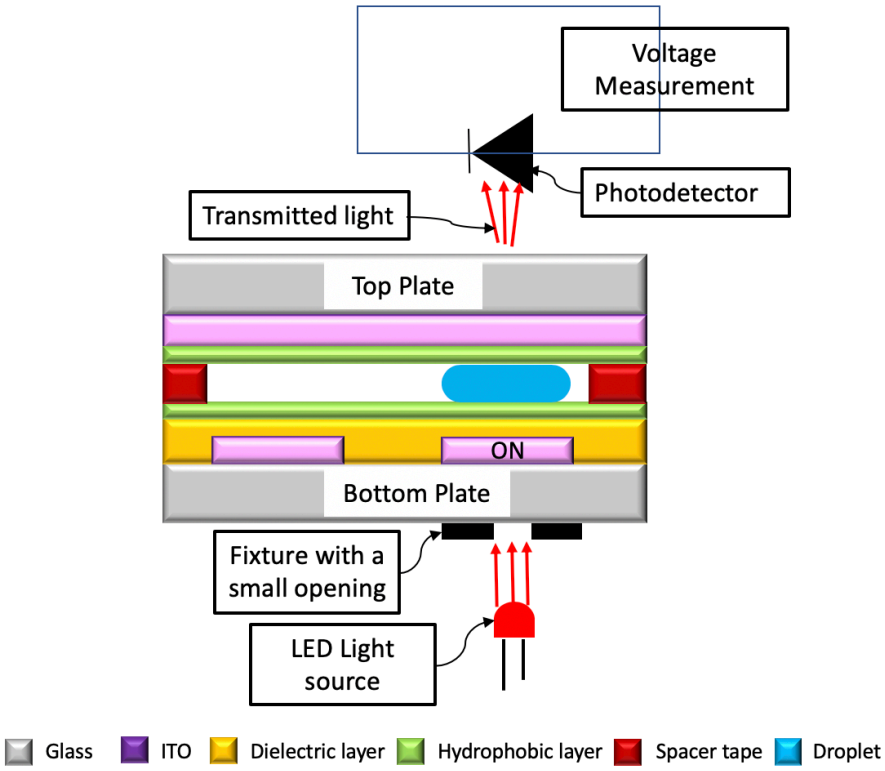

Figure 4.4: Side view of the on-chip concentration measurement system.

The Voltage (V) generated by the photodiode is directly proportional to the intensity of the light incident on the photodiode passing through the sample. The absorbance by the analyte can be calculated with voltage measured by the following equation

$$A = \ln\left(\frac{V_0}{V}\right) \qquad (4.1)$$

where, V_0 refers to voltage generated when the sample concentration is zero and V refers to the voltage generated at a certain concentration.

Absorbance is also given by the Beer Lambert's law,

$$A = \varepsilon \cdot l \cdot C \qquad (4.2)$$

where, ε is the extinction coefficient, l is the optical path length and C is the concentration of an analyte in the solution.

The system was first calibrated for the two dyes separately to get a linear plot between absorbance and concentration. Stock solutions of separate green and yellow dye were made and serially diluted to obtain several standards. The starting concentration was 1230 $\mu g/ml$ and was serially diluted to $156.25\,\mu g/ml$. Different standards of dye solutions were introduced into the EWOD device, and voltage was recorded from the light passing through the droplet and incident on the detector. For each concentration, the samples were exposed to the two LED light sources. Equation 4.1 was used to find the absorbance values for different concentrations of the green, and the yellow dye solutions and calibration curves were plotted.

When working with a mixture of two components in a sample, both the components have a contribution to the absorbance value, and thus the absorbance is given by a new modified form of equation 4.2:

$$A = \varepsilon \cdot l \cdot C_g + \varepsilon \cdot l \cdot C_y \qquad (4.3)$$

where, C_g corresponds to concentration of the green dye and C_y corresponds to the concentration of the yellow dye.

Thus, for two wavelengths of light the following system of equations can be solved to find the concentration of each analyte.

$$\begin{aligned} A_1 &= \varepsilon_g^1 \cdot l \cdot C_g + \varepsilon_y^1 \cdot l \cdot C_y \quad (\text{at } \lambda_1 = 430\,\text{nm}) \\ A_2 &= \varepsilon_g^2 \cdot l \cdot C_g + \varepsilon_y^2 \cdot l \cdot C_y \quad (\text{at } \lambda_2 = 650\,\text{nm}) \end{aligned} \qquad (4.4)$$

where ε_A^X is the coefficient of extinction for a solute A at wavelength X, l is the length of the path the light is travelling, and λ_1 and λ_2 are two different wavelengths, selected to have the greatest differences in absorbance between the two dyes.

The values of $\varepsilon_g^1 \cdot l$, $\varepsilon_g^2 \cdot l$, $\varepsilon_y^1 \cdot l$ and $\varepsilon_y^2 \cdot l$ obtained from the absorbance vs concentration calibration curve for different concentration of each analyte over the two light sources. The slopes of the respective curves give us the $\varepsilon_A^X.l$ values. The absorbance values at each wavelength due to the binary solution can be calculated by using Equation (4.1), with the measured voltage reading. With these known values, the system of linear equations (4.4) can be solved to find the individual dye concentration in the mixture.

4.3 Results and discussions

4.3.1 Off-chip LLE and partition coefficient of analytes

Off-chip LLE experiments were conducted as described in section 4.2.4 and illustrated in Figure 4.5 a-b. It can be observed visually (Figures 4.5 a-b) from the off-chip LLE experiments that the green dye has a higher extraction yield compared to yellow dye.

Standardized curves for both dye samples were obtained separately at their respective wavelengths of maximum absorbance for concentration measurement of off-chip LLE experiments. Standards were prepared by serial dilution of the original stock solution of 1 mg/ml and were loaded into the spectrophotometer to get the absorbance measurement. The standardized curves are plotted in Figure 4.5 c for the green and yellow dye solutions.

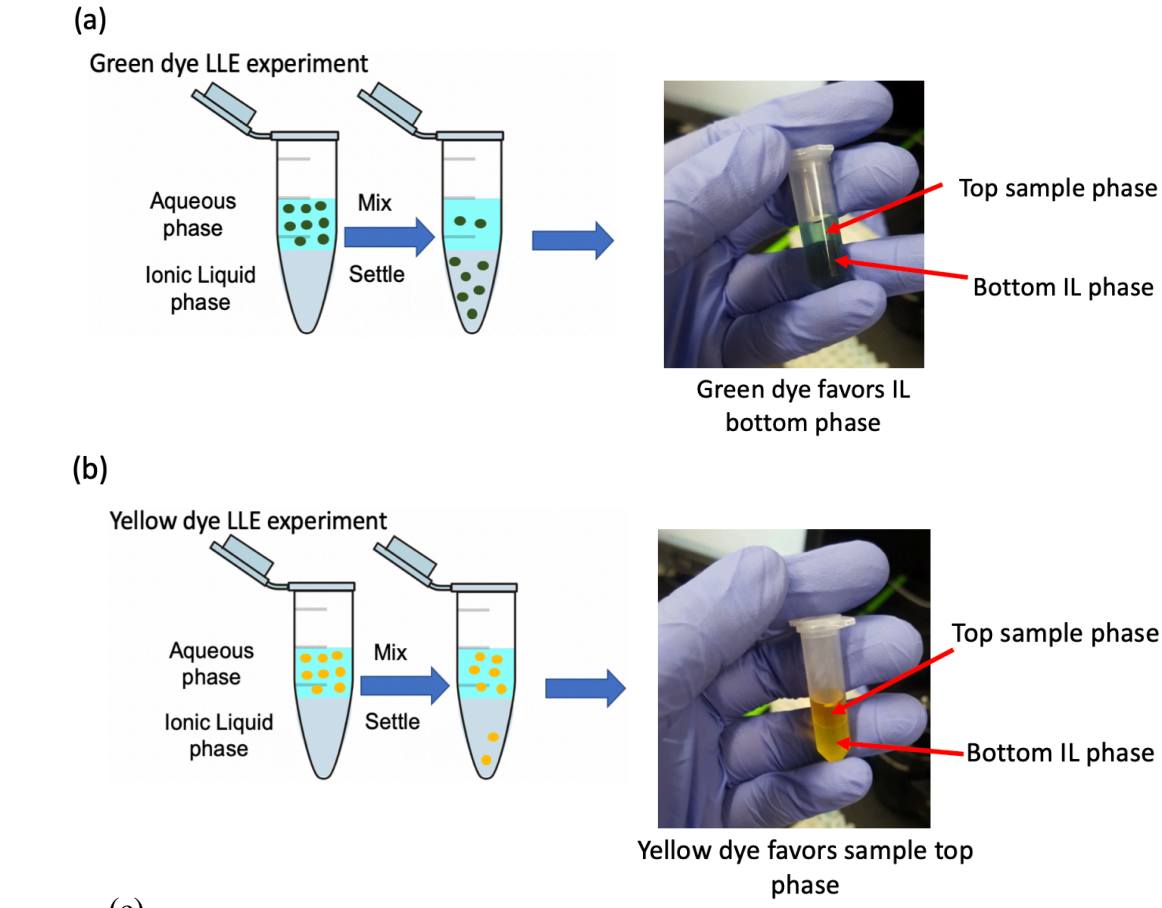

(c)

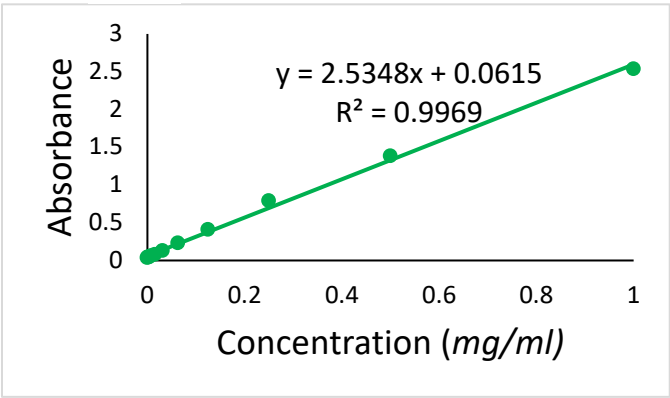

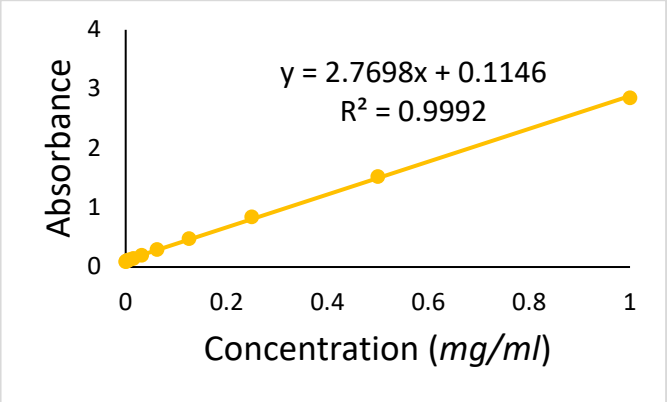

Figure 4.5: a) Off-chip green dye LLE experiment where most of the molecules favor the bottom IL phase. b) Off-chip yellow dye LLE experiment where most of the molecules favor the top sample phase. c) Standardized plots obtained for each of the dye samples separately using a plate-based spectrophotometer - absorbance values measured at the wavelength of maximum absorptivity for each dye.

Partition Coefficient: For a given compound, its solubility between two solvents is given by the quantitative measure called the partition coefficient, which can be calculated given by the equation (4.5).

$$k = \frac{Concentration\ of\ dye\ in\ ionic\ liquid}{Concentration\ of\ dye\ in\ aqueous\ phase} \qquad (4.5)$$

The partition coefficient values of the green and the yellow dye were calculated from the off-chip experiment for the given two-phase system. The k for green dye was found to be 34.3, whereas for the yellow dye was found to be 0.22. Thus, the green dye has much high k value compared to the yellow dye, which indicates that the green dye molecules can be selectively extracted from a mixture of green and yellow dyes. This selective extraction of one analyte may lead to the separation of the compounds in the mixture.

4.3.2 Mixing optimization for higher LLE yield

Different mixing schemes were studied, i.e., different ways of moving the two phases while they are merged to have the maximum extraction from the EWOD LLE process. The goal is to have high extraction in a short time. The higher the rate of transfer of molecules across the interface, the higher the LLE yield can be obtained in a short duration. In this study, the sample consisted of one analyte, and its transfer to the extractant phase was studied under different mixing schemes. Wijethunga et al. reported the stretching of the interface of the two phases to enhance the extraction. The present study was done as an extension to previous work [66], to optimize and fix the mixing protocol with the highest yield possible on EWOD for all the following experiments.

The droplets generation and splitting were done in the same procedure as described in section 4.2.3. While mixing, an interesting phase phenomenon was observed. The phase with comparatively lower resistance to actuate often surrounded the other phase while mixing. In this case, the sample droplet with lower resistance to actuate with the addition of a surfactant (details in section 4.3.3) surrounded the extractant phase. The quantification of the extraction yield for this study was done off-chip using a plate-based spectrophotometer. The sample droplet after LLE on EWOD was collected and transferred to the spectrophotometer for concentration measurement.

Figure 4.6 shows the three different mixing schemes studied. The first scheme, Figure 4.6 (a), demonstrates the back and forth linear motion of the merged droplets. With this scheme of mixing, the dye molecules oscillated along with the droplets, and a very slow rate of diffusion into the extractant phase was observed. It was also observed that after some time, the interface between the phases would get concentrated, which further damped the transfer of molecules. The second scheme that was studied, as shown in Figure 4.6 (b), both the phases were moved in a circular fashion, which enabled a higher rate of diffusion of the dye molecules into the extractant phase than the first scheme. The interface was observed to be less concentrated. The final scheme involved keeping the extractant droplet stationary and moving the sample droplet continuously around the sample phase, as shown in Figure 4.6 (c). With this scheme of droplet motion, the relative velocity of the droplets was high, and the rate of the extraction was observed to be higher than the previous two schemes. However, the interface was observed to get concentrated after 1 minute of mixing. Based on all the visual observations of the rate of extraction during mixing and the final color of the sample after LLE, the most effective method was devised by combining schemes 2 and 3. In this method, the mixing was started by scheme 3, in which the sample phase was made to rotate around the extractant phase for ten times, followed by mixing the droplets by

scheme 2 for proper distribution of the extracted molecules in the IL phase. This method ensured the maximum extraction rate and also reducing the concentration of the interface during mixing.

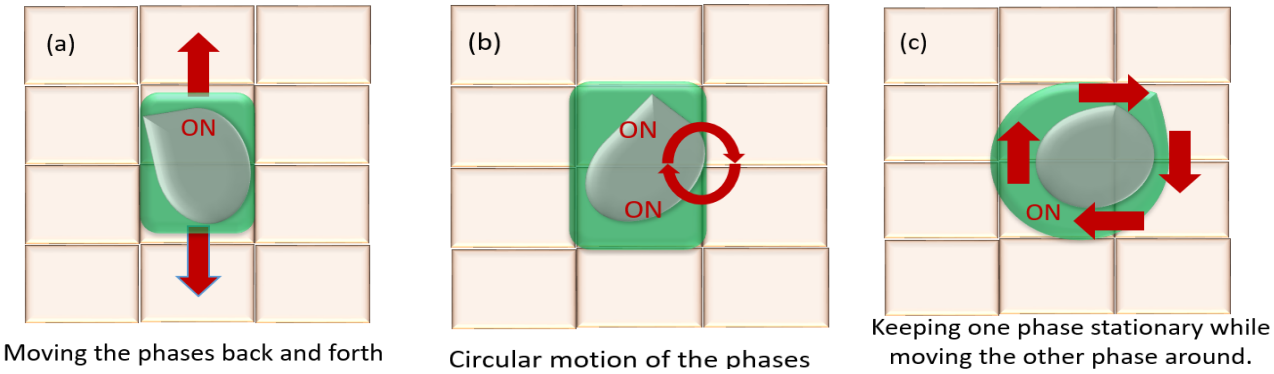

Figure 4.6: The different mixing schemes tried for maximum yield. (a) the two liquid phases are moved in a back and forth motion; (b) in this scheme of mixing, the two liquid phases are moved in a circular motion; and (c) the extractant (IL) phase kept stationary, and the sample droplet moved around.

The results of this study are plotted in Figure 4.7. The error bars in Figure 4.7 indicate standard deviation using a total of three experimental repeats. Extraction efficiency was plotted for each of the mixing schemes by calculating the change in the sample concentration after LLE on EWOD. The extraction time for all the schemes was kept the same at 5 minutes to compare their yield.

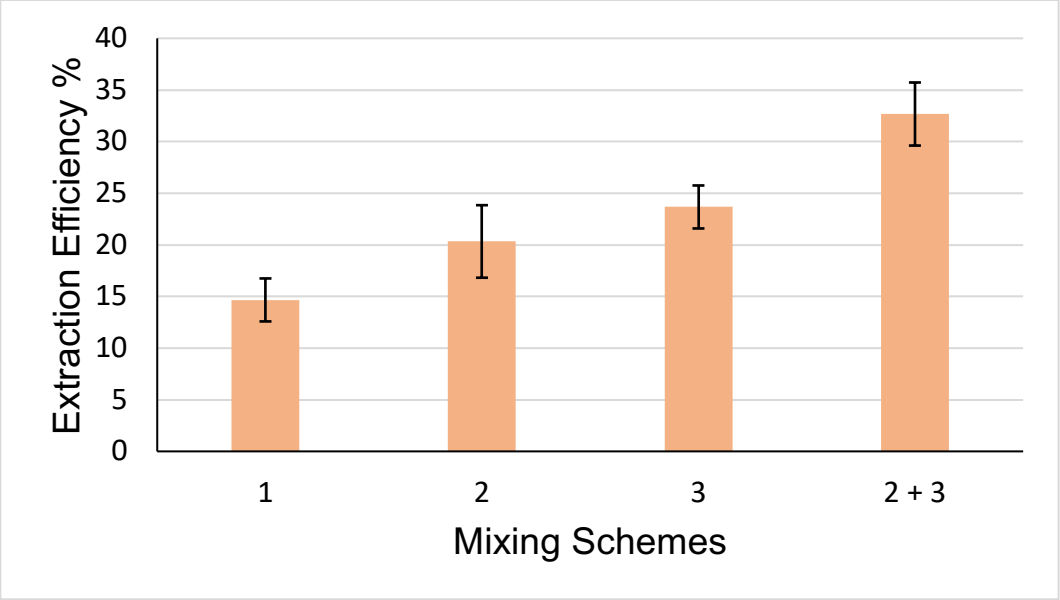

Figure 4.7: Extraction efficiency for different mixing schemes on EWOD.

As was observed visually real-time during the extraction process, the combination of the third and second scheme gave the highest extraction efficiency, the same was also obtained from spectrophotometer concentration measurement. On the other extreme, the extraction efficiency with the first scheme of mixing was found to be the lowest. Thus, it was concluded from the study of the effect of different mixing schemes on LLE that the combination of the third and second mixing schemes found to be the most efficient. This scheme of mixing was adopted for the other LLE studies on EWOD presented in the rest of the dissertation.

4.3.3 Separation of binary solution mixture

The process described in the sections 4.2.3 and 4.3.2 were adopted for droplet generation, mixing and splitting for this study. The sample and extractant droplets were originated from the reservoirs on the EWOD device. These droplets were approximately 200 *nl* in volume. The green

dye molecules were selectively extracted from aqueous solution to IL, and finally, the droplets were split. Snapshots obtained from the entire experiment are presented in Figure 4.8.

One of the observations made was that it was easier to drive the extractant phase compared to the sample phase. In other words, the higher the dye concentration, the more resistant was the sample towards the movement was observed.

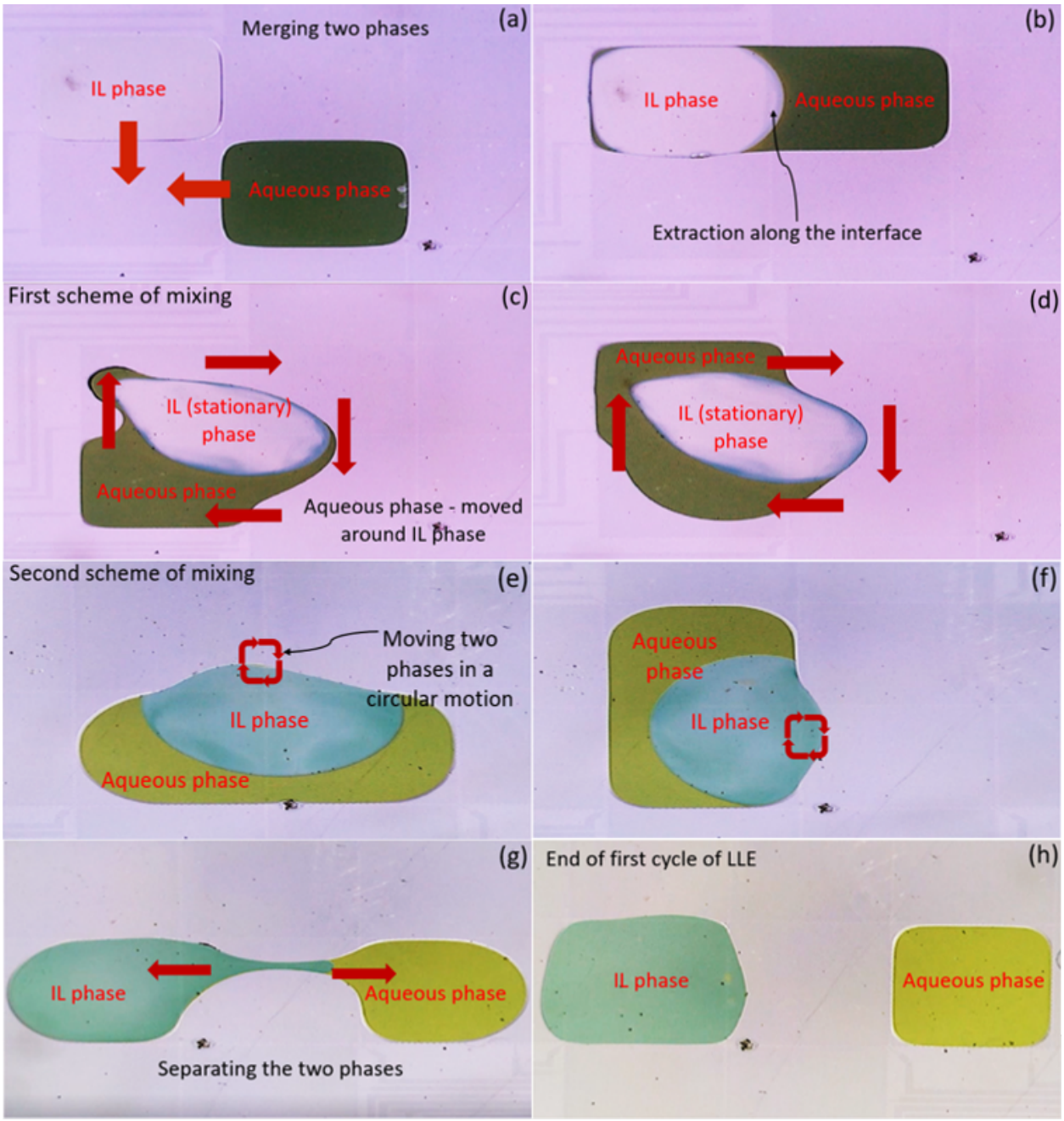

Figure 4.8: Sequential snapshots from the video record of the on-chip extraction experiment demonstrating different stages of the LLE process: (a) the two droplets are about to be brought into contact; (b) merging two droplets and diffusion of dye from sample to the extractant starts; (c) increased inter-face between the two droplets by making the sample droplet surround the extractant droplet; (d-f) mixing the droplets with two schemes for higher extraction (g) create necking to split the extractant phase from the sample phase; (h) the two droplets after splitting.

The difficulty of moving the sample droplet could be due to surface adsorption of solutes. This phenomenon has also been observed for biofluids on EWOD devices [78]. There are reports of several proven solutions to the adsorption issue on EWOD devices [78,79]. We tested one such solution, adding a 1% by volume of the surfactant Tween 20 to the sample. This modification significantly improved the movability of the sample phase so much that it responded even better to EWOD actuation than the extractant phase.

Once the formed droplets are driven along the electrode and merged (Figure 4.8 a), the combined two phases can be mixed. The most efficient mixing scheme was adopted (Figure 4.8 c-f) from the study reported in section 4.3.2. Almost all the green dye color was extracted to the IL drop within 5 min while mixing.

The next step in the LLE process is to split the two phases, which is a critical part of this LLE device. Several studies have been reported on cutting a liquid drop into two droplets on EWOD [80, 81]. The general procedure to split a liquid drop using electrowetting forces is to elongate it over three electrodes by wetting at two ends and keeping the middle electrode nonactivated (0 V). The wetted area gets covered with the fluid as it flows, and a neck is formed in the middle. This study attempted cutting a drop formed by two liquid phases instead of a single-phase droplet. The surface tensions, the pressure differences at the interfaces, are usually different, as the two liquid phases have different interfacial properties. Consequently, the two phases move at different velocities. Therefore, moving two phases onto two separate electrodes requires an intuitive way of activating the electrodes. In previous work, it was reported that the slower phase should be moved first and located on the desired electrode. The two droplet phases are driven to the desired electrode, and once they are placed on two opposite electrodes, as shown in Figure 4.8 g, applying a sudden impulsive potential (i.e., by turning the electrodes on and off simultaneously)

causes phase splitting. It was observed here that the merged droplets tend to break at the interface formed by the two phases. Hence, the relative volumes of the two phases dictate the successful splitting (without any residues from each other liquid phase) of the merged droplets. Thus, it has been shown that two merged immiscible liquid drops, after an LLE process with a 1:1 sample-to-extractant volume ratio, could be successfully separated on the EWOD device. Figure 4.8 h shows the two split phases with the components of the solution mixture separated. A recent study reports a detailed study on two-phase droplets splitting on EWOD [82]. Nahar et al. demonstrated the effective methods of the successful splitting of two merged immiscible droplets on EWOD.

4.3.4 On-chip concentration measurement

The data obtained for calibration using the steps in 4.2.5 was plotted, as shown in Figure 4.9. It shows the calibration curve for the green and yellow dye solution on the EWOD chip. The plot (●) shows the change in the absorbance values of green dye solution with concentration when exposed with the 650 nm light source and (◆) when exposed with the 430 nm. Similarly, (◆) shows the change in the absorbance values of the yellow dye solution with the concentration when exposed with the 430 nm and (●) when exposed with the 650 nm light source.

As is seen from the calibration curves, the green dye has more absorbance for 650 nm, and the yellow dye for 430 nm, as was also found in the plate-based spectrophotometer with the off-chip measurements. Though the green dye has less absorbance for the 430 nm and the yellow dye has less absorbance for the 650 nm, their respective calibration curves are a requirement when working with a binary mixture solution (section 4.2.5).

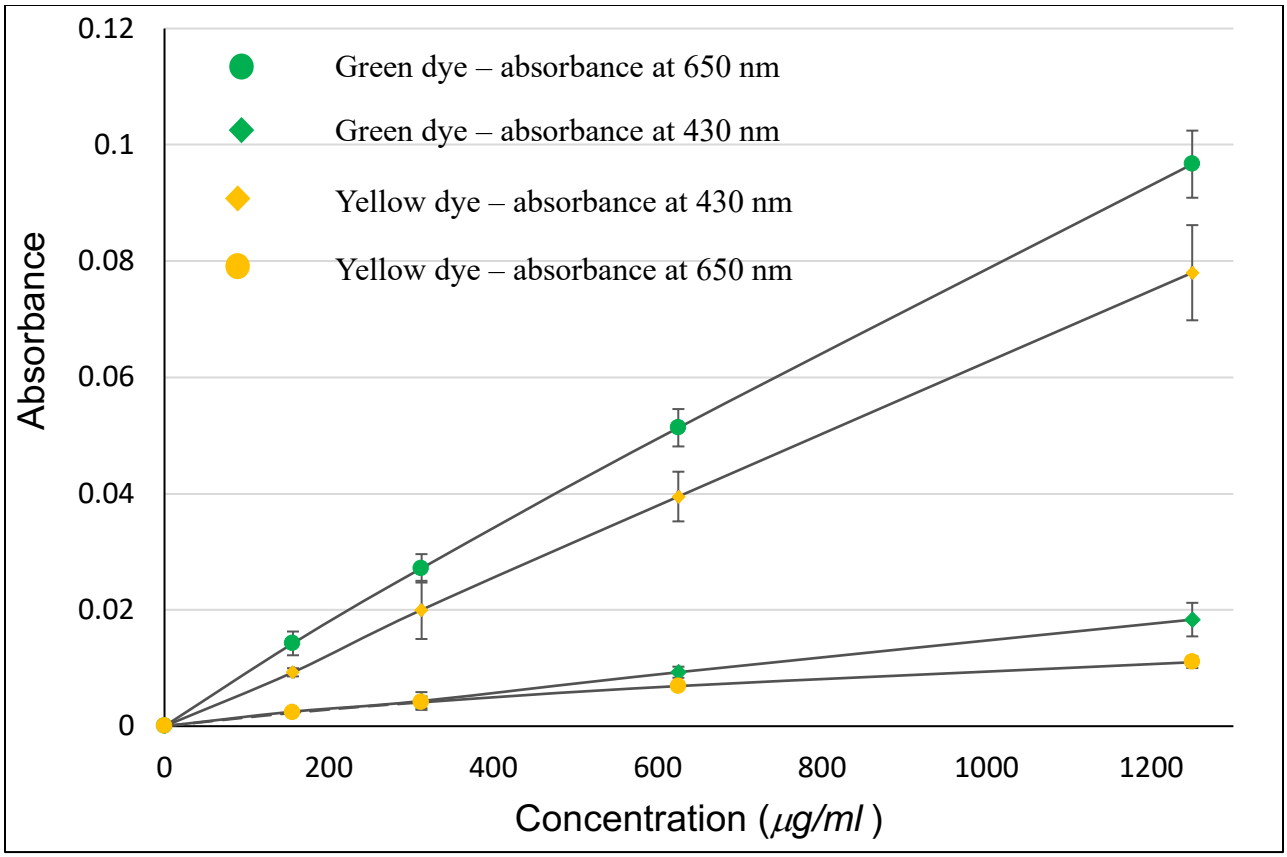

Figure 4.9: Calibration curves for the green and yellow dye solution. (●) and (◆) represents absorbance values for different standards of green dye at 650 nm and 430 nm, respectively; (◆) and (●) represents absorbance values for different standards of yellow dye at 430 nm and 650 nm respectively. The error bar (in black) represents standard deviation from 5 repeats for each data points.

4.3.5 Multistage LLE on EWOD

MLLE is a process where the same extraction steps are repeated to increase the recovery of the target analytes [83]. One of the primary advantages of EWOD devices is its ability to run continuous, a series of multistep processes. When there is a limited transfer of solute in a single step or cycle of LLE, MLLE can be performed on EWOD microfluidics. In the present study, since

there is a vast difference between the partition coefficient of each of the analytes, the MLLE process on EWOD could lead to better separation results for analytes in the binary mixture.

In order to explore this characteristic of EWOD, MLLE was performed in this study with two cycles of LLE. The protocol for the first cycle of LLE was the same as described before (section 4.3.3 and Figure 4.8 for reference). In the second cycle of LLE, a fresh extractant (IL) droplet was generated from the reservoir, and the LLE steps were repeated. After each cycle of the process, the sample droplet was transported to the concentration measurement electrode, and the voltage measurement was done for absorbance.

Figure 4.10 shows changes in the color of the sample and extractant droplets before and after each LLE cycle of MLLE. As is seen in Figure 4.10 (a), the sample droplet becomes very less concentrated with green dye molecules and appears somewhat yellowish, whereas the extractant droplet appears green with most of the green dye extracted. The extraction rate was observed to be very high, given the high concentration gradient between the two phases. It was observed in some experiments there was a decrease in the sample volume phase after the first cycle of LLE, resulting from evaporation during the experiment. Thus, the processing time for each cycle was optimized to minimize the loss of sample volume.

Figure 4.10 (b) shows the image results from the second cycle of the LLE. The final sample drop has very few green dye molecules and mainly concentrated with the yellow dye, whereas the extractant droplet, again turns a little green extracting the rest of the green molecules left after the first cycle of LLE. Further decrease in the volume of the sample was observed at the end of the MLLE process resulting from evaporation, as can be seen in Figure 4.10 (b). In future developments, the evaporation can be damped by controlling the vapor pressure of the surrounding environment of the droplet. With the decrease in the concentration gradient, during the second

cycle, the extraction rate was observed to be quite low compared to the first cycle, with also very fewer molecules being extracted.

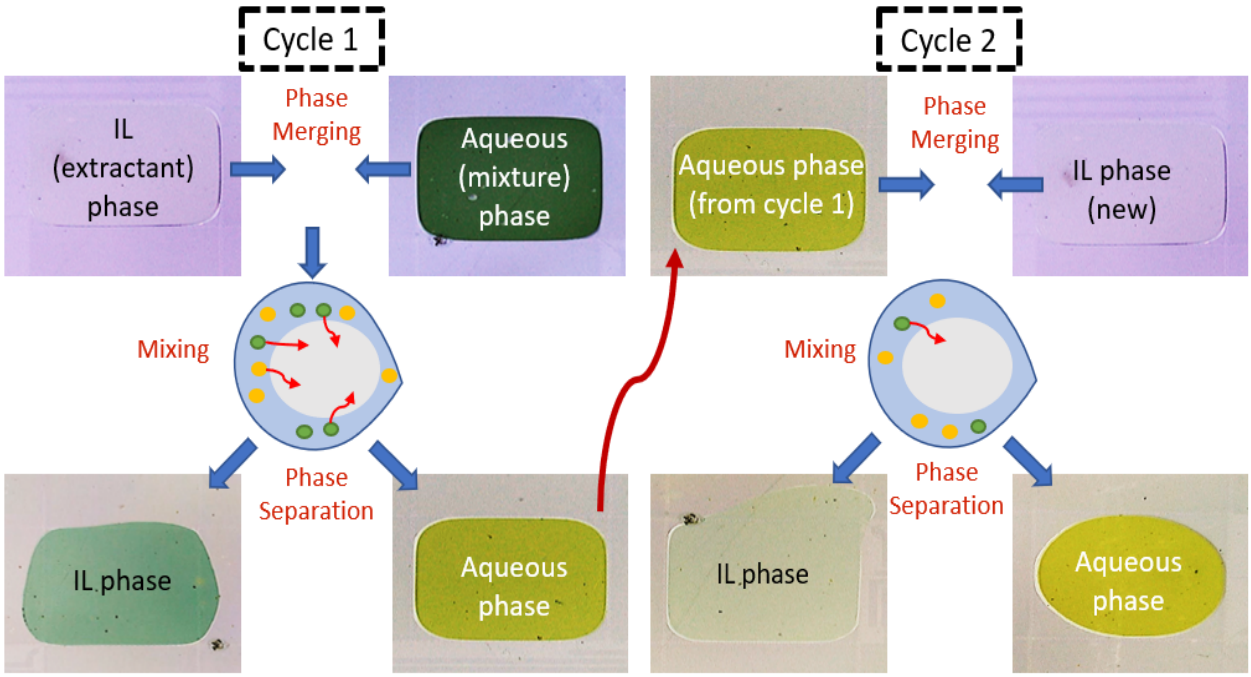

Figure 4.10: MLLE image results of change in the color of the sample and extractant phases at every cycle of LLE: a) The sample phase after the first cycle of LLE, turned more yellow as most of the green molecules are extracted; while the extractant phase turned green b) Rest of the green solutes are extracted in the second cycle making the sample concentrated with yellow dye.

Next, we compare the results of binary separation by MLLE done on the EWOD with theoretical values. The theoretical values were calculated from the partition coefficient values of each solute obtained in section 4.3.1. Figure 4.11 illustrates the drop in the sample concentration ratio of green to yellow dye after each cycle of on-chip LLE and the theoretical values. The blue bar represents the change in the concentration obtained from the on-chip experiments, whereas the orange bar shows the theoretical concentration ratio for each cycle of MLLE.

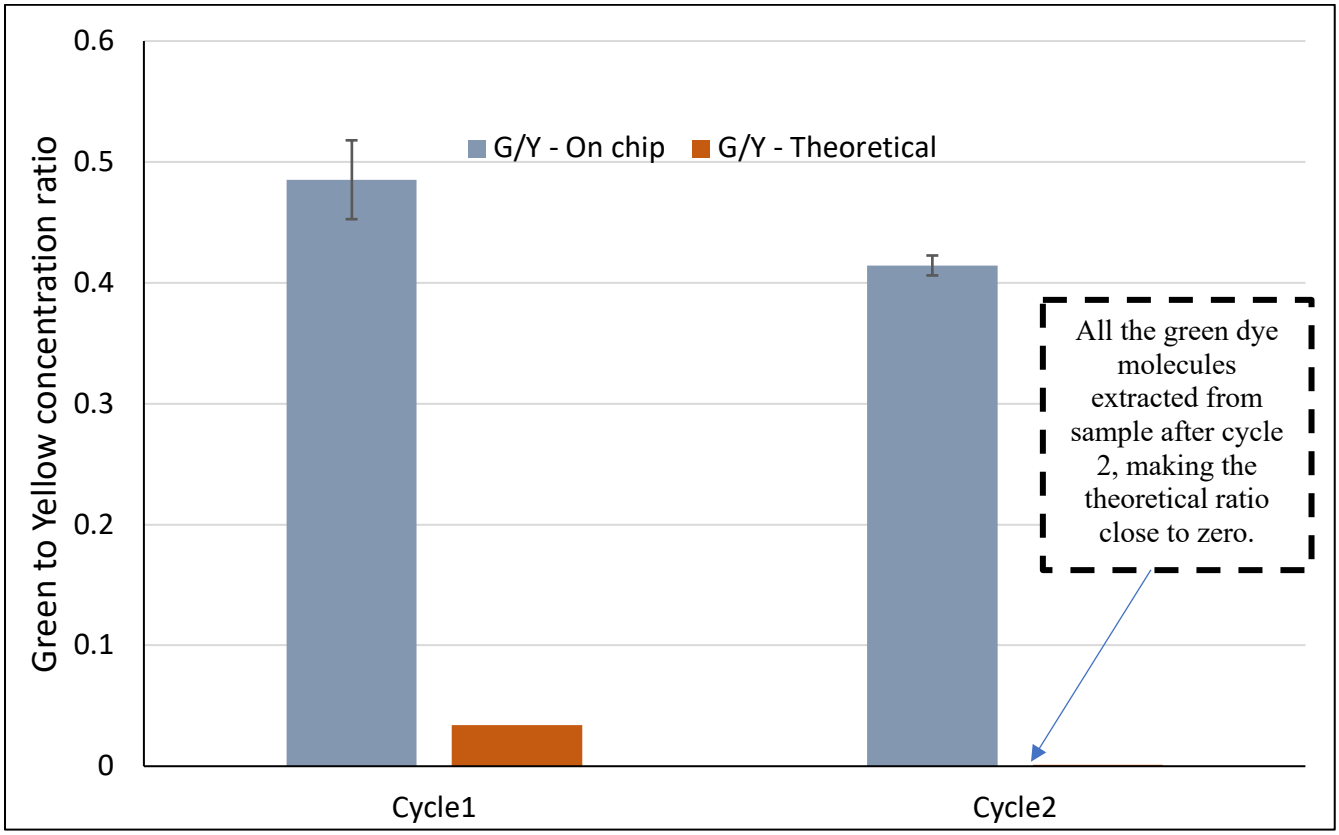

Figure 4.11: The concentration ratio of the green to yellow dye molecules in the sample after each cycle of LLE, where the blue represents on-chip LLE results and orange bar represents theoretical results.

The sample phase was prepared with concentration ratio 1:1 at the beginning of the process, and with each cycle of MLLE, the ratio decreases. A sharp decrease in the concentration ratio is observed after the first cycle of LLE on EWOD. Almost 50% of the green dye was extracted during this step in an extraction time of 5 minutes. The extraction rate was observed to be very high during the first cycle. The drop in the concentration ratio after the second cycle is not very significant as the first cycle. At the end of the second cycle, almost 60% of the initial green dye was extracted, and the concentration ratio drops to 0.4 by the complete MLLE process. The extraction rate in the

second cycle was much less compared to the previous cycle. The error bars in Figure 4.11 indicate standard deviation using a total of two experimental repeats.

The difference in the LLE performance in the EWOD and tube-scale experiments, as illustrated in Figure 4.11, can be attributed to the fact that the mixing of the two phases is limited in the micro-scale system given by the low Reynolds number. Whereas, on the macro scale, the phases undergo a turbulent mixing done by vortexing to have the maximum extraction. Similar problems associated with mixing at the microscale have also been reported elsewhere [66]. Also, because of the evaporation problem, the extraction time was not kept very long, as with longer extraction time, the sample tends to lose its volume.

The results point out that one type of molecule can be separated from the other in a binary solution with LLE on a DMF device. As shown, acid green undergoes more extraction through LLE cycles than yellow dye, proving that this method leads to complete separation of binary mixture solution. Thus, using LLE on EWOD, such a binary mixture of different solutes was successfully separated in this study owing to the different affinity of the solutes for the extracting phase.

4.4 Conclusion

A microfluidic LLE method of separation of compounds in a binary solution is demonstrated in this work. The solutes separate according to their affinity towards respective fluids. For instance, the affinity of the acid green dye is higher towards ionic liquid. This property causes separation of the acid green dye rapidly from the reactive yellow in the aqueous phase. The mixing of two phases, which is critical for a successful LLE process, was studied in this chapter. The splitting of the merged liquid phases at the end of the process occurred in a similar way as breaking a single-phase mother drop into two daughter droplets.

The conventional spectrophotometry method to measure absorbance was used for the concentration measurement of each solute. In order to perform the concentration measurement on a chip, the EWOD device was integrated with LED light sources and photodiode. MLLE was successfully demonstrated on this device for higher recovery of the green dye from the sample. This platform can be used to optimize the number of cycles required for higher separation of different analytes in the MLLE process, instead of performing standard laborious lab-scale experiments.

When the presented on-chip protocol is fully utilized with its downstream assay capability, it will provide a versatile sample preparation platform. This method can be also be applied towards separation and purification of compound of interests (e.g., target proteins, DNA) from a complex solution such as raw blood samples for applications in chemical and biochemical analyses. In the subsequent chapters, we will be examining this platform for the separation of DNA molecules from its other cellular components.

Chapter 5

Magnetic bead free DNA extraction enabled by EWOD digital microfluidics

DNA extraction represents a significant bottleneck in the nucleic acid analysis workflow. With many of the nucleic acid assays being automated thanks to the advancements in fluidics and miniaturization, the DNA extraction protocol is much needed to be integrated into these systems as a sample preparation step for a quick sample-to-result solution. This work reports the first study of on-chip DNA isolation without the use of magnetic beads in EWOD DMF. Instead of using magnetic beads, LLE was employed. Aqueous sample droplet of pure plasmid DNA (pDNA) was introduced on the EWOD platform, and an IL was used as the other extractant phase. All the steps – dispensing, merging, mixing, and splitting of the phases were performed on the EWOD platform. The ease of handling of the two-phase liquid system on this platform makes this integration possible. The selective DNA extraction was also achieved from a DNA-protein mixture solution. The quantification of the on-chip LLE process was done by measuring the sample concentration before and after LLE by using an off-chip instrument.

5.1 Introduction

Nucleic acids, especially DNA, have emerged as one of the essential biomolecules for life science applications [84, 85]. With the developments in sequencing, PCR, and other bioanalytical technologies, it is possible to answer a wide range of biological questions through genotyping and genomic profiling, which has paved the way for precision medicine [86, 87]. Advances in DNA

sequencing and synthesis have begun to enable the possibility of evaluating thousands of gene variants and hundreds of thousands of gene combinations.

Sample preparation for these studies often involves cumbersome bench-top procedures to extract the DNA from a cell sample, which must be of high purity. The most widely used method SPE, in this regard, has been state-of-the-art for isolating DNA from interfering protein and other cellular molecules [85]. Commercially available kits and automated bench-top instruments are available for extracting DNA from different cell lines and prepare the sample for downstream analysis. SPE method of isolating DNA involves the binding of the DNA molecules with solid particles or a surface, which has a specific affinity for the molecule. After capturing the molecules, the particles are washed to remove the unbounded impurities in the sample further and finally eluted to obtain the purified DNA sample (the detailed procedure is provided in section 2.1.1). Although this method has shown great success, the costs involved in this technique are high, with often magnetic beads being used as the solid phase particles [88]. SPE method of DNA extraction has been adopted in standard protocols due to the easiness of scale-up using automatic robotic systems [89].

Microfluidics liquid handling systems have enabled small scale laboratory automation as an alternative to lab robots to decrease the reagent consumptions and increase throughput and efficiency. Significant efforts have been made to develop microfluidic platforms to automate the molecular biology protocols and reduce hands-on labor. Automated microfluidic approaches incorporating all the steps of SPE have been reported by several groups to reduce the cost and reagent consumptions and the footprint when compared to other automated machines [90, 91]. However, these platforms execute the same number of steps involved in SPE-based DNA isolation, which includes binding, washing, buffer exchange, and elution and the use of magnetic bead

particles, as shown in Figure 5.1. As a much simple alternative process, LLE has not much been explored for DNA isolation on a microfluidic device. LLE of DNA traditionally done by the phenol extraction method suffers from the significant drawback of phenol being toxic [92]. Also, phenol having high wavelength absorptivity at 260 nm, it becomes difficult for the quantification of the extractant phase. The continuous microfluidics approach for DNA extraction using the phenol extraction method was reported by Morales et al. [42]. This paper has also been reviewed briefly in section 2.2.1. They showed the successful partition of protein into the extractant phase leaving behind the DNA molecules concentrated in the sample phase. The phase splitting at the end of the process is typically challenging with traditional continuous microfluidics. There is also not much control of the individual phases during the process of LLE inside microchannels. On the other hand, LLE on EWOD platform exploits fully drop-wise flow control for both sample and extractant phase so that parallel and serial extraction as well multiplexing of many different combinatorial extractions on a single chip can be performed. Thus, there is a need for an EWOD microfluidic approach where the operation of the liquid-liquid system is much simpler for DNA isolation.

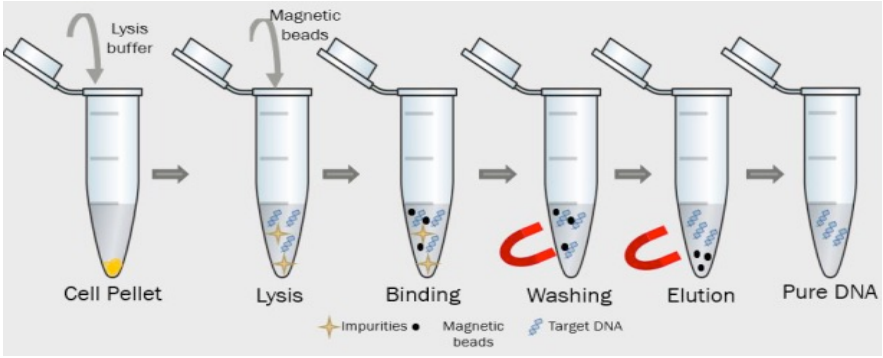

Figure 5.1: The steps of the magnetic bead-based DNA separation method from other impurities (protein, RNA, etc.). The process involves many steps, and the use of magnetic beads and various buffers add to the cost of the process.

When it comes to the alternate liquid-liquid system for LLE of DNA, IL has been proposed as an extractant for encapsulating DNA molecules with LLE [85]. ILs often referred to as green solvents with high thermal stability and low vapor pressure are environment-friendly, and the easy tunability of the ILs structure makes them a favorable extractant for DNA molecules. ILs are synthesized with bulky cations paired with weakly-coordinating anions [93]. The fundamental properties of the IL, such as viscosity, thermal stability, and hydrophobicity, can be customized for a given application by the choices of the cation and anion structures [94]. Thus, a hydrophobic IL can form a two-phase system with the aqueous sample for the extraction of target DNA molecules. It has been reported in the literature that the extraction of DNA molecules is a result of the electrostatic interaction between the cation of the IL with the negatively charged phosphate groups of the DNA molecule [85]. ILs such as 2-hydroxyethylammonium formate (2-HEAF), and trihexyl(tetradecyl)phosphonium tetrachloroferrate [$P_{6,6,6,14}$] [$FeCl_4$] have also been reported to be excellent media for DNA storage for longer durations and as media that is compatible with PCR [95, 96]. Magnetic ionic liquids (MIL) have been reported for DNA extraction with high extraction efficiency using an external magnet to separate the phases at the end [97].

The present study is the first attempt for DNA LLE from other impurities, such as protein molecules performed on the EWOD platform in a DTD format. EWOD platform has been used to demonstrate the DNA extraction process by other groups making use of the magnetic bead-based extraction technique and complex protocols on-chip [25, 26, 53]. By using the LLE method of DNA extraction, we get rid of magnetic beads, external magnets, and perform the DNA isolation in fewer and simpler steps. The use of the EWOD platform has an advantage over traditional continuous microfluidics in moving droplets individually, and thus we have a liquid handling platform where each liquid droplet phase can be accessed and manipulated. This functionality of

EWOD enables the merging of the two phases (sample and extractant), the user-defined mixing time, and ease of splitting of the phases after the LLE process, as was also reported in chapter 4. Besides, the ease of integration of other downstream nucleic acid assays on this platform [21-24] makes it an excellent choice for the sample-to-result platform for various applications. The first study in this chapter includes the LLE of DNA molecules from a control sample containing only pDNA molecules to show the working of the LLE process on EWOD. The second study involves the selective extraction of pDNA from a binary mixture of pDNA and BSA protein molecules in the sample. IL was used as an extractant in both studies.

5.2 Experimental

5.2.1 Reagents

For this study, pDNA pVAX1-hVEGF165 transformed in growth strain DH5-Alpha, obtained from Addgene, was used as the model DNA. Details of the pDNA are provided in section 5.2.3. The bacterial strain was cultured to increase the colony, and from the expanded colony, pure pDNA was extracted using the Qiagen Hispeed kit for all the control LLE experiments, details in section 5.2.4. BSA protein was used as the impurity molecules to show the selective extraction of pDNA from a binary mixture of pDNA and protein. Commercially available IL BMIM-PF_6 (same as used in the study reported in chapter 4) was chosen as the extractant phase. Ethidium bromide (EtBr; Life Technologies, Gaithersburg, MD) was used as received for intercalation with DNA for qualitative analysis of on-chip LLE.

5.2.2 Device design, fabrication and control

Detailed fabrication steps with the layout of the platform and all the different layers of the chip can be found in chapter 3 (section 3.4). The experimental setup and the control parameters are also described in detail in chapter 3.

5.2.3 Plasmid DNA introduction

pDNA are small, circular, double-stranded DNA molecules that are different from cells genomic DNA (gDNA) and are present in bacterial cells, and some eukaryotes [98]. Usually, they exist as a supercoiled structure, as shown in Figure 5.2. The pDNA used in this study has a vector backbone pVAX1 with a size of 3000 bp, and the inserted gene is hVEGF165 with a size of 578 bp [99]. pDNA was used as the model DNA molecule for this study, and the same approach can be extended for the extraction of other targets nucleic acid such as genomic DNA from sample lysate in the future.

Besides, using pDNA as a model DNA for a proof of concept LLE study, pDNA extraction on EWOD finds application when the downstream process is a gene-editing system (transformation or transfection) on-chip [100, 101]. pDNA has been the point of interest in many gene delivery studies where target genes are transferred with pDNA to the targeted tissue. The success of this protocol is measured by achieving a stable transfection, i.e., more pDNA containing the inserted gene should reach the nucleus of the target cells surviving enzymatic degradation for efficient transfection and protein expression studies are done subsequently. The reported studies so far have integrated the downstream protocols such as pDNA transformation in bacterial cells on EWOD with the pDNA extraction done off-chip [102]. The sample preparation step (pDNA

extraction) presented in this work can be integrated with the downstream protocols (i.e., the transformation of bacteria) to have the complete workflow in one platform.

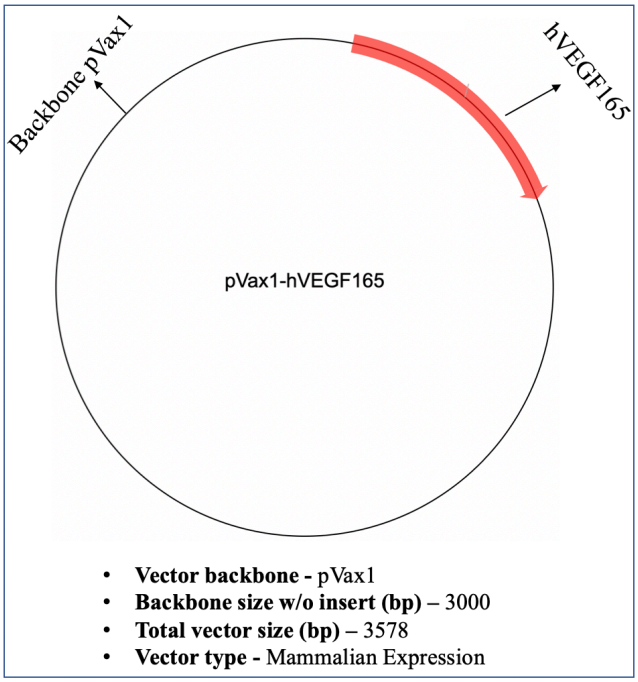

Figure 5.2: Details of model plasmid DNA used in the study [99].

5.2.4 Plasmid DNA production

For all the control experiments, pure pDNA was obtained using a Qiagen Hispeed kit from the bacteria pellet. Plasmid DNA transformed in E. coli strain was expanded to increase the bacterial colony using standard techniques, as described below.

A bacterial stab of E. coli containing the plasmid pVAX1-hVEGF165 obtained from Addgene was streaked on a Kanamycin-agar plate. After overnight incubation at 37° C, individual colonies were picked from the plate into starter cultures. One of the starter cultures were expanded into a 250 ml LB Broth supplemented with Kanamycin and incubated overnight in 37° C shaker. After overnight culture, the bacterial pellet was collected by centrifugation of the 250 ml culture. This pellet was then used to extract the plasmid using Qiagen Hispeed midi prep kit. There are

many lysis processes that can be done. In this study, chemical lysis, as directed in the Qiagen kit protocol, was adopted. The lysis process ends with the precipitation of the denatured proteins, cell debris, and other nucleic acids. Then a filtration step was adopted to filter out the lysate or supernatant from the impurities. In the second filtration step, the pDNA is eluted along with some other impurities. The third filtration step involved washing the pDNA with ethanol to eliminate the impurities and finally eluting the pure pDNA from the filter with the help of ultrapure water. The DNA sample was then checked by measuring the concentration and purity of the pDNA. Pure pDNA obtained from this workflow was used for all the control experiments.

5.2.5 DNA quantification instrument

The DNA quantification was done by using the NanoDrop™ instrument both for the on-chip and tube-based off-chip experiments. The concentration of the DNA sample obtained from the Qiagen kit was measured. Based on the readings of the NanoDrop™, the sample was found to be of pure pDNA with no impurities (RNA, proteins, etc.). For the LLE experiments, the DNA left in the aqueous phase was measured to quantify the yield of the process.

It was observed from the off-chip experiments, that after the LLE process, the sample showed a sharp peak at 230 nm wavelength higher than the peak at 260 nm (wavelength of highest absorptivity of DNA molecules). This peak comes from the ions absorbed by the sample phase from the IL during the LLE process. The following procedure was adopted to decrease the peak at 230 nm and increase the resolution of the measurement at 260 nm wavelength. Instead of using ultra-pure water as the blank for all the DNA concentration measurements, the ultra-pure water was first mixed with the IL and then split as done in the LLE process and used as the blank. In this process of mixing the water with the IL, some of the ions diffuse into the water phase. The water

phase after splitting from the IL phase used as the blank has ions from the IL and was used in all the concentration measurements. This method helped to suppress the peak at 230 nm and increased the resolution of the peak at the desired 260 nm for the sample DNA concentration measurements.

For the EWOD LLE experiments, the sample after the extraction was collected and transferred to the NanoDrop™ for concentration measurement. However, the volume of the sample droplet was too small (~2-3 μl) from a single LLE test for the NanoDrop™ measurement. Three tests were conducted under the same experimental conditions, and the sample droplets were merged to increase the volume (~7-9 μl). The increased sample volume was used for the concentration measurement, which is an average of three on-chip LLE experiments, and thus, one data set was obtained. The final concentrations of the sample after LLE were compared with the initial concentration to find the amount of pDNA transferred to the IL phase.

5.2.6 Off-chip LLE experiments

DNA LLE tests were conducted off-chip (in tubes), as illustrated in Figure 5.3, to find the extraction efficacy of the IL used in the study. A control sample of 100 $ng/\mu l$ of pDNA was prepared and mixed with an equal volume of IL in a 1 ml tube. The mixture was mixed vigorously with constant shaking. After mixing, the phases were let to settle back, and the top sample phase was pipetted out and transferred to NanoDrop™ for concentration measurement.

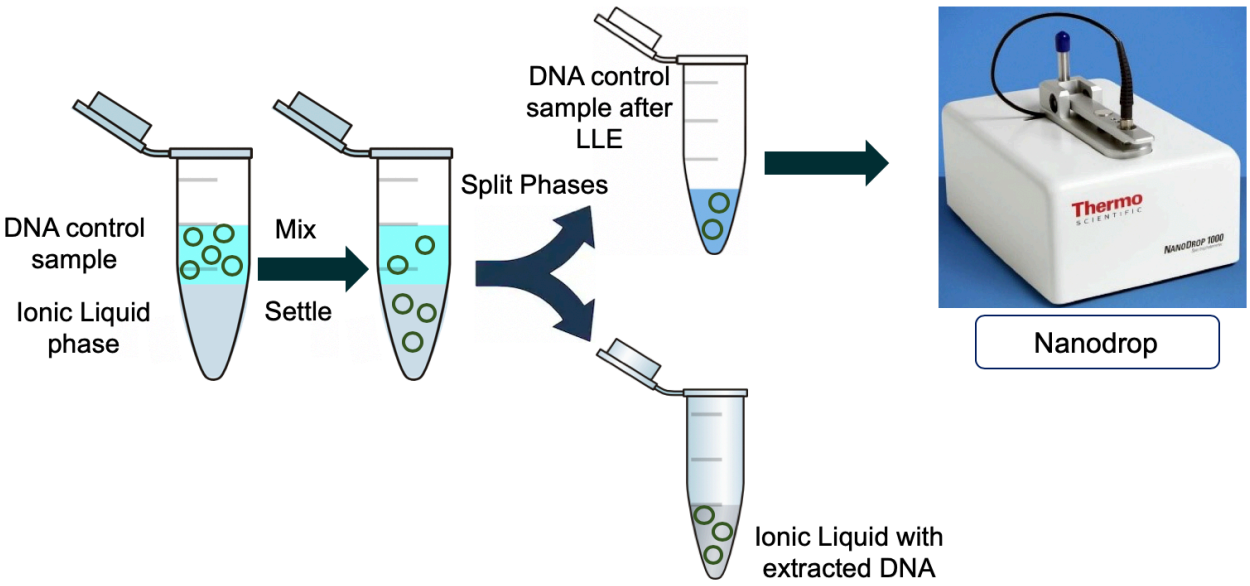

Figure 5.3: Protocol for off-chip DNA LLE experiment.

Wang et al. demonstrated the use of BMIM-PF6 as an excellent candidate for the extraction of DNA from both pure DNA samples and a sample containing other impurities [85]. Almost 100% extraction of DNA from the aqueous phase was observed, and from that, 30% of DNA obtained after back extraction from IL to an aqueous phase. The mechanism of extraction, as proposed in [85], involved electrostatic interactions between the negatively charged phosphate group of DNA and the positively charged cation of the IL (Figure 5.4). However, Khimji et al. reported that this IL is more suitable for DNA staining dye extraction and demonstrated the successful extraction of dye molecules from a DNA-dye mixture sample [103]. Similar to these studies, tube-based DNA LLE experiments were conducted, and the residual DNA concentration in the aqueous phase was measured.

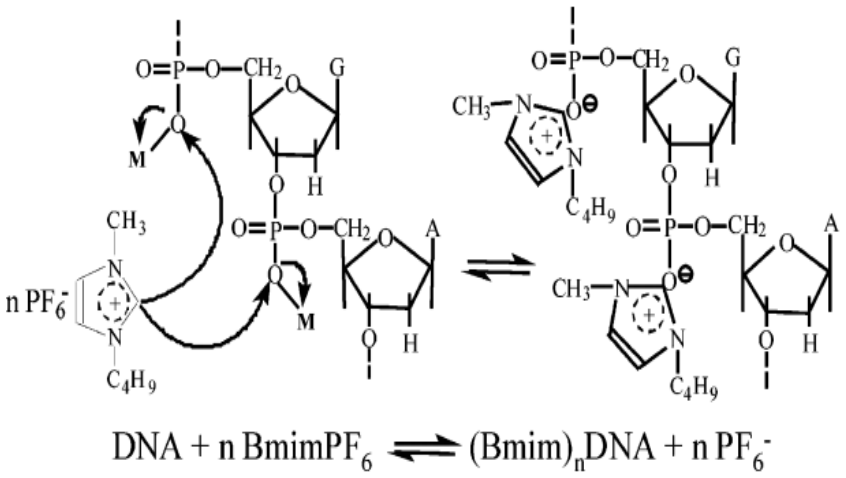

Figure 5.4 - DNA binding to IL mechanism as reported in [85].

It was reported previously that the co-extraction of protein was not observed using this IL [85]. We performed experiments to study the extraction of BSA protein with BMIM-PF_6 separately in the off-chip LLE experiment. In this experiment, pure BSA protein was mixed in ultra-pure water as a control sample, and the concentration was adjusted to 100 $ng/\mu l$. The solution (sample phase) was then mixed with an equal volume of the IL in a 1 ml tube. The sample was mixed vigorously for 5 minutes and then left to settle for the phases to separate. The top sample phase was carefully separated and was transferred for quantification by NanoDrop™ using 280 nm wavelength. The LLE experiments confirmed that no protein was extracted, more detailed results in section 5.3.1. It was concluded from this experiment that when pDNA and BSA molecules are mixed in a sample, the IL can selectively extract pDNA molecules from the mixture, and for all the on-chip LLE experiments, only DNA concentration in the sample was quantified.

5.2.7 On-chip LLE experiments

The protocol for on-chip DNA LLE was the same as demonstrated in Chapter 4, section 4.2.3. Briefly, the sample droplet and an IL droplet were generated from two different reservoirs and were merged to initiate the mixing process. In this study, the optimized mixing scheme obtained in Chapter 4 (section 4.3.2) was adopted. The end step of LLE is to split the two phases, and they can now go for their respective downstream analysis. After the LLE process was done on EWOD, the sample was transferred to Nanodrop™ for DNA concentration measurement.

Before moving to the LLE experiments on-chip, we wanted to confirm that the pDNA lost in the sample is a result of on-chip extraction and not due to device surface adsorption. A study was conducted to quantify the DNA lost to the device surface due to EWOD motion. Different sample concentration droplets were moved on the chip using EWOD operations without LLE. The droplets were moved on four electrodes in a back and forth motion for 15 minutes, which was the maximum time duration of the LLE process that was studied on EWOD. After moving the droplets on the EWOD device, they were transferred to NanoDrop™ to measure the concentration lost to the surface of the device. From this study, it was found when a sample concentration of around 100 $ng/\mu l$ was used, there was no adsorption by the surface due to EWOD motion. Sample concentration higher than 100 $ng/\mu l$ (in the range of 200 $ng/\mu l$ or higher) was found to lose some of the DNA molecules to the surface. The detailed results are shown and discussed in section 5.3.2.

The first DNA LLE study was conducted to show the on-chip LLE of pDNA from a sample containing pure pDNA. The motivation for this study was to show the concept of transfer of DNA molecules in a DTD format using the EWOD platform. A sample concentration of 100 $ng/\mu l$ was used for this study.

The second on-chip LLE study was conducted to show the capability of the platform to extract DNA selectively from its other impurities. The sample was prepared by spiking BSA protein in the pDNA sample and hence, creating a mixture of pDNA and protein. The sample concentration was adjusted such that each analyte had a final concentration of 100 $ng/\mu l$ in the mixture. The steps of the protocol adopted for LLE of pDNA study on EWOD are illustrated in Figure 5.5.

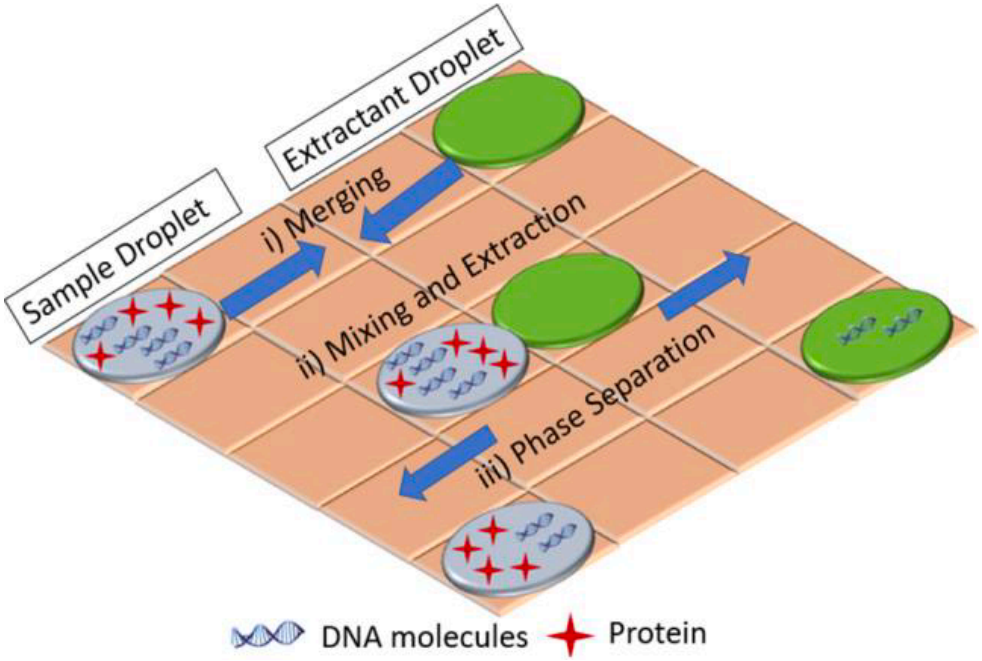

Sample collected and transferred for concentration measurement.

Nanodrop

Figure 5.5: Steps of the protocol of on-chip LLE of DNA. The DNA selectively diffuses into the IL phase through the interface formed by the two immiscible liquids. The sequence of the protocol - 1. merging, 2. mixing, and 3. splitting of phases of sample and extractant droplets. The sample is then collected and transferred to NanoDrop™ to measure the concentration drop.

5.3 Results and discussion

5.3.1 Off-chip LLE experiments

The concentration of the residual DNA left in the sample undergoing off-chip LLE was measured. The off-chip LLE experiment from pure pDNA samples showed an extraction efficiency of 30%. The percentage yield was sufficient to demonstrate the capability of EWOD DMF for LLE of DNA using this IL.

The second off-chip study was done to check the extraction of protein molecules by the IL phase. The protein quantification mode (expose the sample to a wavelength of 260 nm) was chosen in the NanoDrop™, and the sample phase was tested. There was no change in the concentration of the protein in the sample before and after the LLE process. Hence, no protein extraction was observed using the IL as the extractant. A pH of 6.9 for the sample (BSA protein mixed in ultra-pure water) was maintained for this experiment. The isoelectric point of BSA molecules was found to be 4.8 from the literature [104], and given the pH of the environment, the protein molecules should have a small negative charge on them. However, the electrostatic interaction between the charged BSA molecules and the ions of the IL was not strong enough to extract the protein molecules to the IL (extractant) phase. From this experiment, it was concluded that for all the on-chip experiments, if the same conditions are maintained, there will not be any protein co-extraction.

5.3.2 Adsorption on chip surface due to droplet motion

To find a concentration of DNA that would not be adsorbed by the EWOD surface, and to confirm the change in the sample concentration is coming from on-chip LLE, motion tests were conducted with different concentrations of DNA sample, as described in section 5.2.6. The results of this study are plotted in Figure 5.6. Figure 5.6 shows the comparison of DNA concentration before and after the EWOD motion. The x-axis represents the DNA sample concentration tested, and the y-axis represents the concentration after EWOD motion. The blue line represents the sample concentration tested on EWOD. In the ideal situation, DNA should not be adsorbed on the surface, which is represented by the orange reference line in Figure 5.6. Any experimental data point which does not fit the orange reference line is discarded to be used in further LLE experiments. It was found that with concentration close to 100 $ng/\mu l$, there was no loss of DNA due to EWOD motion. As can be seen from the results, the samples of concentration 500 $ng/\mu l$ and 1200 $ng/\mu l$ there was a significant change in the concentration with a higher standard deviation due to surface adsorption. A loss in the sample volume was also observed while retrieving samples from the chip with higher concentration. Hence, it was concluded that a sample concentration of 100 $ng/\mu l$ or less was suitable for the LLE experiments. All the on-chip LLE experiments were done at an initial sample concentration of 100 $ng/\mu l$.

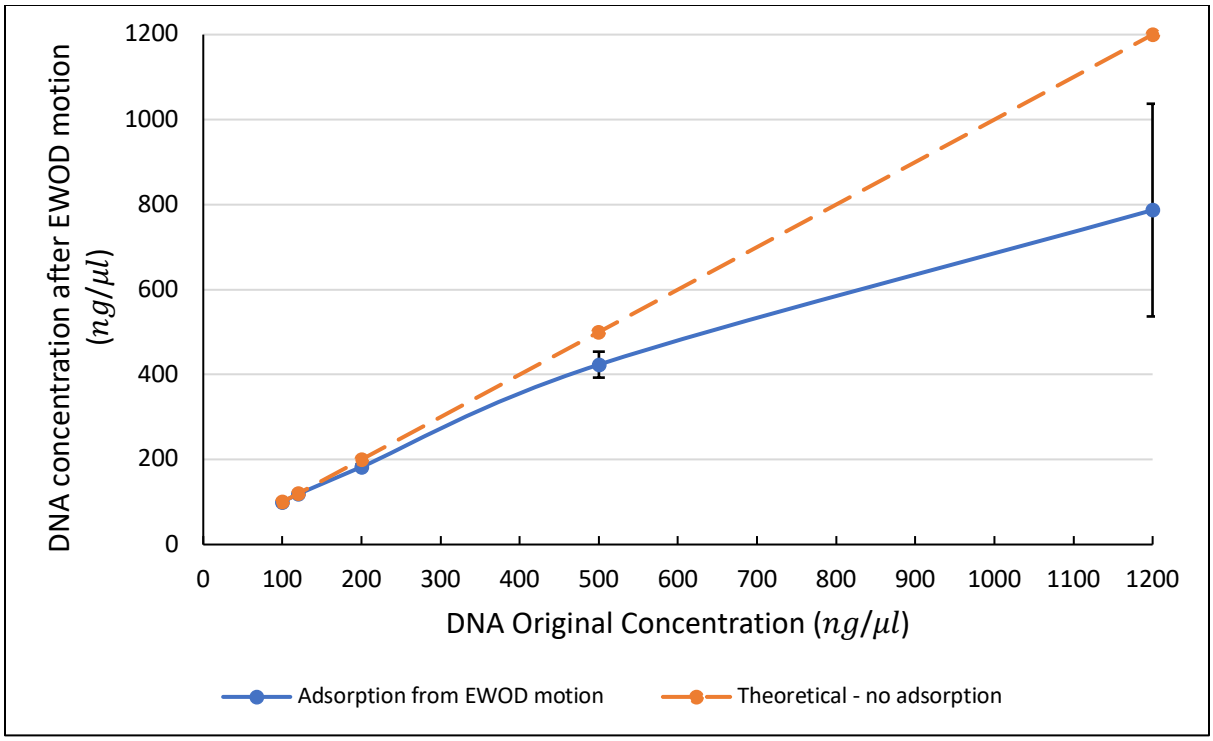

Figure 5.6: The change in the sample DNA concentration with EWOD motion without LLE. The orange line shows the ideal situation when the surface does not adsorb any DNA. The blue line shows the change in the concentration of the sample due to surface adsorption during EWOD motion. The error bar (in black) represents standard deviation from 6 repeats for each data points.

5.3.3 LLE of pDNA on EWOD

The proposed EWOD based microfluidic device was successful in generating the sample and IL phase droplets of equal volume, transporting the droplets to the mixing and extraction zone, and finally split the two phases to complete the LLE process. The optimized mixing, as described in section 4.3.2, was adopted for all the experiments. Similar to the study in Chapter 4, it was observed that the droplet, which was easy to actuate with EWOD forces, would engulf the other phase. In this study, the IL phase was more mobile than the sample phase under the voltage application and hence, completely engulfing the later phase. During mixing, in this study, the

sample phase was kept stationary, and the IL phase was made to rotate around the sample phase. The snapshots from the experiment of the entire protocol are shown in Figure 5.7.

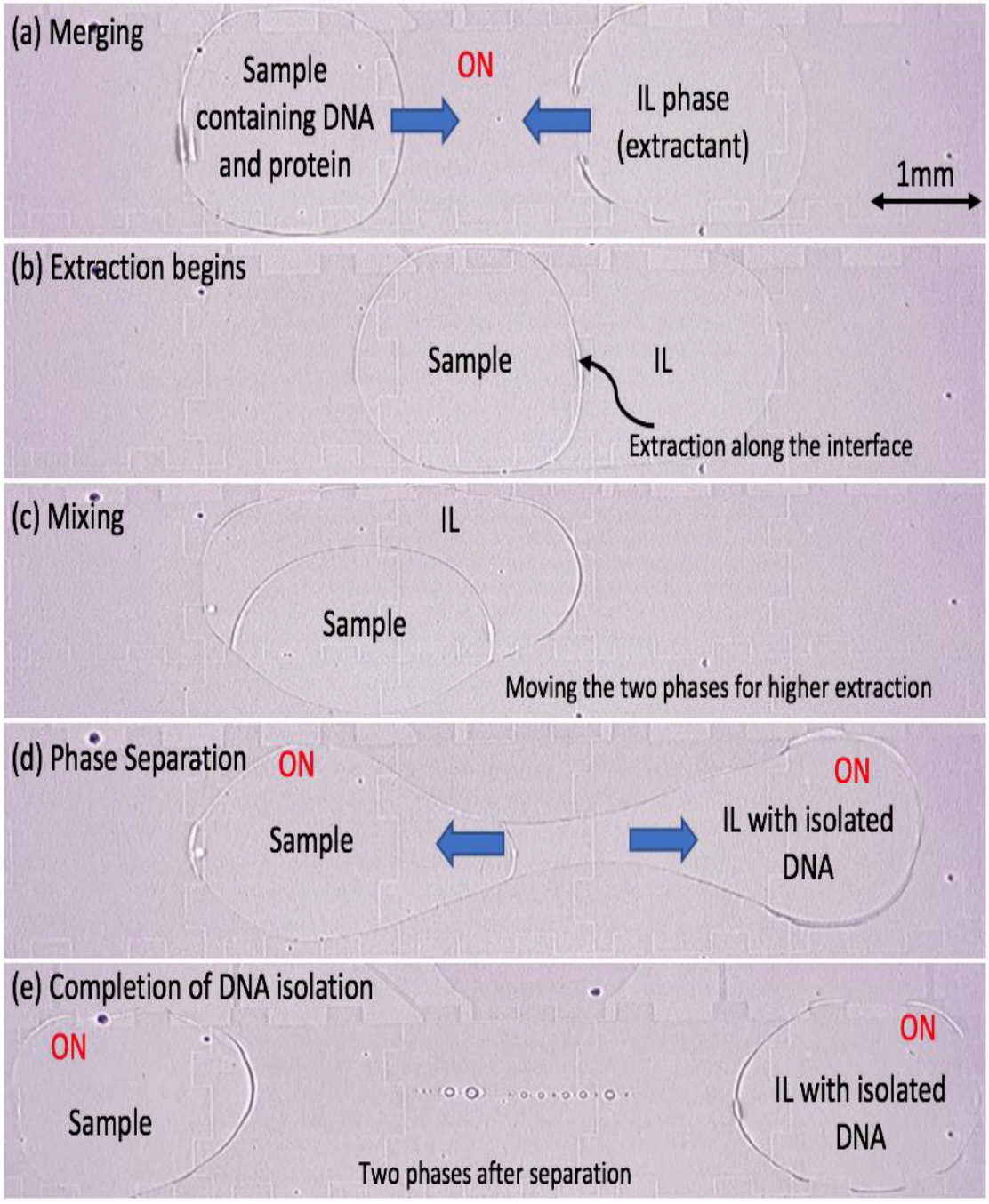

Figure 5.7: Snapshots from experiment of LLE on EWOD: a) the sample and the IL phases are merged, b) DNA extraction takes place along the interface of the phases, c) the phases are moved around to enhance extraction, d) the phases are split to conclude LLE, e) separated phases, the sample droplet is then collected for concentration measurement using NanoDrop™.

5.3.4 On-chip DNA LLE – Fluorescent image

Fluorescent images were taken and compared with a control sample, to have a qualitative result showing the extraction happening from the pDNA sample by the LLE process on-chip. After the LLE process, EtBr dye droplet was mixed with the sample on-chip. The intercalation of DNA-EtBr increases the fluorescent intensity when exposed to a wavelength of 285 *nm* ultraviolet light. The same concentration of EtBr was added to a sample droplet which did not undergo LLE. The device was then taken to a gel doc instrument, and a fluorescent image was taken when exposed to 285 *nm*. The intensity of the sample after LLE was quite less compared to the control sample (which did not undergo LLE), as demonstrated in Figure 5.8. This study demonstrates the successful extraction of DNA with the on-chip LLE process.

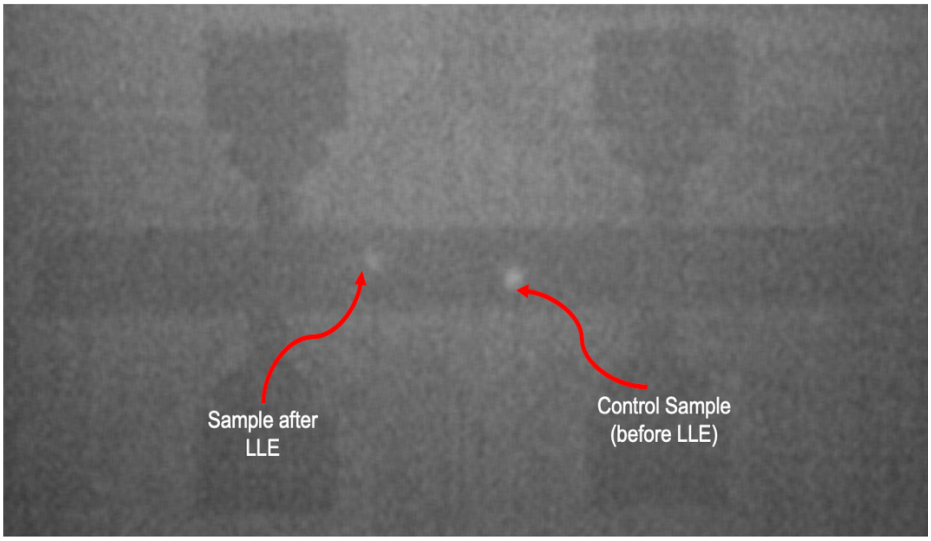

Figure 5.8: The change in the fluorescent intensity of the sample after the pDNA extraction. The sample after LLE and the control sample (without undergoing LLE) has the same EtBr concentration.

5.3.5 On-chip DNA LLE quantification

LLE tests were performed on the EWOD platform with pure pDNA as the sample in the first study. In the EWOD LLE experiments, 2 μl of pure pDNA droplet and 2 μl of IL droplet were transported onto the mixing region. After the splitting of the phases, the sample droplet was collected and transferred to NanoDrop^{TM} for concentration measurements. The residual DNA concentration in the sample was compared, and the extraction efficiency was calculated. Tests with different extraction times were performed. The results of this study are plotted in Figure 5.9. The extraction efficiency was plotted against the extraction time of the LLE process, as demonstrated. Experiments were conducted with each of the extraction time of 5, 10, and 15 minutes. Error bars in Figure 5.9 indicate the standard deviation using 3 data sets. As can be seen in Figure 5.9, the extraction efficiency increases with an increase in the extraction time. Experiments beyond 15 minutes of extraction time can be conducted in a saturated environment condition. In the present experimental setup, we observed a decrease in the volume of the sample due to evaporation beyond 15 minutes of LLE. So, the extraction time was set to an upper limit of 15 minutes. This study demonstrates the successful extraction of pDNA molecules from the sample into the IL phase on the EWOD platform in a DTD format. The IL phase with the extracted DNA molecules can now go for its downstream analysis.

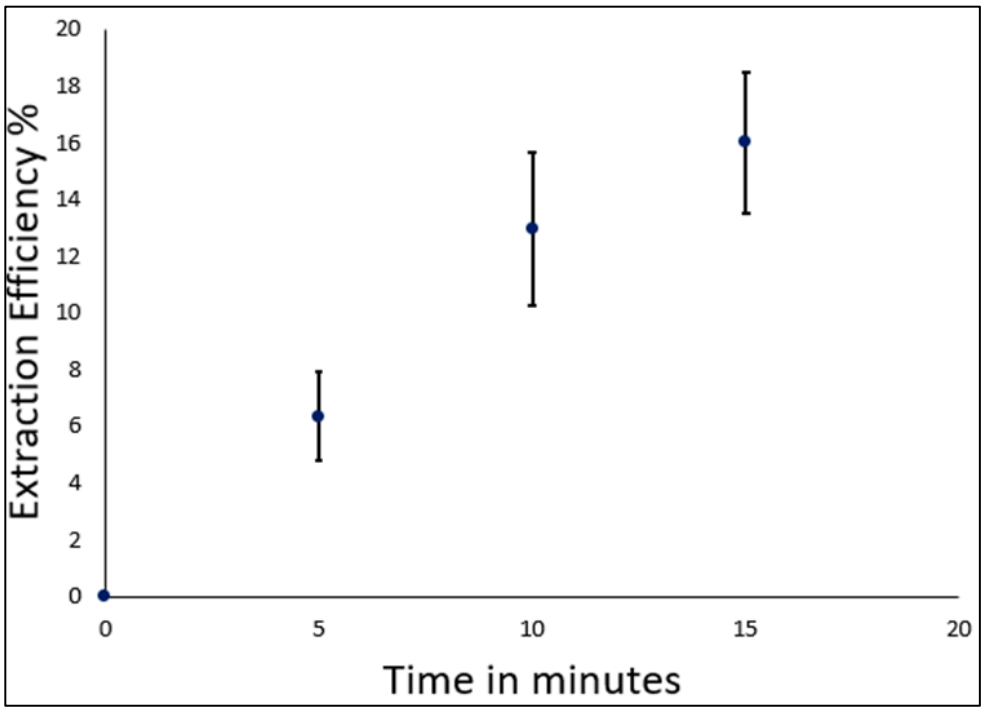

Figure 5.9: Extraction efficiency of pDNA from pure pDNA sample for different duration of LLE on-chip.

5.3.6 On-chip DNA extraction from DNA-protein mixture

Results from off-chip and on-chip LLE experiments showed the extraction of pDNA. These results show that BMIM-PF_6 can extract pDNA molecules. The results in section 5.3.1 also showed that the IL does not extract BSA protein molecules. This study was designed to demonstrate the selective extraction of pDNA on the EWOD platform.

The motion of the DNA sample mixed with protein was found to be very sluggish due to surface adsorption of the protein molecules. The surfactant Tween 20 was mixed with the sample to enhance the motion of the droplet, as was used in Chapter 4. The concentration of the surfactant was maintained the same for all the experiments. The motion was improved significantly, however, not the smoothest motion that can be achieved on EWOD without protein molecules. Separate

studies can be done to further enhance the sample movability with smart coatings of the top layer on EWOD and optimizing electrical parameters for droplet motion [105, 106].

DNA-protein mixture was prepared by adding BSA protein into the pure DNA sample to obtain an equal concentration 100 $ng/\mu l$ of DNA and protein in the sample. The mixture sample was then dispensed on EWOD to study the selective DNA extraction in the presence of protein impurities. Since it was confirmed from off-chip experiments that IL does not extract protein molecules, only DNA molecules were quantified for the on-chip experiments. This study demonstrated the effect on DNA extraction in the presence of protein molecules as impurities. Three sets of experiments were conducted for the mixture with an extraction time of 5, 10, and 15 minutes. After the LLE process, the sample was collected and used for DNA concentration measurement following the same procedure as mentioned before. The extraction efficiency of DNA was calculated and was plotted against time in Figure 5.10 (orange dot), and for comparison, the previous data (section 5.3.5) is also plotted in the same graph (blue dot).

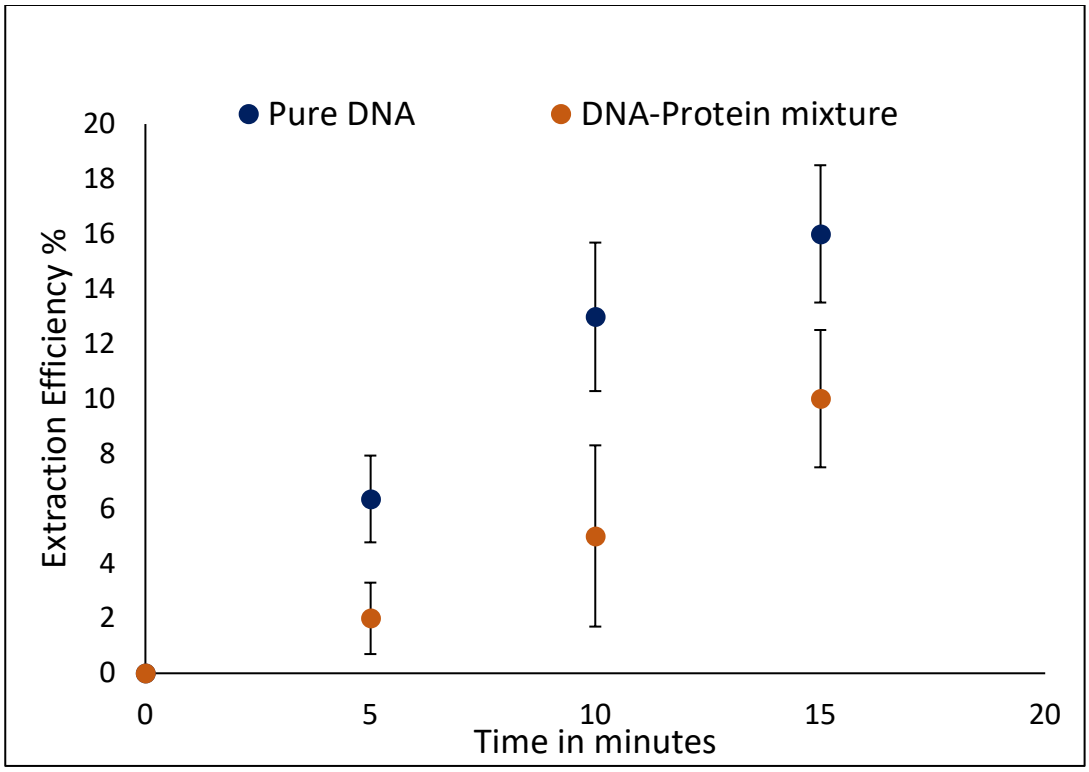

Figure 5.10: Extraction efficiency of pDNA from pure pDNA sample (blue dot), and from pDNA-protein mixture (orange dot) with different time duration of LLE on EWOD.

As shown in Figure 5.10, the extraction efficiency increases with the extraction time. The decrease in the efficiency of DNA extraction can be attributed to the presence of protein molecules in the sample, which damps the yield of the process. The sluggish motion of the two-phase droplets also contributed to the inferior mixing and, in turn, the poor extraction yield from the process. As described in section 5.3.1 and reported in [85], protein co-extraction was not observed with the present liquid-liquid system. Thus, the decrease in the on-chip pDNA extraction in the presence of protein molecules cannot be attributed to protein co-extraction. Although slightly lower extraction efficiency resulted when impurities (i.e., BSA) are present in the sample (Figure 5.10), the result still confirms that the proposed on-chip LLE protocol can selectively isolate DNA from a complex sample solution. The extraction yield can be improved further by designing a liquid-liquid system

in which the extractant has a very high affinity for DNA molecules, which is the basis for Chapter 6. The study reported in this chapter demonstrated the integration of DTD DNA LLE enabled by EWOD using IL as the extractant. It provided a microfluidic platform where quick and parallel DNA extractions can be performed in a fully automated fashion.

5.4 Conclusion

As the demand for automation and microsystems are on the rise for screening different genes and expressing on different cell lines at high throughput and performing parallel experiments, there is a need for integrating a simple automated protocol of DNA isolation and sample preparation in such systems. A novel microfluidic method of separation of DNA from other impurities such as protein was demonstrated in this work.

In this study, the DNA separates and extracts out preferentially from the sample phase because of its affinity for the IL extractant phase. In the first study, the control sample consisted of pure pDNA. The transfer of pDNA to the IL phase was demonstrated on the EWOD device. On-chip LLE was performed for different extraction times, and the extraction efficiency was found to increase with increasing extraction time. In the second study, protein molecules were added to the control sample as impurities, and selective extraction of pDNA was studied on the EWOD device. It was concluded that protein was not co-extracted in the on-chip LLE process, enabling the selective isolation of DNA for downstream analysis. The method presented in this chapter gets rid of both the use of magnetic beads and the use of an external magnetic field to separate DNA from the sample by enabling LLE in the EWOD microfluidic device. The DNA extraction efficiency can be improved further by having an extractant phase that has a much higher affinity for the target molecules. Compared to standard LLE of DNA in tube-based setups, LLE on EWOD platform

fully exploits drop-wise flow control for both sample and extractant phase. The capability of EWOD, when fully exploited it can enable parallel and serial extraction, as well as multiplexing of many different combinatorial extractions on a single chip, can also be readily performed, providing high-throughput capability if required.

Chapter 6

On-chip aqueous two-phase system -based DNA extraction enabled by EWOD digital microfluidics

Aqueous two-phase system (ATPS) is an alternative system for aqueous/organic or aqueous/IL (Aq./IL) extraction media for biomolecule separation. It is a special type of extraction system formed by two aqueous solutions – polymer/polymer (P/P) system or polymer/salt (P/S) system. These systems are known to be efficient for extraction and provide a gentle environment, especially for biomolecules. The study reported in this chapter was done to explore the integration of ATPS-based extraction of DNA on EWOD devices. Two different ATPSs were studied and reported in this chapter - i) polyethylene glycol/sodium citrate system (PEG/SC) and ii) polyethylene glycol /ammonium sulfate (PEG/AS) system. The ATPSs in this study were formed off-chip using a conventional method, and the pDNA was introduced to the PEG-rich phase. In the first study, the extraction of pDNA from the PEG-rich phase to the salt-rich phase was studied on-chip. The two droplets of PEG-rich and salt-rich phases were dispensed, merged, mixed, and split on the EWOD chip to complete the ATPE process. Enhanced efficiency of the DTD extraction of pDNA on EWOD was achieved with the ATPE method, as opposed to the Aq./IL system (presented in chapter 5). The extraction studies with each ATPS were done for various time durations, and the resulting extraction yields were compared. In the second study, BSA protein as interfering molecules was used to show the selective extraction of DNA from the sample mixture. As a demonstration of the screening capability of the EWOD platform to screen different liquid-liquid systems for DNA extraction, the extraction yield of all the systems reported in this dissertation (Aq./IL system and ATPSs) was compared.

6.1 Introduction

Martinus Willem Beijerinck accidentally discovered ATPS by mixing an aqueous solution of gelatin and starch [107]. ATPSs are formed by mixing two polymers of different structures or a polymer and a salt solution [108, 109]. Many other components can be used to form an ATPS, but P/P and P/S systems are the most common. The liquid phases are aqueous in nature, as the name suggests. The process of extraction or mass transfer across the boundary formed by the two phases is known as aqueous two-phase extraction (ATPE). This form of extraction has several advantages over other traditional methods such as – i) these systems are environment-friendly, ii) ease of scale-up and low cost, and iii) finally, they have shown great potential in extracting or separating biomolecules [110]. ATPE method of biomolecule extraction is widely used as a preprocess for concentration and purification of biomolecules such as – cell separations, protein purification, DNA/RNA extraction, and enzymes extraction [111-113].

In ATPSs, water is the primary solvent, and thus the system forms a very gentle environment for the biomolecules. Whereas, in other standard LLE methods, damage of the biomolecules is inevitable due to the harsh environment created by the organic solvents and other conventional extractant fluids. It has been shown in ATPSs, that the structure and biological activities of the molecules can be retained due to the aqueous nature of the medium, thus allowing relatively fewer degradations [110]. The entire process of ATPE, starting from the formation of ATPS, is shown in Figure 6.1. The two polymers or a polymer and a salt are added and then vortexed to have better mixing. It is then left to settle down, and this is when the two phases are formed (Figure 6.1 a).

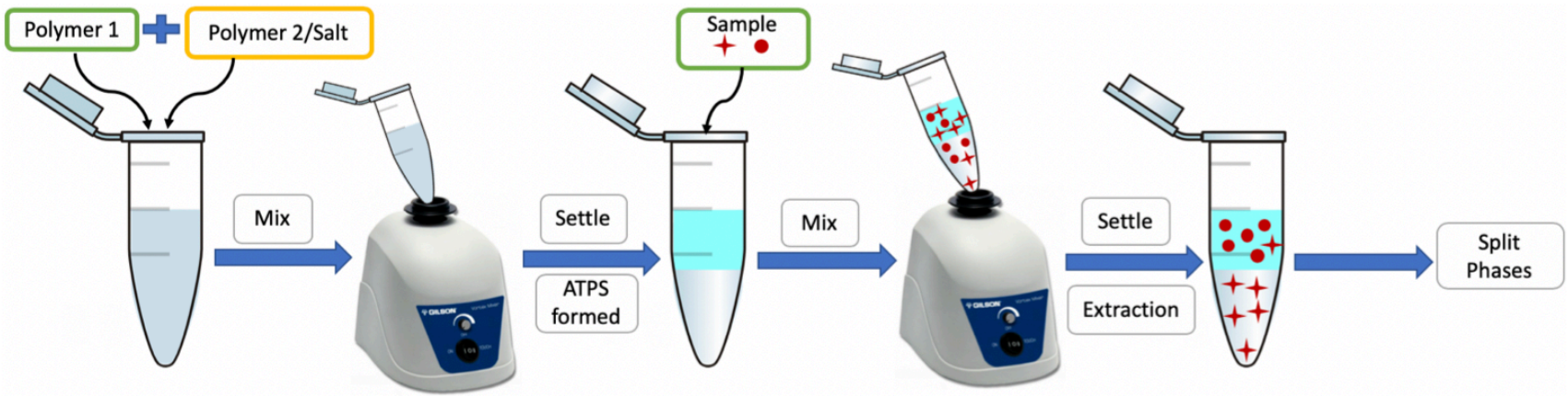
Polymer 1
Polymer 2/Salt
Mix
Sample
Settle
ATPS formed
Mix
Settle
Extraction
Split Phases
(a)
(b)
(c)

Figure 6.1: The overall process of aqueous two-phase formation and extraction by ATPE method. a) The salt solution and polymer are mixed and vortex; after settling down, they form the two phases. b) The sample mixture with the analyte of interest added and vortex for mixing; c) The phases separate again, and the analyte is extracted preferentially to one of the phases, the phases are then split.

The sample mixture of different molecules is then added and mixed to have proper distribution along the whole volume (Figure 6.1 b). After the solution settles back, the target molecules preferentially separate into one of the phases. The phases are then split, and now the molecules of interest are separated (Figure 6.1 c).

The partitioning of biomolecules in ATPS is mainly decided by the factors – hydrostatic and electrostatic interactions, the specific affinity of molecules, molecular size, and conformation. ATPS are mostly optimized by varying several variables, such as - physicochemical properties (e.g., molecular weight of polymer), pH, and temperature of the ATPS. Mujahid et al. provided an excellent review of all these variables on the partitioning of biomolecules in ATPS [110]. The optimization of these variables can be very laborious and may consume many reagents. There could be tremendous advancement with miniaturization and automation of ATPS based partition studies, with the ease of user-defined automated variables optimizations.

There have been attempts to perform ATPE in microscale with the help of microfluidics [114 – 116]. Most of the studies are done in continuous microfluidics. These systems suffer from the drawback of limited mixing capabilities and extraction time, and imperfect phase splitting at the end of the process. In most of the microsystems, ATPS is formed off-chip, and only the ATPE can be performed on-chip. Attempts have been made to study ATPE of different biomolecules in

the microscale, but very few studies have been done for ATPE of DNA molecules. The integration of the ATPE process for DNA molecules in the microscale could lead to a one-step solution for enriching the sample for the downstream nucleic acid assays. Due to the aqueous nature of the extractant phase, the sample can directly go for the next step in the workflow.

Wijethunga et al. reported the first study of the formation of ATPS on EWOD DMF, and the ATPE of dye molecules was demonstrated [117]. The present study is the first attempt to demonstrate the ATPE of DNA from a sample using two ATPSs on EWOD. Several research groups are actively investigating IL as an extractant for DNA isolation (as was studied in chapter 5). However, the DNA extracted by IL needs a buffer exchange step as most of the downstream nucleic acid assays are still done in the aqueous media [85]. Whereas, the extractant phase in ATPS being aqueous can directly go for the downstream assays. In this chapter, two ATPSs were studied for DNA extraction on EWOD. One system consisted of PEG/SC, and the other system consisted of PEG/AS. After the ATPE, the DNA was found to be concentrated in the salt-rich phase. The phases were split, and the salt-rich phase was acquired for DNA concentration measurement. Unlike chapter 5, where the DNA LLE was quantified by an indirect method by measuring the residual DNA concentration in the sample; in this study, the extracted DNA was quantified directly in the extractant phase. In the first study, on-chip ATPE was investigated, introducing pDNA in the PEG-rich phase (formed off-chip) with no other impurities present. The extraction yield for the system using PEG/SC was found to be higher than that of the PEG/AS system. In the second study, BSA protein molecules were spiked in the PEG-rich phase along with the pDNA molecules to study the selective extraction of pDNA from the mixture. The pDNA extraction yields were found to be again higher for the PEG/SC system over PEG/AS system. However, co-extraction of protein was also observed along with the pDNA molecules with both the ATPSs. The protein co-extraction

was found to be quite significant for the PEG/SC system. Thus, the PEG/AS system showed greater selectivity for pDNA extraction resulting in purer final pDNA product in the salt-rich phase.

6.2 Experimental

6.2.1 Chemicals

PEG (molar mass 600 g/mol), AS (molar mass 132.14 g/mol), and SC (molar mass 258.06 g/mol) were used to form the two different ATPSs. To obtain a particular polymer/salt (P/S) ATPS, pure solutions of PEG and AS or SC were mixed at designated concentrations. Altogether, two different ATPSs was formed to study the partition of pDNA in these systems. The ATPSs and their composition were selected by observing the biphasic curves, as reported in [118]. The biphasic curves give the information of the threshold concentrations, beyond which the resultant solution will separate into two phases.

For the DNA extraction study, the same pDNA pVAX1-hVEGF165 transformed in growth strain DH5-Alpha, was used as in the previous study (chapter 5). The bacterial strain was cultured to increase the colony, and from the expanded colony, the plasmid DNA was extracted using the Qiagen Hispeed kit. The pure pDNA sample mixed in the PEG-rich phase was used for all the control ATPE experiments. The details of the plasmid production steps can be found in section 5.2.4. BSA protein was used as the impurity molecules to show the selective extraction of DNA from a mixture of DNA and protein.

6.2.2 Fabrication and device design

The device design and the fabrication steps are the same as described in chapter 3.

6.2.3 ATPS formation

The two ATPSs used for pDNA partition study were prepared off-chip by mixing appropriate amounts of PEG solution and the salt in water, as shown in Figure 6.1 (a). The final composition of the ATPS prepared was 25% (w/w) PEG and 17% (w/w) of the salt. The systems were homogenized by vortexing for 5 minutes and then centrifuged at 4000 rpm for 5 minutes. The two aqueous phases were formed, and they were split very carefully. Pure pDNA was added to the PEG-rich phase, and concentration was adjusted to 100 $ng/\mu l$ and vortexed for proper mixing. The PEG-rich phase with the pDNA and the salt-rich phase were stored for the ATPE experiments. Now, the PEG-rich phase has the pDNA, and the extraction of pDNA from PEG to the salt-rich phase was studied both on EWOD and off-chip experiments.

6.2.4 Off-chip pDNA extraction

The DNA extraction was first studied off-chip using the ATPS formed as described in section 6.2.3. The PEG-rich phase containing the pDNA molecules was mixed with the salt-rich phase and vortex for 5 minutes. Here, the salt-rich phase acts as the extractant phase. The mixture was left to settle back to form the two phases. The phases were then very carefully split, and the bottom salt-rich phase was transferred for spectrophotometric based DNA concentration measurement. The presence of pDNA in the salt-phase confirmed the successful extraction of pDNA by the ATPS in off-chip experiments.

Separate experiments were conducted where BSA protein molecules were spiked into the PEG-rich phase to form a mixture of pDNA and protein. The same procedure of mixing and splitting the two phases was carried out. The salt-rich bottom phase was then analyzed for both pDNA and protein concentration.

6.2.5 On-chip pDNA extraction

The ATPS formed off-chip was used to demonstrate the ATPE process on EWOD, as illustrated in Figure 6.2 a. The PEG-rich phase containing pDNA, and the salt-rich phase were loaded on separate EWOD chip reservoirs. The initial concentration of pDNA in the PEG-rich phase was adjusted to 100 $ng/\mu l$. Two droplets of equal volume were dispensed from each reservoir by operating the EWOD device. The droplets were moved with the EWOD electrodes and were brought into contact, at which point the extraction begins. The merged liquid droplets were mixed by moving them in a particular fashion. The most optimized on-chip mixing scheme from the previous study reported in section 4.3.2 was adopted. This scheme of mixing was adopted to have the maximum extraction of pDNA from the PEG-rich phase to the salt-rich phase.

The end step of the process is to split the phases using EWOD forces, and the extractant droplet with the isolated pDNA can go for its downstream analysis. The phase splitting was achieved on-chip by driving the two phases onto two separate opposite electrodes and applying EWOD forces at opposite ends to split the phases at the interface. The salt-rich phase was analyzed for DNA concentration measurement to quantify the ATPE process on-chip. The entire on-chip ATPE protocol is illustrated in Figure 6.2 b. ATPE experiments were conducted for both the ATPS, and results were compared to find a system with a higher extraction yield.

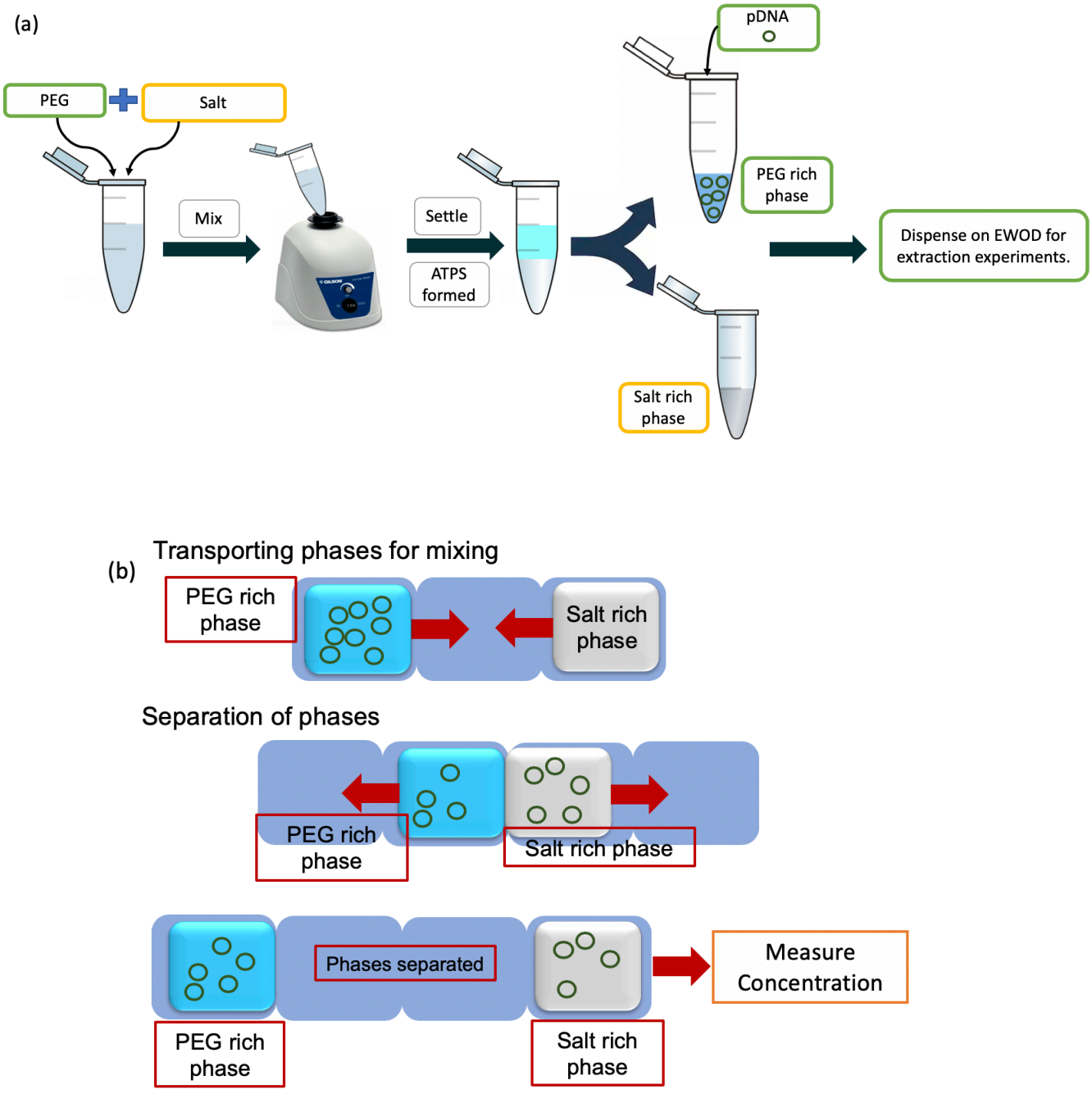

Figure 6.2: The protocol for ATPE – a) The ATPS was formed off-chip. The phases were split, and pDNA was introduced in the PEG-rich phase. b) The two phases were dispensed on EWOD to perform the extraction process.

Protein molecules were spiked into the PEG-rich phase to show the selectivity of on-chip pDNA extraction in a separate study. The concentration of pDNA and BSA in these experiments were adjusted to an equal concentration of 100 $ng/\mu l$.

6.2.6 Extraction quantification

The DNA extraction quantification for both on-chip and off-chip studies were done by using the NanoDrop™ instrument. After the extraction process, the salt-rich phase was collected and transferred to NanoDrop™ for concentration measurements. The DNA concentration measurement was done at 260 nm wavelength. The presence of pDNA in the salt confirmed the success of the ATPE process. Due to the aqueous nature of the extractant (salt-rich phase), it was compatible with NanoDrop™, and hence, the direct quantitation of the extractant phase was possible. This was not the case with the study reported in chapter 5, where the extractant (IL) phase was not compatible with the NanoDrop™ instrument. For the protein quantification, the salt-rich phase was measured at 280 nm wavelength in NanoDrop™. The blank used in all the measurements consisted of the initial salt-rich phase obtained from ATPS but without the pDNA or BSA molecules.

6.3 Results and discussion

6.3.1 Off-chip DNA extraction

The pDNA concentration in the salt-rich phase was measured from the off-chip ATPE experiments. Experiments were performed with both the ATPSs. Figure 6.3 shows peaks at 260 nm from the ATPE experiments in the salt-rich phase due to the presence of pDNA.

The salt-rich phase from the ATPS PEG/SC was analyzed in NanoDrop™, and the absorbance measurement is shown in Figure 6.3 (a). The total partitioning resulted in a 90% extraction of pDNA. The left figure shows no peak at 260 *nm* wavelength for the salt-rich phase before the ATPE experiment was conducted, whereas, the right figure shows a sharp peak at 260*nm* wavelength after the ATPE experiment (Figure 6.3 a). Figure 6.3 (b) represents the absorbance peaks of the salt-rich phase from the PEG/AS system extraction. It resulted in extraction efficiency of almost 70%. There was again no peak observed before the ATPE, and a sharp peak at 260 *nm* wavelength was observed after the extraction process (Figure 6.3 b). The presence of pDNA in the salt-rich phase in both systems confirmed the successful extraction of pDNA by the ATPSs. Thus, the two systems are suitable for studying the pDNA extraction on the EWOD platform.

(a)

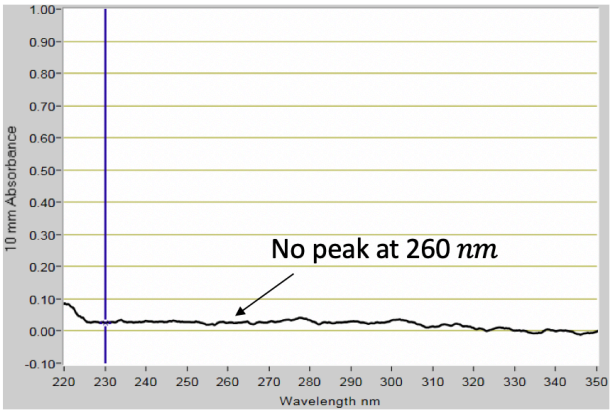

Salt-rich phase before ATPE

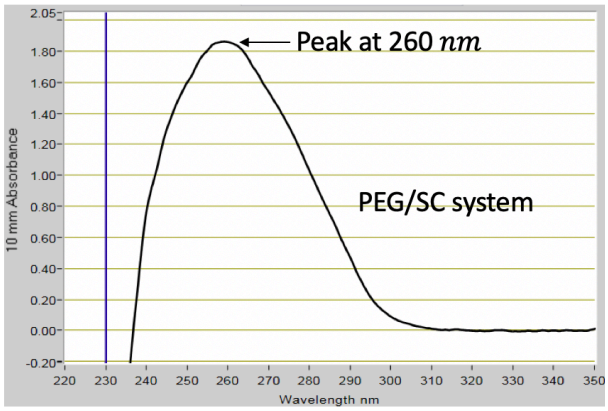

Salt-rich phase after ATPE

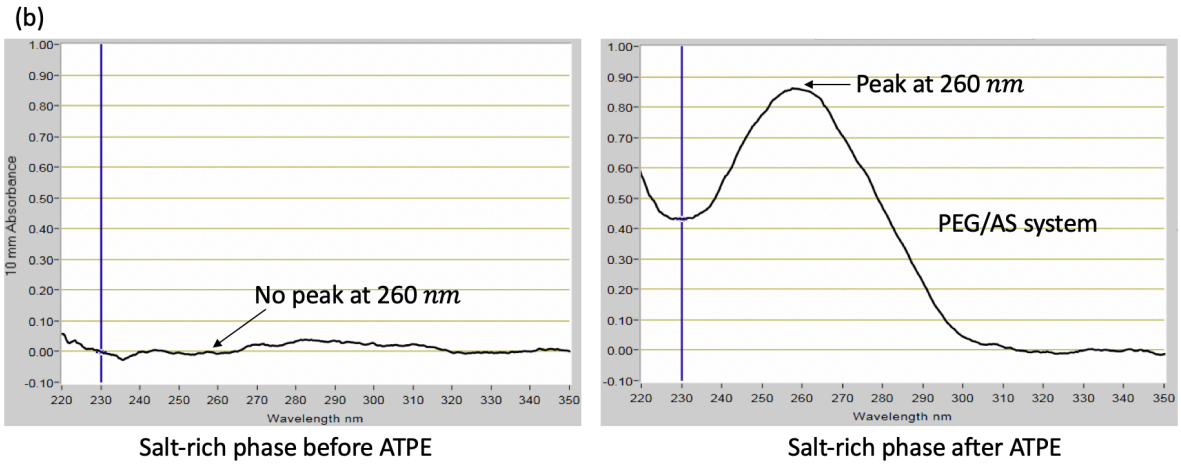

Figure 6.3: The salt-rich phase analyzed to quantify the pDNA extracted from off-chip ATPE at 260 nm wavelength. The peaks in the salt-rich phase before (left) and after (right) the ATPE process with a) PEG/SC and b) PEG/AS systems. Both the systems showing peaks at 260 nm wavelength in the salt-rich phase confirm the extraction of pDNA.

6.3.2 ATPE of pDNA on EWOD

The proposed EWOD based microfluidic device was successful in generating the PEG-rich phase with the pDNA molecules, and the salt-rich phase droplets of equal volume, transporting the droplets to the mixing and extraction zone, and finally split the two phases to complete the ATPE process. The optimized mixing, as described in section 4.3.2, was adopted for all the experiments. Similar to the study in Chapter 4, it was observed that the droplet, which was easy to actuate with EWOD forces, would engulf the other phase. In this study, the PEG-rich phase was more mobile than the salt-rich phase under the voltage application and hence, completely engulfing the later phase. During mixing, in this study, the salt-rich phase was kept stationary, and the PEG-rich phase was made to rotate around. The snapshots from the experiment of the entire protocol are shown in Figure 6.4.

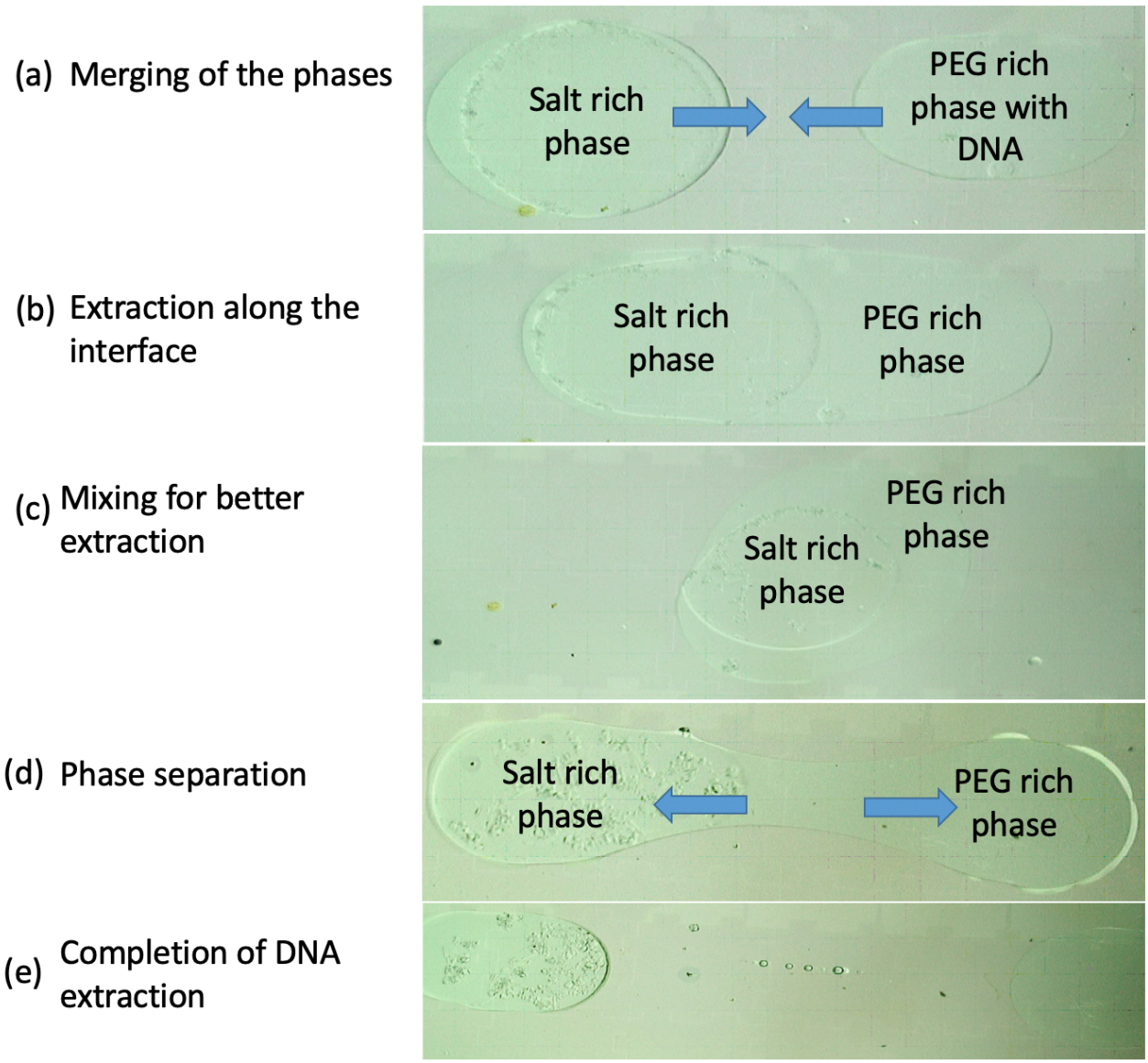

Figure 6.4: Snapshots of ATPE on EWOD: a) the salt-rich phase and the PEG-rich phases are merged, b) DNA extraction takes place along the interface of the phases, c) the phases are moved around to enhance mixing and extraction, d) the phases are split to conclude ATPE, e) split phases, the salt-rich phase is then collected for concentration measurement using NanoDrop™.

After the splitting of the phases, the salt-rich phase droplet was collected for concentration measurement. The volume of the salt-rich phase droplet retrieved from the EWOD device after the

ATPE process was ~2-3 μl. Individual droplet volume from each experiment was too small for multiple concentration measurements in the NanoDrop™ instrument. Thus, three similar experiments were done, and the droplets from each experiment were collected. The combined volume (~7-9 μl) from the three experiments was then used for the concentration measurements. The obtained measurement thus corresponds to one average data set (from three tests) for an experimental condition. Three similar sets of experiments were conducted to obtain three data sets, each consisting of three experimental repeats. Thus, the error bars in each of the following studies indicate standard deviation using a total of nine experimental repeats.

In the first study on EWOD, the PEG-rich phase contained only pDNA molecules to demonstrate the transfer of DNA molecules using ATPS. The results from the off-chip experiments (section 6.3.1), showed the successful extraction of pDNA with the two ATPSs. ATPE experiments were performed on the EWOD platform to demonstrate DTD format extraction. Experiments were performed by varying the extraction time at 5, 10, and 15 minutes. The results of the extraction efficiency are plotted against the extraction time of the on-chip ATPE process in Figure 6.5. The extraction efficiency was calculated by finding the difference in the salt-rich phase pDNA concentration before and after the process.

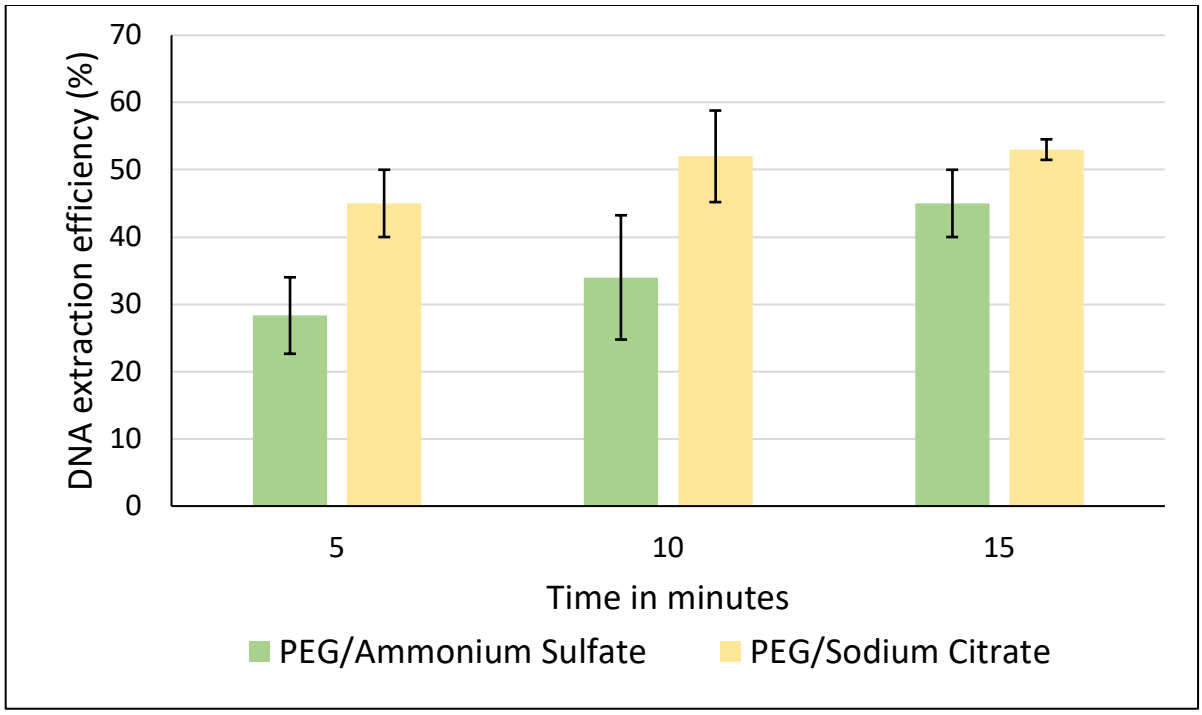

Figure 6.5: ATPE efficiency for the two ATPSs. The green bar represents the efficiency of the PEG/AS system, and the yellow bar represents the efficiency of the PEG/SC system.

Figure 6.5 illustrates the extraction efficiency obtained from two ATPS for different time periods of mixing. The green bar shows the efficiency obtained with the PEG/AS system, and the yellow bar represents that obtained with the PEG/SC system. As can be seen, in Figure 6.5, the extraction efficiency increases with the increase in the extraction time. Experiments beyond 15 minutes of extraction time can be conducted in a saturated environment condition. In our current experimental setup, we observed a decrease in the volume of the droplets (as was seen in the previous studies, chapters 4 and 5) due to evaporation beyond 15 minutes. So, the extraction time was set to an upper limit of 15 minutes in the present test setup. As can be seen in Figure 6.5, the ATPE with the PEG/SC shows a higher yield of pDNA extraction than that by the PEG/AS. The same trend is reported elsewhere with these ATPSs [85]. Also, to be noted here, the extraction

yield from these systems is higher compared to that obtained from the Aq./IL system, as was reported in chapter 5.

6.3.3 On-chip pDNA extraction from pDNA-protein mixture

In the second study, the ATPE performance of the two ATPS with interfering protein BSA molecules was conducted by adding protein to the PEG-rich phase. The control PEG-rich phase now has both the pDNA and the BSA molecules. The same procedure, as in section 6.3.2, was done for the on-chip ATPE process in this study. A droplet of the PEG-rich phase containing pDNA and protein and a droplet of salt-rich phase were introduced to the device. The two droplets were merged, and after proper mixing, they were split. The salt-rich phase was transferred for both DNA and protein quantification. Figure 6.6 shows the DNA extraction efficiency with protein spiked as an impurity. The pink bar represents the DNA extraction efficiency with the PEG/AS system, and the grey bar represents the DNA extraction efficiency with the PEG/SC system. The same trend, as was observed in section 6.3.2, is also seen here. The PEG/SC system shows a higher extraction yield compared to PEG/AS system. Not much decrease in DNA extraction efficiency (from the study in Figure 6.5) in the presence of protein was observed, as was the case with the Aq./IL system (section 5.3.6). The droplet motion was smooth in the case of ATPS on the EWOD platform upon the addition of the surfactant Tween 20 in the same procedure as described in section 4.3.3. Due to the ease of the movement of the ATPS droplets, it was possible to replicate the exact optimized mixing scheme, as was described in section 4.3.2. It was observed that the response of the ATPS to EWOD actuation was better compared to the Aq./IL system (reported in chapter 5).

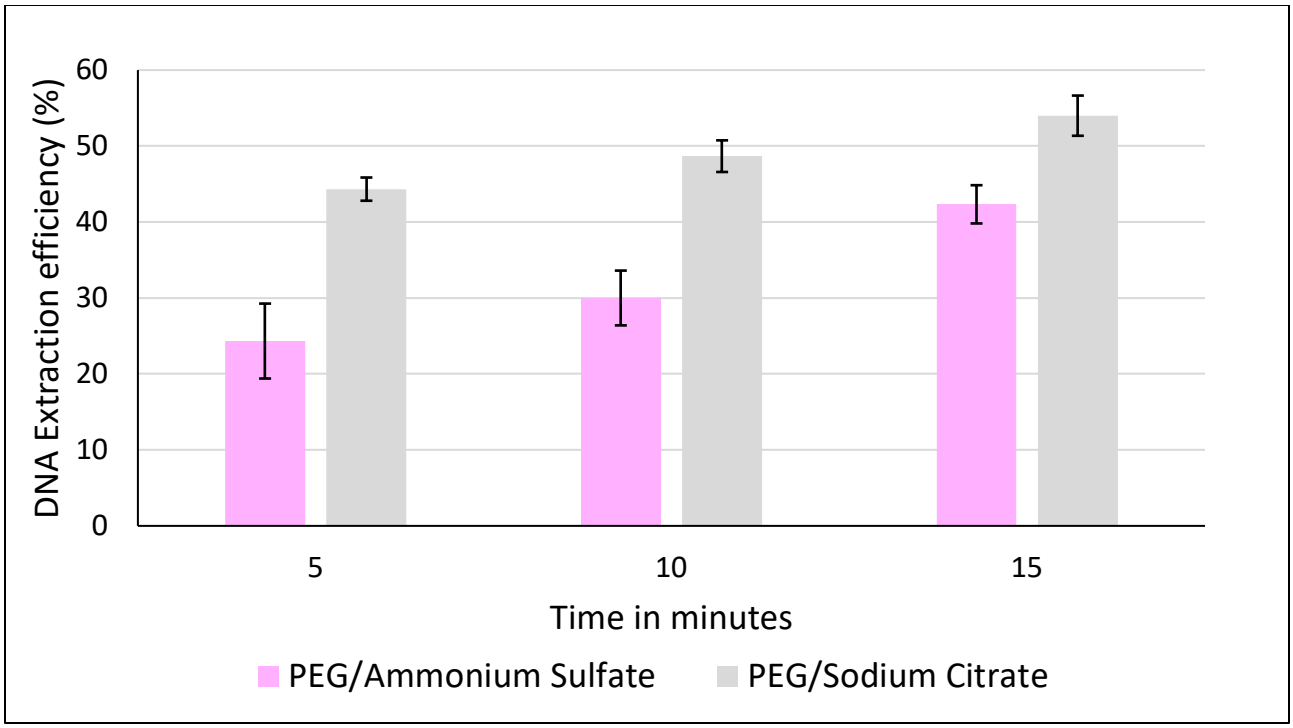

Figure 6.6: ATPE efficiency for the two ATPS with protein spiked in the PEG-rich phase. The pink bar represents the efficiency for the PEG-AS system and the grey bar represents the efficiency for the PEG-SC system.

The protein co-extraction was quantified by measuring the protein content in the salt-rich phase with NanoDrop™. It was found that with the PEG/AS system, the protein co-extraction was less, leading to much pure pDNA in the salt-rich phase than the PEG/SC system. Although the on-chip pDNA extraction with PEG/SC was high, the high protein co-extraction makes it less selective to pDNA extraction in the presence of other impurities (protein). The protein co-extraction by the salt-rich phase can be attributed to the pH of the system [110]. The pH of the two systems in this study was found to be in the range of 6.8-6.9 for all the experiments, which can induce a negative charge on the BSA protein molecules (isoelectric point of BSA is 4.8 [104]). The negative charge of the BSA molecules could be a factor for the electrostatic interaction with the positive

components of the salt-rich phase, which causes the co-extraction. The ratio of the DNA to protein extraction results for the two systems are plotted in Figure 6.7. The blue bar representing the PEG/AS system shows the increase in the ratio of DNA to protein extracted over time and is higher than the orange bar, which represents the PEG/SC system. The orange bar decreases with time as more protein molecules are also co-extracted with more extended extraction experiments, thus decreasing the purity of the final extracted pDNA. Hence, from these experiments, the PEG/AS system was found to be a better choice among the two ATPSs. As mentioned above, in future experiments, the pH of the system can be adjusted to study the effect on protein co-extraction.

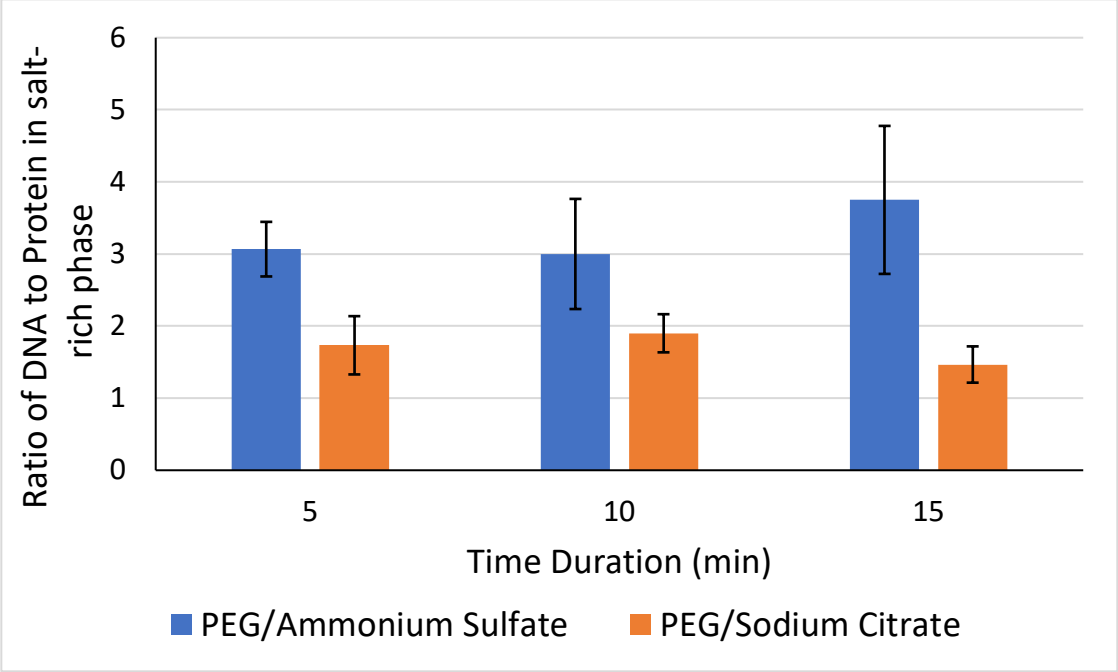

Figure 6.7: DNA to Protein ratio in the salt-rich phase after on-chip extraction.

6.3.4 Effect of initial pDNA concentration

For all the tests so far, the initial pDNA concentration in the PEG-rich phase was kept at 100 $ng/\mu l$. The extraction efficiency of 35% was achieved with the PEG/AS system when the

extraction is done for 10 minutes (Figure 6.5). However, if the initial pDNA (or lysate load, when the starting sample is cells) concentration is high, it can give the same extraction yield in a short period of extraction time. This study was done to see the effect of initial pDNA concentration in the extraction rate, where the extraction time was kept constant at 10 minutes. PEG/AS system was used for this study, and the PEG-rich phase contained only pDNA molecules. Sets of experiments were done with two initial pDNA concentrations in the PEG-rich phase: 100 $ng/\mu l$, and 300 $ng/\mu l$. The results of this study are plotted in Figure 6.8. With 300 $ng/\mu l$ initial pDNA concentration in the PEG-rich phase, a yield of 45% was reached within 10 minutes of the extraction. The same yield of 45% could be reached in 15 minutes when the pDNA concentration in the PEG-rich phase was 100 $ng/\mu l$ instead, as observed in section 6.3.2. The extraction yield was found to be proportional to the initial pDNA concentration. This observation can be explained in terms of the concentration gradient. When the concentration gradient between the two liquid phases are high, the extraction yield (or rate) is higher. Thus, this study shows that when the initial concentration can be estimated, then the extraction time can be optimized accordingly.

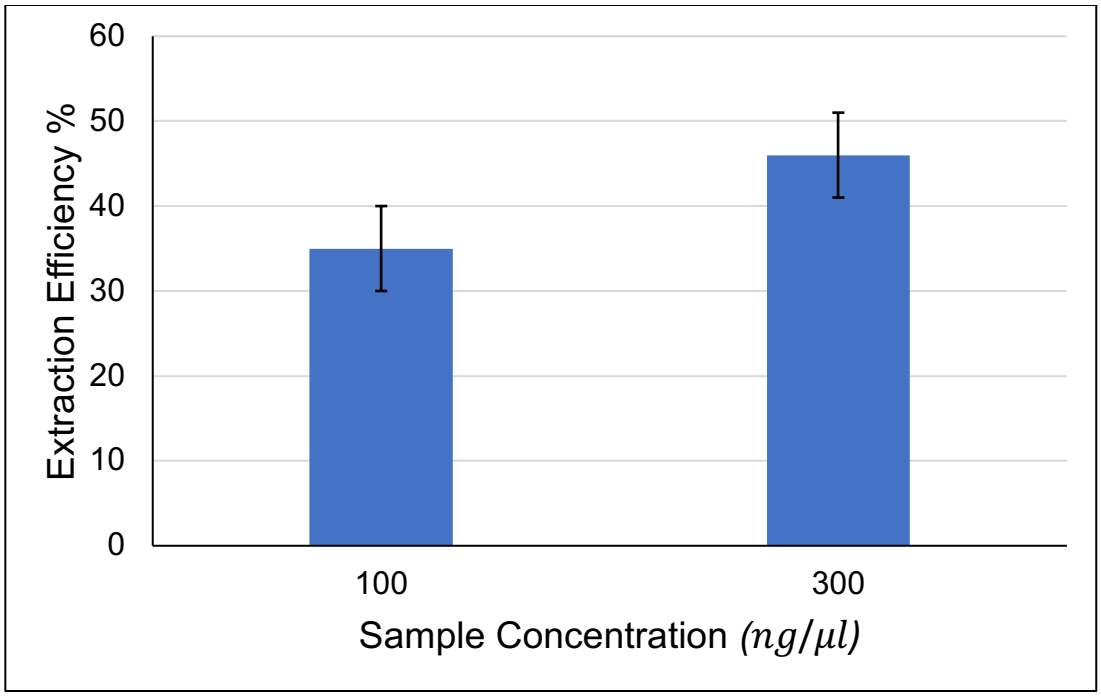

Figure 6.8: DNA extraction efficiency with PEG/AS system for different initial pDNA concentrations in the PEG-rich phase. Extraction time kept constant at 10 minutes.

6.3.5 EWOD capability of screening liquid-liquid systems for DNA extraction

Two-phase liquid system conditions often need to be optimized to achieve efficient extraction yield. The condition variables like- type of the liquid-liquid system (such as ATPS, Aq./IL, phenol extraction, etc.) pH, temperature, polymer/salt concentration can change the extraction efficiency. Typically, the system can be optimized on the final extraction yield from the process. Such optimization is a tedious process that requires substantial resources, including time and effort. On the contrary, an EWOD DMF technology becomes useful to address this problem. An EWOD device can easily produce droplet arrays where each droplet can act as individually controlled miniaturized systems bringing in unique ATPS formulation conditions on which several liquid-liquid systems, and variables can be tested.

As a demonstration of this capability of EWOD microfluidics, three different liquid-liquid systems were used in this entire work to study pDNA extraction in a DTD format on EWOD. The performance of the three systems studied is plotted in Figure 6.9. The grey bar for each system represents the DNA extraction efficiency, and the black bar represents the selectivity percentage for extraction experiments done for 15 minutes. The extraction with the Aq./IL system had minimal pDNA extraction. However, with protein molecules spiked in, no protein co-extraction was observed, making the pDNA selectivity to be maximum with the Aq./IL system, leading to a very pure pDNA in the extractant. The results from the two ATPS show higher pDNA extraction compared to IL, but with also some protein co-extraction. From Figure 6.9, it can be concluded that the PEG/AS has a better compromise of both with DNA extraction as high as 45% and selectivity as high as 80% as attained on the EWOD platform.

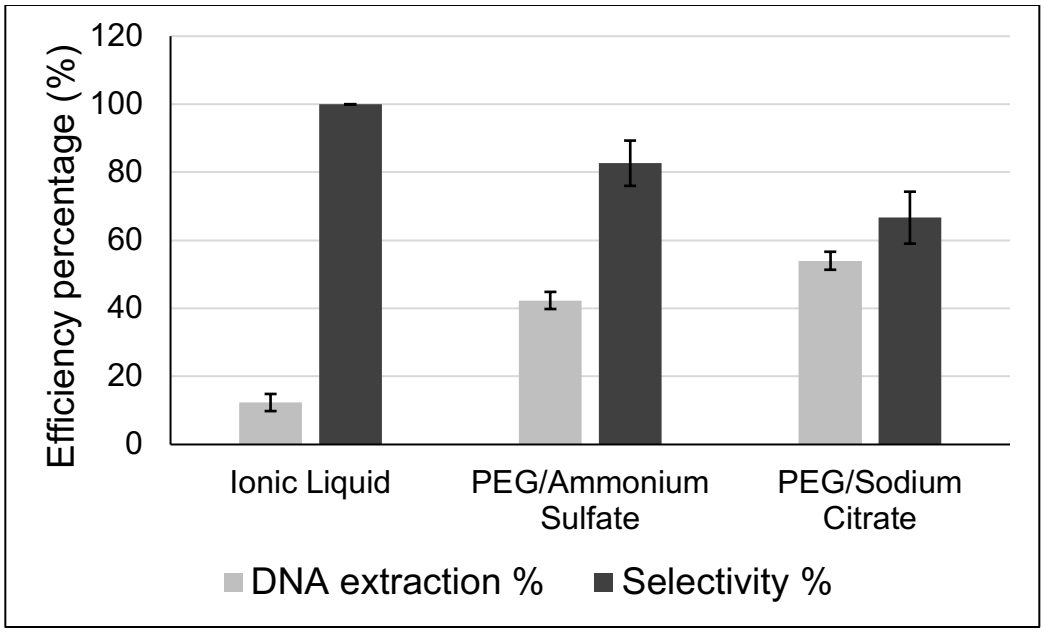

Figure 6.9: DNA extraction and selectivity with three liquid-liquid systems. The grey bar demonstrates the DNA extraction percentage efficiency from the pDNA-protein mixture, and the black bar demonstrates the selectivity percentage of DNA extraction - less selective means protein co-extraction along with DNA molecules.

This platform can be used to study several such liquid-liquid systems with varying parameters that make it very suitable for screening a library of systems. In this study, we have shown that by changing the salt in the ATPS, different DNA extraction yield, and purity of the final sample can be achieved. Similarly, several other ILs can also be screened for higher extraction, besides the one studied here.

6.4 Conclusion

ATPE of DNA was demonstrated in the EWOD DMF platform for the first time. DNA was successfully isolated in the salt-rich phase using this platform. The procedures of extraction and separation require only a few minutes, and thus, this process is much faster than the traditional beaker aqueous two-phase extraction, which takes a few hours. The aqueous nature of the extractant makes the DNA extracted readily available for the next analysis in the workflow.

The idea behind this study has been twofold. The initial study was to demonstrate the successful transfer of pDNA from the PEG-rich phase to the salt-rich phase in a DTD format on EWOD microfluidics without the presence of any other impurities. The extraction by the two ATPSs obtained on-chip was compared, and it was found that the PEG/SC system showed a higher extraction yield. The second study consisted of spiking protein molecules in the PEG-rich phase, along with pDNA, and on-chip ATPE was studied for the two systems. The motivation of this study was to show the on-chip selective extraction of pDNA using the two ATPSs. PEG/SC system showed higher pDNA extraction; however, the protein co-extraction with the PEG/SC system was also significant. The conclusion can be made that the PEG/AS system is the best system for pDNA isolation and purification on-chip in the experimental conditions studied here, as it successfully eliminated major protein impurities and selectively extracted pDNA molecules.

Due to the versatile nature of the device, the ATPS can be formed on the device for future studies. Further, different liquid-liquid systems and conditions can be quickly tested on-chip for rapid screening of their extraction performance. Parameters like different salt concentrations, salt combinations, pH, etc., can be rapidly tested in this platform. Altogether, this system provides a convenient as well as an effective method of studying different liquid-liquid systems as opposed to conducting experiments in lab-scale protocols.

References

[1] Reece JB, Urry LA, Cain ML, Wasserman SA, Minorsky PV, Jackson RB. Campbell biology. 9th ed. San Francisco, CA: Pearson Education, Inc.; 2011.

[2] Gormally, Emmanuelle, et al. "Circulating free DNA in plasma or serum as biomarker of carcinogenesis: practical aspects and biological significance." *Mutation Research/Reviews in Mutation Research* 635.2-3 (2007): 105-117.

[3] Juliano, R. L., Xin Ming, and Osamu Nakagawa. "The chemistry and biology of oligonucleotide conjugates." *Accounts of chemical research* 45.7 (2012): 1067-1076.

[4] Blau, Soren, et al. "The contributions of anthropology and mitochondrial DNA analysis to the identification of the human skeletal remains of the Australian outlaw Edward 'Ned'Kelly." *Forensic science international* 240 (2014): e11-e21.

[5] Whitcomb, David C., Celeste A. Shelton, and Randall E. Brand. "Genetics and genetic testing in pancreatic cancer." *Gastroenterology* 149.5 (2015): 1252-1264.

[6] Parsons, Juliana, et al. "A gene responsible for prolyl-hydroxylation of moss-produced recombinant human erythropoietin." *Scientific reports* 3 (2013): 3019.

[7] Kalia, Awdhesh, Ashok Rattan, and Prem Chopra. "A method for extraction of high-quality and high-quantity genomic DNA generally applicable to pathogenic bacteria." *Analytical biochemistry* 275.1 (1999): 1-5.

[8] Green, Michael R., and Joseph Sambrook. "Isolation of high-molecular-weight DNA using organic solvents." *Cold Spring Harbor Protocols* 2017.4 (2017): pdb-prot093450.

[9] Abdel-Latif, Amani, and Gamal Osman. "Comparison of three genomic DNA extraction methods to obtain high DNA quality from maize." *Plant Methods* 13.1 (2017): 1.

[10] Monteiro, Lurdes, et al. "Complex polysaccharides as PCR inhibitors in feces: Helicobacter pylori model." *Journal of clinical microbiology* 35.4 (1997): 995-998.

[11] Rogacs, Anita, Lewis A. Marshall, and Juan G. Santiago. "Purification of nucleic acids using isotachophoresis." *Journal of Chromatography A* 1335 (2014): 105-120.

[12] Alaeddini, Reza. "Forensic implications of PCR inhibition—a review." *Forensic Science International: Genetics* 6.3 (2012): 297-305.

[13] Figeys, Daniel, and Devanand Pinto. "Lab-on-a-chip: a revolution in biological and medical sciences." (2000): 330-A.

[14] Huang, Chao-Wei, et al. "Efficient SNP discovery by combining microarray and lab-on-a-chip data for animal breeding and selection." *Microarrays* 4.4 (2015): 570-595.

[15] Chong, Zhuang Zhi, et al. "Active droplet generation in microfluidics." *Lab on a Chip* 16.1 (2016): 35-58.

[16] Fouillet, Yves, et al. "Digital microfluidic design and optimization of classic and new fluidic functions for lab on a chip systems." *Microfluidics and Nanofluidics* 4.3 (2008): 159-165.

[17] Chang, Yi-Hsien, et al. "Integrated polymerase chain reaction chips utilizing digital microfluidics." *Biomedical microdevices* 8.3 (2006): 215-225.

[18] Li, Xiujun James, and Yu Zhou, eds. *Microfluidic devices for biomedical applications*. Elsevier, 2013.

[19] Shen, Hsien-Hua, et al. "EWOD microfluidic systems for biomedical applications." *Microfluidics and Nanofluidics* 16.5 (2014): 965-987.

[20] Brennan, Des, et al. "An integrated hybrid system for genetic analysis combining EWOD sample preparation and magnetic detection." *Journal of Physics: Conference Series*. Vol. 307. No. 1. IOP Publishing, 2011.

[21] Lin, Tai-Hsuan, and Da-Jeng Yao. "Applications of EWOD systems for DNA reaction and analysis." *Journal of Adhesion Science and Technology* 26.12-17 (2012): 1789-1804.

[22] Delattre, Cyril, et al. "Macro to microfluidics system for biological environmental monitoring." *Biosensors and Bioelectronics* 36.1 (2012): 230-235.

[23] Petralia, Salvatore, Daniele Motta, and Sabrina Conoci. "EWOD silicon biosensor for multiple nucleic acids analysis." *Biotechnology and bioengineering* (2019).

[24] Coelho, Beatriz, et al. "Digital microfluidics for nucleic acid amplification." *Sensors* 17.7 (2017): 1495.

[25] Hung, Ping-Yi, et al. "Genomic DNA extraction from whole blood using a digital microfluidic (DMF) platform with magnetic beads." *Microsystem Technologies* 23.2 (2017): 313-320.

[26] Kim, Hanyoup, et al. "Automated digital microfluidic sample preparation for next-generation DNA sequencing." *JALA: Journal of the Association for Laboratory Automation* 16.6 (2011): 405-414.

[27] Abdel-Latif, Amani, and Gamal Osman. "Comparison of three genomic DNA extraction methods to obtain high DNA quality from maize." *Plant Methods* 13.1 (2017): 1.

[28] McCormick, Randy M. "A solid-phase extraction procedure for DNA purification." *Analytical biochemistry* 181.1 (1989): 66-74.

[29] Kudr, Jiri, et al. "Magnetic nanoparticles: From design and synthesis to real world applications." *Nanomaterials* 7.9 (2017): 243.

[30] QIAprep® Miniprep Handbook

[31] "Nucleic Acid Separation." *Nucleic Acid Separation - Technical Platform - Creative Diagnostics*, www.cd-bioparticles.com/t/Nucleic-Acid-Separation_49.html.

[32] "Chemagic™ 360 Nucleic Acid Extractor." *Biocompare*, 21 Dec. 2019, www.biocompare.com/9977.

[33] Albariño, César G., and Víctor Romanowski. "Phenol extraction revisited: a rapid method for the isolation and preservation of human genomic DNA from whole blood." *Molecular and cellular probes* 8.5 (1994): 423-427.

[34] Hummon, Amanda B., et al. "Isolation and solubilization of proteins after TRIzol® extraction of RNA and DNA from patient material following prolonged storage." *Biotechniques* 42.4 (2007): 467-472.

[35] Tan, Siun Chee, and Beow Chin Yiap. "DNA, RNA, and protein extraction: the past and the present." *BioMed Research International* 2009 (2009).

[36] Drábková, Lenka, J. A. N. Kirschner, and Ĉestmír Vlĉek. "Comparison of seven DNA extraction and amplification protocols in historical herbarium specimens of Juncaceae." *Plant Molecular Biology Reporter* 20.2 (2002): 161-175.

[37] Liu, Mei, et al. "Extraction of DNA from complex biological sample matrices using guanidinium ionic liquid modified magnetic nanocomposites." *RSC advances* 9.40 (2019): 23119-23128.

[38] Tateishi-Karimata, Hisae, and Naoki Sugimoto. "Biological and nanotechnological applications using interactions between ionic liquids and nucleic acids." *Biophysical reviews* 10.3 (2018): 931-940.

[39] Trindade, Inês P., et al. "Purification of plasmid DNA vectors by aqueous two-phase extraction and hydrophobic interaction chromatography." *Journal of Chromatography A* 1082.2 (2005): 176-184.

[40] Ali, Nasir, et al. "Current nucleic acid extraction methods and their implications to point-of-care diagnostics." *BioMed research international* 2017 (2017).

[41] Breadmore, Michael C., et al. "Microchip-based purification of DNA from biological samples." *Analytical chemistry* 75.8 (2003): 1880-1886.

[42] Morales, Mercedes C., and Jeffrey D. Zahn. "Droplet enhanced microfluidic-based DNA purification from bacterial lysates via phenol extraction." *Microfluidics and nanofluidics* 9.6 (2010): 1041-1049.

[43] Stanley, Claire E., Robert CR Wootton, and Andrew J. deMello. "Continuous and segmented flow microfluidics: Applications in high-throughput chemistry and biology." *CHIMIA International Journal for Chemistry* 66.3 (2012): 88-98.

[44] Jeon, Noo Li, et al. "Microfluidics section: design and fabrication of integrated passive valves and pumps for flexible polymer 3-dimensional microfluidic systems." *Biomedical Microdevices* 4.2 (2002): 117-121.

[45] Cady, Nathaniel C., Scott Stelick, and Carl A. Batt. "Nucleic acid purification using microfabricated silicon structures." *Biosensors and Bioelectronics* 19.1 (2003): 59-66.

[46] Perez-Toralla, Karla, et al. "Microfluidic extraction and digital quantification of circulating cell-free DNA from serum." *Sensors and Actuators B: Chemical* 286 (2019): 533-539.

[47] Zhang, Rui, et al. "A microfluidic liquid phase nucleic acid purification chip to selectively isolate DNA or RNA from low copy/single bacterial cells in minute sample volume followed by direct on-chip quantitative PCR assay." *Analytical chemistry* 85.3 (2013): 1484-1491.

[48] Torabinia, Matin, et al. "On-chip organic synthesis enabled using an engine-and-cargo system in an electrowetting-on-dielectric digital microfluidic device." *Lab on a Chip* 19.18 (2019): 3054-3064.

[49] Aizenberg, Joanna, Tom Krupenkin, and Paul Kolodner. "Accelerated chemical reactions for lab-on-a-chip applications using electrowetting-induced droplet self-oscillations." *MRS Online Proceedings Library Archive* 915 (2006).

[50] Miller, Elizabeth M., and Aaron R. Wheeler. "A digital microfluidic approach to homogeneous enzyme assays." *Analytical Chemistry* 80.5 (2008): 1614-1619.

[51] Chang, Yi-Hsien, et al. "Integrated polymerase chain reaction chips utilizing digital microfluidics." *Biomedical microdevices* 8.3 (2006): 215-225.

[52] Wheeler, Aaron R., et al. "Digital microfluidics with in-line sample purification for proteomics analyses with MALDI-MS." *Analytical Chemistry* 77.2 (2005): 534-540.

[53] Rival, A., et al. "An EWOD-based microfluidic chip for single-cell isolation, mRNA purification and subsequent multiplex qPCR." *Lab on a Chip* 14.19 (2014): 3739-3749.

[54] Samiei, Ehsan, Maryam Tabrizian, and Mina Hoorfar. "A review of digital microfluidics as portable platforms for lab-on a-chip applications." *Lab on a Chip* 16.13 (2016): 2376-2396.

[55] Novotný, Jakub, and František Foret. "Fluid manipulation on the micro-scale: Basics of fluid behavior in microfluidics." *Journal of separation science* 40.1 (2017): 383-394.

[56] Nelson, Wyatt C., and Chang-Jin 'CJ Kim. "Droplet actuation by electrowetting-on-dielectric (EWOD): A review." *Journal of Adhesion Science and Technology* 26.12-17 (2012): 1747-1771.

[57] Nahar, Mun Mun. *NUMERICAL AND EXPERIMENTAL STUDY OF SINGLE PHASE AND MULTIPHASE DROPLET DYNAMICS ON ELECTROWETTING-ON-DIELECTRODE DIGITAL MICRO-FLUIDICS*. Diss. 2018.

[58] Nanayakkara, Yasith Sameera. "Electrowetting of ionic liquids and development of an electrowetting based tunable RC filter and its uses as an analytical detector." (2011).

[59] Nikapitiya, NY Jagath B., Mun Mun Nahar, and Hyejin Moon. "Accurate, consistent, and fast droplet splitting and dispensing in electrowetting on dielectric digital microfluidics." *Micro and Nano Systems Letters* 5.1 (2017): 24.

[60] S. Pedersen-Bjergaard and K.E. Rasmussen, Liquid-Liquid Microextraction for Sample Preparation of Biological Fluids Prior to Capillary Electrophoresis, Anal. Chem., vol. 71, no. 14, pp. 26502656, Jan. 1999.

[61] Hanai, Toshihiko. "Chromatography and computational chemical analysis for drug discovery." Current medicinal chemistry 12.5 (2005): 501-525.

[62] Pearson, David. The chemical analysis of foods. No. Ed. 7. Longman Group Ltd., 1976.

[63] Kula, Maria-Regina, Karl Heinz Kroner, and Helmut Hustedt. "Purification of enzymes by liquid-liquid extraction." reaction engineering. Springer, Berlin, Heidelberg, 1982. 73-118.

[64] H. Liu and P. K. Dasgupta. "Analytical chemistry in a drop. Solvent extraction in a Microdrop," Analytical Chemistry, vol. 68, no. 11, pp. 1817-1821, Jan. 1996.J. Clerk Maxwell, A Treatise on Electricity and Magnetism, 3rd ed., vol. 2. Oxford: Clarendon, 1892, pp.68–73.

[65] Guo, Mira T., et al. "Droplet microfluidics for high-throughput biological assays." Lab on a Chip 12.12 (2012): 2146-2155.

[66] P. A. L. Wijethunga, Y. S. Nanayankar, P. Kunchala, D. W. Armstrong, and H. Moon, "Onchip drop-to- drop liquid Microextraction coupled with real-time concentration monitoring technique." Analytical chemistry, vol. 83, no. 5, pp. 1658-1664, Mar. 2011.

[67] Wheeler, A. R. Science 2008, 322, 539.

[68] Moon, H.; Wheeler, A. R.; Garrell, R. L.; Loo, J. A.; Kim, C. J. Lab Chip 2006, 6, 1213–1219.

[69] Srinivasan, V.; Pamula, V. K.; Fair, R. B. Anal. Chim. Acta 2004, 507, 145–150

[70] Srinivasan, V.; Pamula, V. K.; Fair, R. B. Lab Chip 2004, 4, 310–315.

[71] Srinivasan, V.; Pamula, V.; Pollack, M.; Fair, R. A Digital Microfluidic Biosensor for Multianalyte Detection. In Proceedings of the IEEE 16th Annual International Conference on Micro Electro Mechanical Systems, Cho, Y.-H., Tabata, O., Eds.; IEEE explore digital library: Kyoto, Japan, January 19-23, 2003; pp 327-330.

[72] Satoh, W.; Hosono, H.; Suzuki, H. Anal. Chem. 2005, 77, 6857–6863.

[73] Dubois, P.; Marchand, G.; Fouillet, Y.; Berthier, J.; Douki, T.; Hassine, F.; Gmouh, S.; Vaultier, M. Anal. Chem. 2006, 78, 4909–4917.

[74] Tateishi-Karimata, Hisae, and Naoki Sugimoto. "Biological and nanotechnological applications using interactions between ionic liquids and nucleic acids." *Biophysical reviews* 10.3 (2018): 931-940.

[75] Emaus, Miranda N., et al. "Preconcentration of DNA using magnetic ionic liquids that are compatible with real-time PCR for rapid nucleic acid quantification." *Analytical and bioanalytical chemistry* 410.17 (2018): 4135-4144.

[76] https://en.wikipedia.org/wiki/1-Butyl-3-methylimidazolium_hexafluorophosphate.

[77] Srinivasan, Vijay, Vamsee K. Pamula, and Richard B. Fair. "Droplet-based microfluidic lab-on-a-chip for glucose detection." *Analytica Chimica Acta* 507.1 (2004): 145-150.

[78] Yoon, Jeong-Yeol, and Robin L. Garrell. "Preventing biomolecular adsorption in electrowetting-based biofluidic chips." *Analytical Chemistry* 75.19 (2003): 5097-5102.

[79] Latip, EN Abdul, et al. "Protein droplet actuation on superhydrophobic surfaces: A new approach toward anti-biofouling electrowetting systems." *Rsc Advances* 7.78 (2017): 49633-49648.

[80] Cho, Sung Kwon, Hyejin Moon, and Chang-Jin Kim. "Creating, transporting, cutting, and merging liquid droplets by electrowetting-based actuation for digital microfluidic circuits." *Journal of Microelectromechanical systems* 12.1 (2003): 70-80.

[81] Walker, Shawn W., and Benjamin Shapiro. "Modeling the fluid dynamics of electrowetting on dielectric (EWOD)." *Journal of Microelectromechanical Systems* 15.4 (2006): 986-1000.

[82] Nahar, Mun Mun, and Hyejin Moon. "Phase separation of multiphase droplets in a digital microfluidic device." *Micro and Nano Systems Letters* 7.1 (2019): 19.

[83] Schuur, Boelo, et al. "Chiral separation by enantioselective liquid–liquid extraction." *Organic & Biomolecular Chemistry* 9.1 (2011): 36-51.

[84] Clark, Kevin D., et al. "Extraction of DNA by magnetic ionic liquids: tunable solvents for rapid and selective DNA analysis." Analytical chemistry 87.3 (2015): 1552-1559.

[85] Wang, Jian-Hua, et al. "Direct extraction of double-stranded DNA into ionic liquid 1-butyl-3-methylimidazolium hexafluorophosphate and its quantification." Analytical chemistry 79.2 (2007): 620-625.

[86] Pavlović, Sonja, et al. "Genomics as a basis for precision medicine." Biologia Serbica 39.1 (2017).

[87] Fackler, Jennifer L., and Amy L. McGuire. "Paving the way to personalized genomic medicine: steps to successful implementation." Current Pharmacogenomics and Personalized Medicine (Formerly Current Pharmacogenomics)7.2 (2009): 125-132.

[88] Berensmeier, Sonja. "Magnetic particles for the separation and purification of nucleic acids." *Applied microbiology and biotechnology* 73.3 (2006): 495-504.

[89] Witt, Sebastian, et al. "Establishing a novel automated magnetic bead-based method for the extraction of DNA from a variety of forensic samples." *Forensic Science International: Genetics* 6.5 (2012): 539-547.

[90] Chung, Yung-Chiang, et al. "Microfluidic chip for high efficiency DNA extraction." Lab on a Chip 4.2 (2004): 141-147.

[91] Hui, Wing C., et al. "Microfluidic systems for extracting nucleic acids for DNA and RNA analysis." Sensors and Actuators A: Physical 133.2 (2007): 335-339.

[92] Sambrook, Joseph, and David W. Russell. "Purification of nucleic acids by extraction with phenol: chloroform." Cold Spring Harbor Protocols 2006.1 (2006): pdb-prot4455.

[93] Lethesh, Kallidanthiyil Chellappan, et al. "Synthesis of magnesium complexes of ionic liquids with highly coordinating anions." *Dalton Transactions* 48.3 (2019): 982-988.

[94] Dobler, Dorota, et al. "Ionic liquids as ingredients in topical drug delivery systems." *International journal of pharmaceutics* 441.1-2 (2013): 620-627.

[95] Singh, Nripat, et al. "Very High Concentration Solubility and Long-Term Stability of DNA in an AmmoniumBased Ionic Liquid: A Suitable Medium for Nucleic Acid Packaging and Preservation." ACS Sustainable Chemistry & Engineering 5.2 (2017): 1998-2005.

[96] Clark, Kevin D., et al. "Magnetic ionic liquids as PCR-compatible solvents for DNA extraction from biological samples." Chemical Communications 51.94 (2015): 16771-16773.

[97] Bowers, Ashley N., et al. "Extraction of DNA with magnetic ionic liquids using in situ dispersive liquid–liquid microextraction." *Analytical and bioanalytical chemistry* 411.28 (2019): 7375-7385.

[98] https://www.sciencelearn.org.nz/resources/1900-bacterial-dna-the-role-of-plasmids

[99] Marshall Jr, William G., et al. "Electroporation-mediated delivery of a naked DNA plasmid expressing VEGF to the porcine heart enhances protein expression." *Gene therapy* 17.3 (2010): 419.

[100] Sinha, Hugo, et al. "An automated microfluidic gene-editing platform for deciphering cancer genes." *Lab on a Chip* 18.15 (2018): 2300-2312.

[101] Madison, Andrew C., et al. "Scalable device for automated microbial electroporation in a digital microfluidic platform." *ACS synthetic biology* 6.9 (2017): 1701-1709.

[102] Gach, Philip C., et al. "Droplet microfluidics for synthetic biology." *Lab on a Chip* 17.20 (2017): 3388-3400.

[103] JimmyáHuang, Po-Jung. "Extraction of DNA staining dyes from DNA using hydrophobic ionic liquids." *Chemical Communications* 49.40 (2013): 4537-4539.

[104] Salis, Andrea, et al. "Measurements and theoretical interpretation of points of zero charge/potential of BSA protein." *Langmuir* 27.18 (2011): 11597-11604.

[105] McHale, Glen, et al. "Apparent Contact Angles on Lubricant-Impregnated Surfaces/SLIPS: From Superhydrophobicity to Electrowetting." *Langmuir* 35.11 (2019): 4197-4204.

[106] Torabinia, Matin, Ali Farzbod, and Hyejin Moon. "Electromechanical model to predict the movability of liquids in an electrowetting-on-dielectric microfluidic device." *Journal of Applied Physics* 123.15 (2018): 154902.

[107] Ola, Pius Dore, and Michiaki Matsumoto. "Metal Extraction with Ionic Liquids-Based Aqueous Two-Phase System." *Recent Advances in Ionic Liquids* (2018): 145.

[108] Asenjo, Juan A., and Barbara A. Andrews. "Aqueous two-phase systems for protein separation: a perspective." *Journal of Chromatography A* 1218.49 (2011): 8826-8835.

[109] Hann, Sarah D., et al. "One-step generation of cell-encapsulating compartments via polyelectrolyte complexation in an aqueous two phase system." *ACS applied materials & interfaces* 8.38 (2016): 25603-25611.

[110] Iqbal, Mujahid, et al. "Aqueous two-phase system (ATPS): an overview and advances in its applications." *Biological procedures online* 18.1 (2016): 18.

[111] Hann, Sarah D., et al. "One-step generation of cell-encapsulating compartments via polyelectrolyte complexation in an aqueous two phase system." *ACS applied materials & interfaces* 8.38 (2016): 25603-25611.

[112] Ramakrishnan, Vrinda, et al. "Extraction and purification of lipase from Enterococcus faecium MTCC5695 by PEG/phosphate aqueous-two phase system (ATPS) and its biochemical characterization." *Biocatalysis and agricultural biotechnology* 6 (2016): 19-27.

[113] Matos, Tiago, et al. "Isolation of PCR DNA fragments using aqueous two-phase systems." *Separation and Purification Technology* 122 (2014): 144-148.

[114] Hardt, Steffen, and Thomas Hahn. "Microfluidics with aqueous two-phase systems." *Lab on a Chip* 12.3 (2012): 434-442.

[115] SooHoo, Jeffrey R., and Glenn M. Walker. "Microfluidic aqueous two phase system for leukocyte concentration from whole blood." *Biomedical microdevices* 11.2 (2009): 323-329.

[116] Silva, D. F. C., et al. "Design of a microfluidic platform for monoclonal antibody extraction using an aqueous two-phase system." *Journal of Chromatography A* 1249 (2012): 1-7.

[117] Wijethunga, Pavithra AL, and Hyejin Moon. "On-chip aqueous two-phase system (ATPS) formation, consequential self-mixing, and their influence on drop-to-drop aqueous two-phase extraction kinetics." *Journal of Micromechanics and Microengineering* 25.9 (2015): 094002.

[118] Gomes, Gabriela A., et al. "Purification of plasmid DNA with aqueous two phase systems of PEG 600 and sodium citrate/ammonium sulfate." *Separation and Purification Technology* 65.1 (2009): 22-30.